Chekhov, L., and Shapiro, M. (2009) "Log-canonical coordinates for symplectic groupoid and cluster algebras," International Mathematics Research Notices, Vol. 2009, Article ID rnn999, 54 pages. doi:10.1093/imrn/rnn999

Log-canonical coordinates for symplectic groupoid and cluster algebras

Leonid O. Chekhov¹ and Michael Shapiro²

¹Steklov Mathematical Institute, Moscow, Russia, National Research University Higher School of Economics, Russia, and Michigan State University, East Lansing, USA. Email: chekhov@msu.edu and ²Michigan State University, East Lansing, USA and National Research University Higher School of Economics, Russia. Email: mshapiro@msu.edu

Correspondence to be sent to: mshapiro@msu.edu

Using Fock-Goncharov higher Teichmüller space variables we derive log-canonical coordinate representation for entries of general symplectic leaves of the \mathcal{A}_n groupoid of upper-triangular matrices and, in a more general setting, of higher-dimensional symplectic leaves for algebras governed by the reflection equation with the trigonometric R-matrix. The obtained results are in a perfect agreement with the previously obtained Poisson and quantum representations of groupoid variables for \mathcal{A}_3 and \mathcal{A}_4 in terms of geodesic functions for Riemann surfaces with holes. We realize braid-group transformations for \mathcal{A}_n via sequences of cluster mutations in the special \mathcal{A}_n -quiver. We prove the groupoid relations for normalized quantum transport matrices and, as a byproduct, obtain the Goldman bracket in the semiclassical limit. We prove the quantum algebraic relations of transport matrices for arbitrary (cyclic or acyclic) directed planar network.

Dedicated to the memory of great mathematician and person Boris Dubrovin.

1 Introduction

1.1 Symplectic groupoid, induced Poisson structure on the unipotent upper triangular matrices

Let V denote an n-dimensional vector space, \mathcal{A} be some subspace of bilinear forms on V. Fixing the basis in V, one can identify \mathcal{A} with a subspace in the space of $n \times n$ matrices. The matrix B of a change of a basis in V takes a matrix of bilinear form $\mathbb{A} \in \mathcal{A}$ to $B\mathbb{A}B^{\mathrm{T}}$.

Below we consider an important particular case when \mathcal{A} is the space of unipotent forms identified with the space of the unipotent matrices. The space of unipotent forms is equipped with a natural Poisson structure as follows. The basis change B acts on \mathcal{A} only if the product $B \mathbb{A} B^{\mathrm{T}}$ is unipotent itself. We thus introduce the space of morphisms identified with admissible pairs of matrices (B, \mathbb{A}) such that

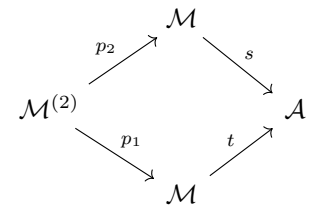
$$\mathcal{M} = \big\{ (B, \mathbb{A}) \; \big| \; B \in GL(V), \; \mathbb{A} \in \mathcal{A}, \; B \mathbb{A} B^{\mathrm{T}} \in \mathcal{A} \big\}.$$

We then have the standard set of maps:

Received 1 Month 20XX; Revised 11 Month 20XX; Accepted 21 Month 20XX Communicated by A. Editor

[©] The Author 2009. Published by Oxford University Press. All rights reserved. For permissions, please e-mail: journals.permissions@oxfordjournals.org.

such that the following diagram, where p_1 and p_2 are natural projections to the first and the second morphism in an admissible pair of morphisms, is commutative:



The crucial point of the construction is the existence of a *symplectic structure*: a smooth groupoid endowed with a symplectic form $\omega \in \Omega^2 \mathcal{M}$ on the morphism space \mathcal{M} that satisfies the splitting (consistency) condition [28, 43]

$$m^*\omega = p_1^*\omega + p_2^*\omega,$$

which implies, in particular, that the source and target maps Poisson commute being respectively an automorphism and an anti-automorphism of the initial Poisson algebra. Since $p_1^*\omega$ and $p_2^*\omega$ are nondegenerate, they admit a (unique) Poisson structure, and because the immersion map e is Lagrangian, this Poisson structure yields a Poisson structure on A.

Identifying \mathcal{A} with \mathcal{A}_n —the space of unipotent upper triangular matrices, in 2000, Bondal [3] obtained the Poisson structure on \mathcal{A}_n using the algebroid construction; assuming $B = e^{\mathfrak{g}}$, we obtain the Bondal algebroid using the anchor map $D_{\mathbb{A}}$ to the tangent space $T_{\mathbb{A}}\mathcal{A}_n$

$$D_{\mathbb{A}}: \quad \mathfrak{g}_{\mathbb{A}} \quad \to \quad T_{\mathbb{A}} \mathcal{A}_{n} g \quad \mapsto \quad \mathbb{A}g + g^{\mathsf{T}} \mathbb{A}, \quad \mathbb{A} \in \mathcal{A}_{n},$$

$$(1.1)$$

where $\mathfrak{g}_{\mathbb{A}}$ is the linear subspace

$$\mathfrak{g}_{\mathbb{A}} := \left\{ g \in \mathfrak{gl}_n(\mathbb{C}), | \mathbb{A} + \mathbb{A}g + g^{\mathsf{T}} \mathbb{A} \in \mathcal{A}_n \right\}$$

of elements g leaving \mathbb{A} unipotent

Lemma 1.1. [3] The map

$$P_{\mathbb{A}}: T_{\mathbb{A}_n}^* \mathcal{A} \to \mathfrak{g}_{\mathbb{A}} w \mapsto P_{-,1/2}(w\mathbb{A}) - P_{+,1/2}(w^{\mathsf{T}}\mathbb{A}^{\mathsf{T}}),$$

$$(1.2)$$

where $P_{\pm,1/2}$ are the projection operators:

$$P_{\pm,1/2}a_{i,j} := \frac{1 \pm \text{sign}(j-i)}{2}a_{i,j}, \quad i, j = 1, \dots, n,$$
(1.3)

and $w \in T^*\mathcal{A}_n$ is a strictly lower triangular matrix, defines an isomorphism between the Lie algebroid $(\mathfrak{g}, D_{\mathbb{A}})$ and the Lie algebroid $(T^*\mathcal{A}_n, D_{\mathbb{A}}P_{\mathbb{A}})$.

The Poisson bi-vector Π on \mathcal{A}_n is then obtained by the anchor map on the Lie algebroid $(T^*\mathcal{A}_n, D_{\mathbb{A}}P_{\mathbb{A}})$ (see Proposition 10.1.4 in [33]) as:

$$\Pi: T_{\mathbb{A}}^* \mathcal{A}_n \times T_{\mathbb{A}}^* \mathcal{A}_n \mapsto \mathcal{C}^{\infty}(\mathcal{A}_n) (\omega_1, \omega_2) \to \operatorname{Tr}(\omega_1 D_{\mathbb{A}} P_{\mathbb{A}}(\omega_2))$$

$$(1.4)$$

It can be checked explicitly that the above bilinear form is in fact skew-symmetric and gives rise to the Poisson bracket

$$\{a_{i,k}, a_{j,l}\} := \frac{\partial}{\partial da_{i,k}} \wedge \frac{\partial}{\partial da_{j,l}} \operatorname{Tr} \left(da_{i,k} D_{\mathbb{A}} P_{\mathbb{A}} (da_{j,l}) \right), \tag{1.5}$$

having the following form in components:

$$\{a_{i,k}, a_{j,l}\} = 0, \quad \text{for } i < k < j < l, \text{ and } i < j < l < k,
 \{a_{i,k}, a_{j,l}\} = 2 (a_{i,j} a_{k,l} - a_{i,l} a_{k,j}), \quad \text{for } i < j < k < l,$$
(1.6)

$$\begin{aligned} &\{a_{i,k}, a_{k,l}\} = a_{i,k} a_{k,l} - 2a_{i,l}, & \text{for } i < k < l, \\ &\{a_{i,k}, a_{j,k}\} = -a_{i,k} a_{j,k} + 2a_{i,j}, & \text{for } i < j < k, \\ &\{a_{i,k}, a_{i,l}\} = -a_{i,k} a_{i,l} + 2a_{k,l}, & \text{for } i < k < l. \end{aligned}$$

Another approach to this Poisson structure as a Dirac bracket on the subset of a natural involution in the dual group was developed in [2], see Appendix A.

This bracket turned out to coincide with the bracket previously known in mathematical physics as Gavrilik-Klimyk-Nelson-Regge-Dubrovin-Ugaglia bracket [23, 35, 36, 15, 42] and it arises from skein relations satisfied by a special finite subset of geodesic functions (traces of monodromies of SL_2 Fuchsian systems, which are in 1-1 correspondence with closed geodesics on a Riemann surface $\Sigma_{q,s}$) described in [7]; a simple constant log-canonical bracket on the space of Thurston shear coordinates z_{α} on the Teichmüller space $T_{g,s}$ of Riemann surfaces $\Sigma_{g,s}$ of genus g with s=1,2 holes was shown [6] to induce the above bracket on a special subset of geodesic functions identified with the matrix elements $a_{i,k}$.

Recall that coordinates $\{x_i\}_{i=1}^n$ on an *n*-dimensional Poisson variety are called *log-canonical* if the Poisson structure written in such coordinates is log-canonical: i.e., $\{x_i, x_j\} = \lambda_{ij} x_i x_j$, or, equialently, $\{\log(x_i), \log(x_j)\} = \sum_{i=1}^{n} x_i x_i x_j$ λ_{ij} , where $(\lambda_{ij})_{i,j=1}^n$ is a constant skew-symmetric rational matrix.

All such geodesic functions admit an explicit combinatorial description [16], which immediately implies that they are Laurent polynomials with positive integer coefficients of $e^{z_{\alpha}/2}$. The algebra of Casimirs of the Poisson bracket has s generators c_1, \ldots, c_s , which are independent linear combinations of shear coordinates incident to the holes. The linear subspace of the vector space $\operatorname{span}\{z_{\alpha}\}$ orthogonal to the subspace $\operatorname{span}\{c_1,\ldots,c_s\}$ parametrizes a symplectic leaf in the Teichmüller space which we call a geometric symplectic leaf.

In [7], the Poisson embedding of a geometric symplectic leaf into A_n was constructed. Note however that the size n of matrix A is related to the genus and the number of holes as n=2g+s (with s taking only two values, 1 and 2) and that the (real) dimension of $T_{g,s}$ is 6g-6+3s increasing linearly with g whereas the total dimension of A_n is obviously n(n-1)/2 increasing quadratically with n; for n=3 and n=4 these two dimensions coincide and the geometric symplectic leaf having the dimension 6g - 6 + 2s is of maximum dimension.

For n=5, the dimension of the geometric symplectic leaf has still the maximum value 8 of dimensions of symplectic leaves in A_5 , but we have just one central element in the corresponding Teichmüller space $T_{2,1}$ and two central elements in A_5 . For all larger n the dimension of geometric symplectic leaf is strictly less than the maximal dimension of symplectic leaf in A_n , so the geometric systems do not describe maximal symplectic leaves in the total Poisson space of A_n .

The log-canonical coordinates in geometric situation are well known to be the above shear coordinates, but, as just mentioned, they can not help in constructing log-canonical coordinates in A_n for $n \geq 5$.

The first problem addressed in this publication is a construction of log-canonical coordinates for a general symplectic leaf of A_n and explicit expressions of matrix elements $a_{i,j}$ in terms of these log-canonical coordinates. It was expected for long, and we show below that these log-canonical coordinates are related to cluster algebras, similar to the geometric cases n=3,4. More exactly, Fock and Goncharov described in [17] the space of parameters $\{Z_{\alpha}\}$ defining an element (of Borel subgroup \mathcal{B}) of SL_n equipped with the Poisson structure (see details in Section 2.3). We construct a Poisson map $\mathcal{B} \to \mathcal{A}_n$. Poisson structure in Fock-Goncharov coordinates has the log-canonical form $\{\log Z_{\alpha}, \log Z_{\beta}\} = \lambda_{\alpha\beta}$, are described by the corresponding \mathcal{A}_n -quiver, see for example Figure 13. Parameters Z_{α} 's are attached to the vertices of \mathcal{A}_n -quiver: for two vertices α and β the corresponding constant $\lambda_{\alpha,\beta}$ equals the number of arrows from α to β minus the number of arrows from β to α . Canonical Darboux coordinates can be obtained as rational linear combinations of log Z_{α} 's. In particular, generators of algebra of Casimirs are obtained as monomials in Z_{α} 's.

From the integrable models standpoint, algebras (1.6) (either with a unipotent A or with a general $\mathbb{A}_{gen} \in \mathfrak{gl}_n$ are known under the name of reflection equation algebras. A task closely related to the first problem is to construct a log-canonical coordinate representation for a general matrix \mathbb{A}_{gen} enjoying the reflection equation.

We also define a quantized symplectic groupoid utilizing explicit construction of (normalized) quantum transport matrices. Both normalized and non-normalized quantum transport matrices satisfy standard RTT =TTR relations. We prove additionally that normalized transport matrices enjoy quantum groupoid relations [11].

1.2Braid-group action on the unipotent matrices

The next important result concerning A_n is that this space admits the discrete braid-group action generated by morphisms $\beta_{i,i+1}: \mathcal{A}_n \to \mathcal{A}_n$, $i = 1, \ldots, n-1$, such that

$$\beta_{i,i+1}[\mathbb{A}] = B_{i,i+1} \mathbb{A} B_{i,i+1}^T \equiv \widetilde{\mathbb{A}} \in \mathcal{A}_n, \tag{1.7}$$

where the matrix $B_{i,i+1}$ has the block form

$$B_{i,i+1} = \begin{bmatrix} 1 & & & & & & \\ \vdots & & \ddots & & & & \\ i & & 1 & & & & \\ i & & & 1 & & & \\ & & & 1 & & & \\ & & & 1 & & & \\ \vdots & & & & & 1 & \\ & & & & & \ddots & \\ & & & & & & 1 \end{bmatrix},$$
(1.8)

and this action is a Poisson morphism [3], [42]. When acting on \mathbb{A} , $\beta_{i,i+1}$ satisfy the standard braid-group relations $\beta_{i,i+1}\beta_{i+1,i+2}\beta_{i,i+1}\mathbb{A} = \beta_{i+1,i+2}\beta_{i,i+1}\beta_{i+1,i+2}\mathbb{A}$ for $i=1,\ldots,n-2$ together with the additional relation $\beta_{n-1,n}\beta_{n-2,n-1}\cdots\beta_{2,3}\beta_{1,2}\mathbb{A} = S_n\mathbb{A}$, where S_n is an element of the group of permutations of matrix entries $a_{i,j}$ whose nth power is the identity transformation. Note that $\beta_{i,i+1}^2\mathbb{A} \neq \mathbb{A}$.

In [8], the quantum version of the above transformations was constructed for a quantum upper-triangular matrix

$$\mathbb{A}^{\hbar} := \begin{bmatrix} q^{-1/2} & a_{1,2}^{\hbar} & a_{1,3}^{\hbar} & \dots & a_{1,n}^{\hbar} \\ 0 & q^{-1/2} & a_{2,3}^{\hbar} & \dots & a_{2,n}^{\hbar} \\ 0 & 0 & q^{-1/2} & \ddots & \vdots \\ \vdots & \vdots & \ddots & \ddots & a_{n-1,n}^{\hbar} \\ 0 & 0 & \dots & 0 & q^{-1/2} \end{bmatrix}.$$

$$(1.9)$$

In the geometric cases n=3,4 elements $a_{i,j}$ are identified with geodesic functions—traces of monodromy elements of Fuchsian systems and double hyperbolic cosines of half-lengths of geodesics on a Riemann surface; these elements were identified with "observables" in physical literature on 2D gravity thus being, by postulates of quantum mechanics, self-adjoint operators. Kashaev in [29] found presentation of the quantum elements $a_{i,j}^{\hbar}$ self-adjoint unbounded operators acting in the dense subspace of a Hilbert space \mathcal{H} of $L^2(\mathbb{R}^d)$ and made an extensive analysis of their spectrum; note that, even in a non-geometrical case, all these operators have continuous spectrum $[2,\infty)$. This postulate is consistent with the quantum algebra of these operators and with their quantum modular transformations (Dehn twists in the geometrical case). However, if we want to express these modular transformations in the matrix form $\mathbb{A}^{\hbar} \to B^{\hbar} \mathbb{A}^{\hbar} [B^{\hbar}]^{\dagger}$, we have to require [8] all diagonal elements of \mathbb{A}^{\hbar} to be non-selfadjoint constant operators $g^{-1/2}$.

of \mathbb{A}^{\hbar} to be non-selfadjoint constant operators $q^{-1/2}$.

We assume that $a_{i,j}^{\hbar}$ are self-adjoint unbounded operators for larger n>4 also. This statement is shown in Corollary 4.3 to follow from the expression (4.1) for \mathbb{A}^{\hbar} in terms of quantum Fock-Goncharov parameters Z_{α}^{\hbar} .

Operators $a_{i,j}^{\hbar}$ are enjoying quadratic-linear algebraic relations following from the quantum reflection

Operators $a_{i,j}^{\hbar}$ are enjoying quadratic–linear algebraic relations following from the quantum reflection equation (see Theorem 4.2) and coinciding with the relations obtained for quantum geodesic functions upon imposing quantum skein relations on the corresponding geodesics and $q = e^{-i\hbar}$. The analogous quantum braid-group action is $\mathbb{A}^{\hbar} \to B_{i,i+1}^{\hbar} \mathbb{A}^{\hbar} \left[B_{i,i+1}^{\hbar} \right]^{\dagger}$ with

$$B_{i,i+1}^{\hbar} = \begin{array}{c} \vdots \\ i \\ i \\ i+1 \\ \vdots \end{array} \qquad \begin{array}{c} 1 \\ 0 \\ 1 \\ 1 \\ 0 \\ 0 \\ \vdots \end{array} \qquad \begin{array}{c} 1 \\ 0 \\ 1 \\ 0 \\ 0 \\ \vdots \end{array} \qquad \begin{array}{c} (1.10)$$

In the geometric cases, the above braid-group morphisms are related to modular transformations generated by (classical or quantum [29]) Dehn twists along geodesics corresponding to the geodesic functions $a_{i,i+1}$ (see [7]). In the absence of geometric interpretation, the only possibility we may resort to is to address the **second problem**: to find a sequence of cluster mutations in a quiver still to be constructed that produces the above braid-group transformation for a generic symplectic leaf of A_n .

We solve both of the formulated problems in this paper: we explicitly construct the quiver (called an A_n quiver) such that the entries $a_{i,j}$ of the unipotent matrix A are positive Laurent polynomials of the cluster quiver variables, construct a quantum version of these Laurent polynomials thus realizing the representation (1.9) and finding explicitly chains of mutations of the A_n -quiver that produce the braid-group transformations.

1.3 Results of the paper

Below we list the main results of the paper divided into three groups.

Results on a special PGL_n Fock-Goncharov-Shen quiver for $\Sigma_{0,1,3}$

For a triangular network corresponding to monodromies on the disc with three marked points on the boundary, we established the following results.

- Theorem 2.12 establishes R-matrix commutation relations for normalized transport matrices M_1 and M_2 of the PGL_n -quiver.
- Theorem 2.14 contains the proof of the groupoid condition $T_3T_2T_1 = \text{Id}$ for quantum transport matrices T_i in the triangular network of $\Sigma_{0,1,3}$. This condition can be easily generalized to PGL_n -monodromies on any Riemann surface $\Sigma_{g,s,n}$ with n > 0.
- In Theorem 3.1 we show that a corollary of Theorem 2.12 establishes quantum Goldman commutation relations for monodromy matrices corresponding to graph-simple paths in the fat graph dual to the triangle decomposition of $\Sigma_{g,s,n}$.
- 1.3.2 Results on a symplectic groupoid of upper-triangular matrices and algebras of quantum reflection equation
 - Theorem 4.2: For any $n \times 2n$ quantum transport matrix composed out of two (nonnormalized) $n \times n$ matrices \mathcal{M}_1 and \mathcal{M}_2 , their combination $\mathbb{A}^{\hbar} := \mathcal{M}_1^{\mathrm{T}} \mathcal{M}_2$ satisfies the quantum reflection equation $\mathcal{R}_n(q)\mathbb{A}^{\hbar}\mathcal{R}_n^{\mathrm{t}_1}(q)\mathbb{A}^{\hbar} = \mathbb{A}^{\hbar}\mathcal{R}_n^{\mathrm{t}_1}(q)\mathbb{A}^{\hbar}\mathcal{R}_n(q)$.
 - If we identify $n \times 2n$ quantum transport matrix with that of the PGL_n -quiver, \mathbb{A}^{\hbar} becomes upper triangular, and we construct a special (nonplanar) A_n quiver corresponding to it. Lemma 5.5 describes a special sequence of Y-variable cluster mutations of this quiver that leaves invariant the form of this quiver acting therefore by an automorphism on its variables. We prove in Theorem 5.6 that these automorphisms are braid-group transformations on the entries $a_{i,j}$ of a classical A-matrix. We leave constructing quantum version of these automorphisms to future studies.
 - In a separate Section 6 we describe Casimir operators of the general PGL_n -quiver and those of the \mathcal{A}_n -quiver.

1.3.3 Results on general quantum directed networks

- The most general statement is Theorem 8.3 establishing quantum algebra of elements of a transport matrix of any planar network, with or without cycles.
- In Lemma 7.16 we prove R-matrix commutation relations $R_m(q) \overset{1}{Q}_q \otimes \overset{2}{Q}_q = \overset{2}{Q}_q \otimes \overset{1}{Q}_q R_n(q)$ valid for the quantum transport matrix Q_q of any acyclic planar network with separated n sources and m sinks. Here $R_k(q)$ is the quantum trigonometric R-matrix (2.17) of size $k^2 \times k^2$.
- For an oriented acyclic graph embedded in the disk we develop the theory of quantum measurements parallel to the theory of commutative Grassmann measurements by A.Postnikov. We proved that the quantum Grassmann measurement does not change under orientation reversing of rigid oriented path. This establishes groupoid relations (see Theorem 2.14) for normalized quantum transport matrices.

The structure of the paper is as follows:

In Sec. 2, we describe quantum algebras of transport matrices in the Fock-Goncharov PGL_n -quiver (Theorem 2.12); this quantum algebra is based on a more general Lemma 7.16 proven in Sec. 7 for any planar (acyclic) directed network. We also prove the groupoid condition (Theorem 2.14) satisfied by normalized quantum transport matrices in the PGL_n -quiver as a corollary of the fact that quantum Grassmannian measurement map does not change under reversion of orientation of a rigid path (see Lemma 7.14).

In Sec. 3, we briefly describe general algebraic relations enjoyed by (normalized) quantum transport matrices for SL_n character variety on a general triangulated Riemann surface $\Sigma_{q,s,p}$ with p>0 marked points on the hole boundaries; namely we demonstrate that quantum Goldman relations are satisfied.

Section 4 contains the first main result: out of cluster variables of the PGL_n -quiver we construct a unipotent \mathbb{A} satisfying the quantum reflection equation (Theorem 4.2). We generalize this construction to solutions of quantum reflection equation that are not necessarily unipotent (Theorem 4.5).

Taking the semiclasical limit of Theorem 4.5 we observe in Theorem 5.1 that Fock-Goncharov parameters provide log-canonical coordinates for the Poisson bracket (1.5).

In Sec. 5, we associate the unipotent \mathbb{A} constructed in the preceding section with a special \mathcal{A}_n -quiver and prove that special sequences of mutations at vertices of this quiver generate braid-group transformations of elements of \mathbb{A} (Theorem 5.6).

In Sec. 6, we collect statements about Casimir elements of PGL_n - and A_n -quivers.

In Sec. 7 we consider quantum transport matrices for general acyclic planar directed networks, establish the relation to Postnikov's quantum Grassmannians and measurement maps, and prove the general *R*-matrix relation for the corresponding quantum transport matrices (Lemma 7.16).

In Sec. 8, we generalize the results of Sec. 7 to arbitrary planar directed network (relaxing the acyclicity condition) showing in Theorem 8.3 that quantum transport elements in any such network satisfy the same closed algebraic relations as elements of an acyclic planar directed network.

Section 9 is a brief conclusion.

2 SL_n -algebras for the triangle $\Sigma_{0,1,3}$

Let $\Sigma_{g,s,p}$ denote a topological genus g surface with s boundary components and p marked points. In this section, we concentrate on the case of the disk with 3 marked points on the boundary $\Sigma_{0,1,3}$. (To simplify notations, we use $\Sigma = \Sigma_{0,1,3}$.)

2.1 Quantum torus and (quantum) cluster mutations

Let lattice $\Lambda = \mathbb{Z}^m$ be equipped with a skew-symmetric $\mathbb{Z}/2$ -valued form $\langle \cdot, \cdot \rangle$. Introduce the q-multiplication operation in the module $\Upsilon = \operatorname{Span}\{Z_{\lambda}\}_{{\lambda} \in \Lambda}$ over the ring $k[q^{\pm \frac{1}{2}}]$ by the following formula

$$Z_{\lambda}Z_{\mu} = q^{\langle \lambda, \mu \rangle} Z_{\lambda + \mu}. \tag{2.1}$$

The algebra Υ is called a *quantum torus*. Fix a basis $\{e_i\}$ in Λ , we consider Υ as a non-commutative algebra of Laurent polynomials in variables $Z_i := Z_{e_i}, i \in [1, m]$. For any sequence $\mathbf{s} = (s_1, \dots, s_t), s_j \in [1, m]$, let $\Pi_{\mathbf{s}}$ denote the monomial $\Pi_{\mathbf{s}} = Z_{s_1} Z_{s_2} \dots Z_{s_t}$. Let $\lambda_{\mathbf{s}} = \sum_{j=1}^t e_{s_j}$. Element $Z_{\lambda_{\mathbf{s}}}$ is called in physical literature the Weyl form of $\Pi_{\mathbf{s}}$ and we denote it by two-sided colons $\Pi_{\mathbf{s}}$ It is easy to see that $\Pi_{\mathbf{s}} = Z_{\lambda_{\mathbf{s}}} = q^{-\sum_{j<\mathbf{s}} \langle e_{s_j}, e_{s_k} \rangle} \Pi_{\mathbf{s}}$.

Below we need to consider also an extension $\Upsilon^{\frac{1}{n}}$ of Υ that contains n-th roots $Z_i^{\frac{1}{n}}$ for a fixed n. We replace Λ by $\frac{1}{n}\Lambda = \Lambda \otimes \frac{1}{n}\mathbb{Z}$. Let $\Upsilon^{\frac{1}{n}}$ be an $k[q^{\pm \frac{1}{2n^2}}]$ -module spanned by $\frac{1}{n}\Lambda$ with the same commutation relations $Z_{\lambda}Z_{\mu} = q^{\langle \lambda, \mu \rangle}Z_{\lambda+\mu}$ as before. Weyl ordering is naturally extended to elements of $\Upsilon^{\frac{1}{n}}$. Υ is naturally embedded in $\Upsilon^{\frac{1}{n}}$

In what follows, a fractional power of Z_i means an element of $\Upsilon^{\frac{1}{n}}$.

2.2 Positive representation of quantum torus Υ

Let $Z_j = Z(e_j)$, $i = 1 \dots m$ be generators of quantum torus Υ as above, $b \in \mathbb{R}$, $\omega_{jk} = \langle e_j, e_k \rangle$. An associated topological *-Heisenberg algebra \mathcal{H} is an algebra over \mathbb{C} with generators x_j satisfying $[x_j, x_k] = \frac{1}{2\pi i}\omega_{jk}$. Here * acts as a antiholomorphic, involutive antiisomorphism mapping $z \in \mathbb{C}$ to \bar{z} , *b = b, $*x_j = x_j$. Then, expressions $Z_j = e^{2\pi b x_j}$ and $q = e^{\pi i b^2}$ define an embedding of quantum torus into Heisenberg algebra $\Upsilon \hookrightarrow \mathcal{H}$.

Denote by $\Lambda_{\mathbb{R}} = \Lambda \otimes \mathbb{R}$, and by $\mathfrak{k} \subset \Lambda_{\mathbb{R}}$ the kernel of the form $\langle *, * \rangle$. A central character $\chi \in \Lambda_{\mathbb{R}}^*$ determines an irreducible *-representation V_{χ} where x_j act by unbounded operators in the Hilbert space and a central element $k \in \mathfrak{k}$ acts by scalar $\chi(k)$. More exactly, let us pick a symplectic basis $\{p_i, q_i\}$ in $\Lambda_{\mathbb{R}}/\mathfrak{k}$ and set Λ_{χ} to be the Hilbert space of L^2 -functions on the Lagrangian subspace in $\Lambda_{\mathbb{R}}/\mathfrak{k}$ spanned by q_i s. Operators q_j act by multiplication while p_j act as $\frac{1}{2\pi i}\partial/\partial q_j$. Different choices of symplectic basis lead to unitary equivalent realizations of V_{χ} . All Z_j act by positive, essentially self-adjoint, unbounded operators [26, 40].

In particular, the *n*-th root $Z_j^{\frac{1}{n}}$ is a well defined unique positive essentially self-adjoint operator, $q^{\frac{1}{2n^2}} = \exp(\frac{\pi i b^2}{2n^2})$. Hence, the Weyl ordering of monomial $\prod_{\alpha} Z_{\alpha}^{\frac{t_{\alpha}}{n}} = \exp(\frac{1}{n} \sum_{\alpha} t_{\alpha} x_{\alpha})$ is well defined and coincides with $\prod_{\alpha} Z_{\alpha}^{t_{\alpha} \bullet \frac{1}{n}}$ for all $t_{\alpha} \in \mathbb{Z}$.

We recall the definition of quantum mutations of Υ .

Definition 2.1. A cluster seed σ is a quadruple $\sigma = (\Lambda, \langle , \rangle, \{\mathbf{e}_i\}, I_0)$ where

- Λ is a lattice
- $I_0 \subset [1, rank(\Lambda)]$
- $\{\mathbf{e}_i\}$ is a basis of Λ
- $\langle \ , \ \rangle$ is a skew-symmetric $\mathbb{Z}/2$ -valued form on Λ and $\omega_{ij} = \langle \mathbf{e}_i, \mathbf{e}_j \rangle \in \mathbb{Z}$ unless $(i,j) \in I_0 \times I_0$.

Definition 2.2. For $k \in [1, rank(\Lambda)]$ the cluster mutation μ_k transforms the seed σ to the seed $\mu_k(\sigma)$ by the basis change $\{\mathbf{e}_i\}$ to $\{\mathbf{e}_i' = \mu_k(\mathbf{e}_i)\}$, where $\mathbf{e}_i' = -\mathbf{e}_k$, if i = k; and $\mathbf{e}_i' = \mathbf{e}_i + [\omega_{ik}]_+ \mathbf{e}_k$, otherwise.

Recall the compact quantum dilogarithm function $\Psi^q(z) = \prod_{i=1}^{\infty} \frac{1}{1 + q^{2i+1}z}$. The mutation μ_k induces an automorphism $Ad_{\Psi^q(X_{\mathbf{e}'_k})}$ of the fraction field $Frac(\Upsilon)$. Despite that $\Psi^q(z)$ is an infinite series its properties imply that $Ad_{\Psi^q(X_{\mathbf{e}'_k})}$ is a rational transformation. Namely, $\mu^q_k(X_k) = X_k^{-1}$, $\mu_k^q(X_i) = X_i \prod_{\ell=1}^{\omega_{ki}} \left(1 + q^{2\ell-1} X_k^{-1}\right)^{-1}$ if $i \neq k$ and $\omega_{ki} \geq 0$ and $\mu_k^q(X_i) = X_i \prod_{\ell=1}^{-\omega_{ki}} \left(1 + q^{2\ell-1} X_k\right)$ if $i \neq k$ and $\omega_{ki} \leq 0$ which become the classical commutative mutation formulas for q = 1.

2.3 Moduli space $\mathcal{X}_{PGL_n,\Sigma}(\mathbb{R}_{>0})$

In this section we review the definition of quantized moduli space $\mathcal{X}_{PGL_n,\Sigma}$ of framed PGL_n -local systems on the disk with three marked points Σ ([17]). We call disk with three marked points 1, 2, 3 on its boundary triangle with vertices 1, 2, 3 and use also notation $\triangle 123 = \Sigma$ (see Fig 6) when we want to distinguish the roles of particular sides and vertices.

A framed PGL_n -local system on Σ is defined in [17] as a triple of flags in \mathbb{R}^n . If the flags are pairwise in general position the framed PGL_n -local system in the triangle $\triangle 123$ (see Figure 1) determines transport matrices \widehat{T}_i . If \widehat{T}_i is associated to a directed path then the inverse matrix $(\widehat{T}_i)^{-1}$ corresponds to the same path in the opposite direction.

Recall that a complete flag F_{\bullet} is a collection of consecutively embedded subspaces $\{0 = F_0 \subset F_1 \subset F$ $\cdots \subset F_k \subset \cdots \subset F_{n-1} \subset F_n = \mathbb{R}^n$ where F_k is a linear subspace of dimension k. Denote by $F^a = F_{n-a}$, $a=0,1,\ldots,n$, the vector subspace of codimension a. Let $(F_1)_{\bullet},(F_2)_{\bullet},(F_3)_{\bullet}$ be three complete flags in general position in \mathbb{R}^n assigned to the vertices 1, 2, 3 of triangle $\triangle 123$ (see Fig. 1).

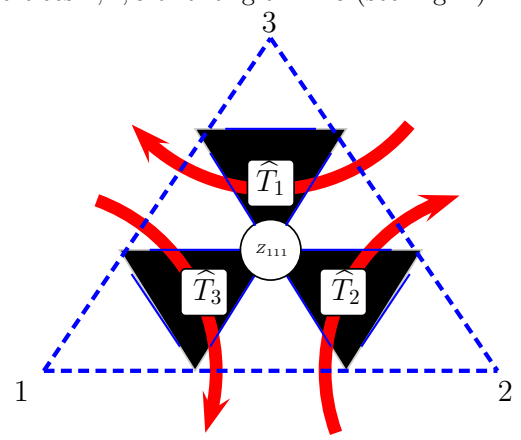


Fig. 1. Fock-Goncharov parameters for $\mathcal{X}_{SL_3,\Sigma}$. Arrows shows the direction of transport matrices $\widehat{T}_1,\widehat{T}_2,\widehat{T}_3$.

Consider the subtriangulation of $\triangle 123$ into $\binom{n}{2}$ white upright triangles and $\binom{n-1}{2}$ black upside-down triangles. Label all white upright triangles by triples $\{(a,b,c)|a,b,c\geq 0\ \&\ a+b+c=n-1\}$. Each white triangle (a,b,c) corresponds to a line $\ell_{abc}=(F_1)^a\cap (F_2)^b\cap (F_3)^c$. Similarly, label black upside-down triangles by triples $\{(a,b,c)|a,b,c\geq 0 \& a+b+c=n-2\}$. Each upside-down triangle (a,b,c) is associated with the plane $P_{abc}=(F_1)^a\cap (F_2)^b\cap (F_3)^c$. Note that every plane P_{abc} of a black triangle contains all three lines $\ell_{(a+1)bc}, \ell_{a(b+1)c}, \ell_{ab(c+1)}$ of white triangles which are neighbors of the black one. In Figures 2, 3, 5 we draw gray triangles with vertices $\ell_{(a+1)bc}, \ell_{a(b+1)c}, \ell_{ab(c+1)}$. Each such gray triangle corresponds to the plane P_{abc} . For every such plane P_{abc} choose three vectors $\mathbf{v}_{(a+1)bc} \in \ell_{(a+1)bc}, \mathbf{v}_{a(b+1)c} \in \ell_{a(b+1)c}, \mathbf{v}_{ab(c+1)} \in \ell_{ab(c+1)}$ such

that they satisfy condition $\mathbf{v}_{(a+1)bc} = \mathbf{v}_{a(b+1)c} + \mathbf{v}_{ab(c+1)}$. Hence, given a configuration of lines corresponding to triple of flags $((F_1)_{\bullet}, (F_2)_{\bullet}, (F_3)_{\bullet})$, the choice of one vector $\mathbf{v}_{abc} \in \ell_{abc}$ determines uniquely all other vectors in the lines $\ell_{a'b'c'}$ for all (a'b'c') (see Fig. 2).

Thus, the configuration of lines ℓ_{abc} determines projective collection of vectors $\{\mathbf{v}_{abc}\}$ modulo scalar scaling. Note that exactly two vectors at vertices of any gray triangle are independent.

Define a *snake* as an oriented piecewise linear path running downwards from the top black triangle containing the line ℓ_{00n-1} to a bottom black triangle containing ℓ_{ab0} consisting of sides of gray triangles (for example, bold red path in Fig 2).

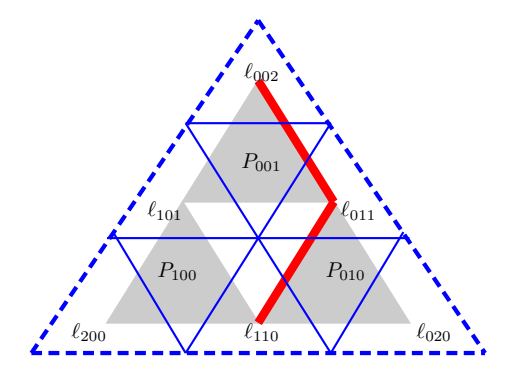


Fig. 2. Configuration of lines corresponding to triple of flags in \mathbb{R}^3 . Black triangles are equipped with planes P_{abc} . Plane P_{100} contains lines ℓ_{200} , ℓ_{110} , ℓ_{101} , P_{010} contains lines ℓ_{110} , ℓ_{020} , ℓ_{011} , P_{001} contains lines ℓ_{101} , ℓ_{011} , ℓ_{002} . Vectors $\mathbf{v}_{abc} \in \ell_{abc}$ satisfy relations $\mathbf{v}_{101} = \mathbf{v}_{002} + \mathbf{v}_{011}$, $\mathbf{v}_{200} = \mathbf{v}_{101} + \mathbf{v}_{110}$, $\mathbf{v}_{110} = \mathbf{v}_{011} + \mathbf{v}_{020}$. The bold red broken line indicates a snake.

Any snake defines a projective basis $\mathbf{v}_{\alpha_1}, \dots, \mathbf{v}_{\alpha_n}$ of \mathbb{R}^n . Note that choosing another corner of triangle as a top one leads to different choice of projective basis. In particular, if the basis defined by the only snake running from ℓ_{00n-1} to ℓ_{n-100} is $\mathbf{v}_{\alpha_1}, \dots, \mathbf{v}_{\alpha_n}$ then the basis defined by the only snake in the opposite direction from ℓ_{n-100} to ℓ_{00n-1} is $\mathbf{v}_{\alpha_n}, -\mathbf{v}_{\alpha_{n-1}}, \dots, (-1)^{n-1}\mathbf{v}_{\alpha_1}$.

Denote by $\mathbf{b_p}$ the basis defined by snake \mathbf{p} . Let \mathbf{b}_{32} be the basis defined by the unique snake from ℓ_{00n-1} to ℓ_{0n-10} in the triangle $\triangle 123$ and by \mathbf{b}_{13} the basis defined by the snake ℓ_{n-100} to ℓ_{00n-1} (see Figure 3). The bases take the following form $\mathbf{b}_{32} = (\mathbf{v}_{002}, \mathbf{v}_{101}, \mathbf{v}_{020})$, the basis $\mathbf{b}_{13} = (\mathbf{v}_{200}, -\mathbf{v}_{101}, \mathbf{v}_{002})$.

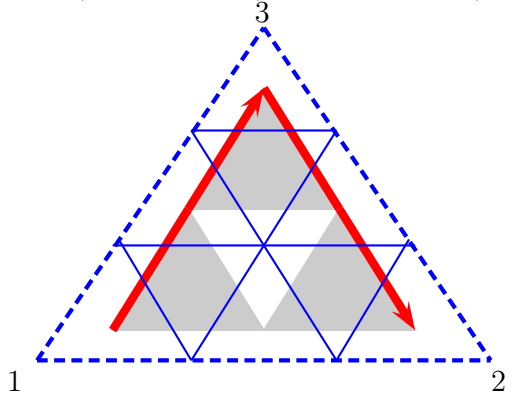


Fig. 3. Snakes \mathbf{b}_{32} on the right and \mathbf{b}_{13} on the left.

Note that such construction identifies each inner vertex of barycentric subdivision (i,j,k), $i,j,k \in Z_{>0}, i+j+k=n$ with three-dimensional vector subspace W space spanned by the three lines $\ell_{i-1,j,k},\ell_{i,j-1,k}$, and $\ell_{i,j,k-1}$. By construction, W contains three planes $P_{i-1,j-1,k} = \operatorname{span}\{\ell_{i-1,j,k},\ell_{i,j-1,k}\}$, $P_{i-1,j,k-1} = \operatorname{span}\{\ell_{i-1,j,k},\ell_{i,j,k-1}\}$, and $P_{i,j-1,k-1} = \operatorname{span}\{\ell_{i,j-1,k},\ell_{i,j,k-1}\}$, and lines $\ell_{i-1,j-1,k+1} \subset P_{i-1,j-1,k},\ell_{i-1,j-1,k-1} \subset P_{i-1,j-1,k-1} \subset P_{i+1,j-1,k-1}$ also lie in W. Projectively, we obtain a plane with three lines and three points (one point on each line). It is well known that such projective configuration is described by one projective invariant parameter. These projective invariant parameters form Fock-Goncharov coordinates $Z_{i,j,k}$ inside triangle $i,j,k\in\mathbb{Z}_{>0},\ i+j+k=n$ (see Figure 1). $Z_{i,j,k}$ parametrize change of basis corresponding to snakes under elementary snake transformations.

In what follows we restrict ourselves only to positive parameters $Z_{i,j,k}$. It is well known [17] that the choice of positive Fock-Goncharov parameters is compatible with flipping surface triangulations and describes one connected component $\mathcal{X}_{PGL_n,\Sigma}(\mathbb{R}_{>0})$ of the moduli space of framed PGL_n -local systems called higher Teichmüller space. Such restriction determines, in particular, the canonical (positive) choice of n-th root of any monomial in Z_{ijk} .

Let $\mathbf{b}_r, \mathbf{b}_b, \mathbf{b}_g$ be the bases corresponding to red, blue, and green snakes on Figure 4. Then, $L_2 = \begin{pmatrix} 1 & 0 & 0 \\ 0 & 1 & 0 \\ 0 & 1 & 1 \end{pmatrix}$

is a transformation matrix from \mathbf{b}_r to \mathbf{b}_b ; $L_1H_2(Z_{111})$ is a transformation matrix from \mathbf{b}_b to \mathbf{b}_g , where

$$L_{1} = \begin{pmatrix} 1 & 0 & 0 \\ 1 & 1 & 0 \\ 0 & 0 & 1 \end{pmatrix}, H_{2}(Z_{111}) = \begin{pmatrix} Z_{111}^{-1/3} & 0 & 0 \\ 0 & Z_{111}^{-1/3} & 0 \\ 0 & 0 & Z_{111}^{2/3} \end{pmatrix}, S = \begin{pmatrix} 0 & 0 & 1 \\ 0 & -1 & 0 \\ 1 & 0 & 0 \end{pmatrix}.$$

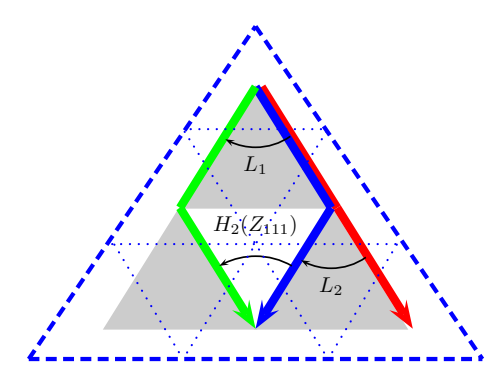


Fig. 4. Snakes \mathbf{b}_r (red), \mathbf{b}_b (blue) and \mathbf{b}_g (green).

Define $\widehat{T}_1 \in SL_n$ as the transformation matrix from basis \mathbf{b}_{13} to \mathbf{b}_{32} , namely, *i*-th column of \widehat{T}_1 is $[(\mathbf{b}_{13})_i]_{\mathbf{b}_{32}}$, i.e. coordinate vector $(\mathbf{b}_{13})_i$ with respect to basis \mathbf{b}_{32} . It is factorizable in a product of elementary basis changes corresponding to the following left-to-right sequence of snake transformations.



Fig. 5. Sequence of elementary snake moves factorizing transport matrix \hat{T}_1

Note that both b_{32} and b_{13} are projective bases defined up to the same multiplicative scalar, because, in particular, each of these two bases contains either \mathbf{v}_{00n} or $-\mathbf{v}_{00n}$. Hence, the transformation matrix T_1 does not depend on the choice of this scalar and is well defined as an element of SL_n . To define a T_2 (T_3) we rotate the triangle $\triangle 123$ by $2\pi/3$ $(4\pi/3)$ counterclockwise and then use the rule for \widehat{T}_1 .

Moduli space of pinnings $\mathcal{P}_{PGL_n,\Sigma}(\mathbb{R}_{>0})$ and transport matrices. 2.4

Next we will add some additional parameters to the sides of $\triangle 123$ and obtain modified versions T_i of transport matrices T_i . We recall the moduli space of pinnings $\mathcal{P}_{PGL_n,\Sigma}$ introduced by Goncharov and Shen in [26]. Let (B, B_{-}) be a generic pair of flags. Let U = [B, B] and $U_{-} = [B_{-}, B_{-}]$ be maximal unipotent subgroups. Let $x_i: \mathbb{A}^1 \to U$ be a unipotent subgroup associated to the simple root α_i . Equivalently, the choices of x_1, \ldots, x_{n-1}

determine an additive isomorphism
$$(\chi_1, \dots, \chi_{n-1}) : U/[U, U] \simeq \mathbb{A}^{n-1}$$
, $\chi_i(x_j(a)) = \begin{cases} a, & \text{if } i = j \\ 0, & \text{, if } i \neq j. \end{cases}$

Let $y_i: \mathbb{A}^1 \to U_-$ be a unipotent subgroup associated to the simple root $-\alpha_i$.

Fig. 6. Triangle $\triangle 123$.

Definition 2.3. The datum $p = (B, B_-, x_i, y_i, i \in [1, n-1])$ is called a pinning over (B, B_-) if it gives rise to a homomorphism $\gamma_i : SL_2 \to PGL_n$ for each $i \in [1, n-1]$ such that $\gamma_i \begin{pmatrix} 1 & a \\ 0 & 1 \end{pmatrix} = x_i(a), \gamma_i \begin{pmatrix} 1 & 0 \\ a & 1 \end{pmatrix} = y_i(a), \gamma_i \begin{pmatrix} a & 0 \\ 0 & a^{-1} \end{pmatrix} = \alpha_i^{\vee}(a)$, where α_i^{\vee} is a simple positive coroot.

 $\mathcal{P}_{PGL_n,\Sigma}$ extends $\mathcal{X}_{PGL_n,\Sigma}$ assigning a pinning to each side of the triangle Σ , hence equipping each oriented side of triangle Σ with additional Cartan element. This Cartan element can be parametrized by assigning one parameter $Z_{i,j,k}$ to each of n-1 vertices of barycentric subdivision on the corresponding side. More exactly, we add $Z_{i,j,k}$, $i=0,j+k=n,j,k\in\mathbb{Z}_{>0}$, $Z_{i,j,k}$, $j=0,i+k=n,i,k\in\mathbb{Z}_{>0}$, and $Z_{i,j,k}$, $k=0,i+j=n,i,j\in\mathbb{Z}_{>0}$ shown on Figure 7 (see [26] for details). Pinning of sides allows an amalgamation of two sets of parameters for two different triangles creating the set of parameters describing moduli space $\mathcal{P}_{PGL_n,\mathbb{O}}$ where \mathbb{O} is the quadrangle obtained by gluing of two triangles along the common side. Amalgamation identifies two tuples of n-1 vertices of the baricentric subdivisions of the common sides in two glued triangles. In the case when such vertex α_1 of the first triangle is glued to vertex α_2 of the second triangle forming vertex α of the common subtriangulation we have $Z_{\alpha} = Z_{\alpha_1} Z_{\alpha_2}$. Note that by our agreement the parameters in different triangles commute and $Z_{\alpha_1} Z_{\alpha_2} = \mathcal{Z}_{\alpha_1} Z_{\alpha_2}$.

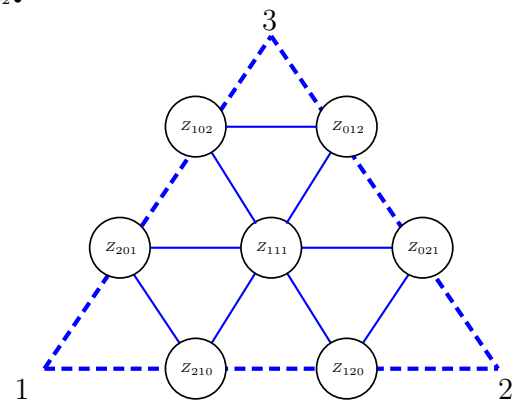


Fig. 7. Fock-Goncharov parameters for $\mathcal{P}_{PGL_3,\Sigma}$. Arrows shows the direction of transport matrices $\widehat{T}_1,\widehat{T}_2,\widehat{T}_3$.

Define transport matrix T_1 as \widehat{T}_1 precomposed and postcomposed with multiplications by diagonal matrices defined by the pinnings on the sides 3-2 and 1-3, which can be thought as elements of SL_n for $PGL_n(\mathbb{R}_{>0})$. In terms of Z_{ijk} transport matrix takes form (2.3). Similarly, we define the transport matrix T_2 as similar transformation matrix from side 2-3 to 1-2 and T_3 as transformation from 2-1 to 1-3.

Finally, denote

$$M_1 = T_1, M_2 = T_2^{-1}$$
 (see Fig. 6). (2.2)

Matrix M_1 is an upper-anti-triangular matrix and M_2 is a lower-anti-triangular matrix (see Example 2.7). The expressions for classical transport matrices were first found in [19], (see also [14] Appendix A.2). Let $u(k) = \{0, k < 0, \text{ and } 1, k \ge 0\}$ denote the integer step function.

Definition 2.4. Define $n \times n$ matrices

1. $(S)_{ij} = (-1)^{i-1} \delta_{i,n+1-j}$. 2. $H_k(t) = t^{-\frac{n-k}{n}} \operatorname{diag}(t^{u(1-k-1)}, t^{u(2-k-1)}, \dots, t^{u(n-k-1)})$,

- 3. $\check{H}_k(t) = SH_k(t)S^T = t^{-\frac{n-k}{n}} \operatorname{diag}(t^{u(n-k-1)}, \dots, t^{u(2-k-1)}, t^{u(1-k-1)}),$
- 4. E_k , where $(E_k)_{i,j} = \delta_{k+1,i} \cdot \delta_{k,j}$ is the matrix whose only nonzero element is 1 at the position (k+1,k).
- 5. $L_k = \operatorname{Id}_n + E_k$ for $k \in [1, n-1]$ where Id_n is the identity $n \times n$ matrix.

Remark 2.5. Note that
$$S^T = S^{-1}$$

Then,

$$T_1 = H_{out}^{13} \cdot \hat{T}_1 \cdot H_{in}^{32}$$
, where (2.3)

$$H_{out}^{13} = \prod_{j=1}^{n-1} \check{H}_{n-j}(Z_{n-j,0,j}) \text{ is the diagonal matrix induced by the pinning of the side } 1-3; \tag{2.4}$$

$$H_{in}^{32} = \prod_{j=1}^{n-1} H_j(Z_{0,j,n-j}) \text{ is the diagonal matrix induced by the pinning of the side } 3-2;$$
 (2.5)

$$\widehat{T}_{1} = S L_{n-1} \prod_{p=1}^{n-2} \left[\prod_{q=1}^{p} L_{n-q-1} H_{n-q}(Z_{p,q,n-p-q}) \right] L_{n-1} \text{ is the transformation matrix from } \mathbf{b}_{13} \text{ to } \mathbf{b}_{32}. \quad (2.6)$$

Equally, the transport matrix can be written as

$$T_{1} = S \left[\prod_{j=1}^{n-1} H_{n-j}(Z_{n-j,0,j}) \right] L_{n-1} \prod_{p=1}^{n-2} \left[\prod_{q=1}^{p} L_{n-q-1} H_{n-q}(Z_{p,q,n-p-q}) \right] L_{n-1} \left[\prod_{j=1}^{n-1} H_{j}(Z_{0,j,n-j}) \right].$$
(2.7)

Here, $H_{out}^{31} = \left[\prod_{j=1}^{n-1} H_{n-j}(Z_{n-j,0,j})\right]$ and H_{out}^{13} satisfy relation $H_{out}^{13} = SH_{out}^{31}S^T$.

Let $\mathbb{I} = \{(a, b, c) | a, b, c \in \mathbb{Z}_{>0}, a + b + c = n\}$ be the set of barycentric indices in the triangle with side n, τ : $\mathbb{I} \to \mathbb{I}$ be the clockwise rotation by $2\pi/3$, τ acts naturally on the sequences of barycentric parameters and hence on sequences of Fock-Goncharov parameters: for $\mathbf{Z}=(Z_{\alpha_1},\ldots,Z_{\alpha_k})$ the sequence $\tau\mathbf{Z}=(Z_{\tau(\alpha_1)},\ldots,Z_{\tau(\alpha_k)})$, if $O(\mathbf{Z})$ is an object depending on the collection $\mathbf{Z} = (Z_{\alpha_i})_{i=1}^k$ of Fock-Goncharov parameters then $\tau O = O(\tau \mathbf{Z})$. Note that $T_2 = \tau T_1$, $T_3 = \tau^2 T_1$ (see Fig. 1). The transport matrix $M_2 = (\tau M_1)^{-1}$.

Example 2.6. For
$$n = 3$$
, we have $H_1(t) = \begin{pmatrix} t^{-2/3} & 0 & 0 \\ 0 & t^{1/3} & 0 \\ 0 & 0 & t^{1/3} \end{pmatrix}$, $H_2(t) = \begin{pmatrix} t^{-1/3} & 0 & 0 \\ 0 & t^{-1/3} & 0 \\ 0 & 0 & t^{2/3} \end{pmatrix}$, $L_1 = \begin{pmatrix} 1 & 0 & 0 \\ 1 & 1 & 0 \\ 0 & 0 & 1 \end{pmatrix}$, $L_2 = \begin{pmatrix} 1 & 0 & 0 \\ 0 & 1 & 0 \\ 0 & 1 & 1 \end{pmatrix}$, $S = \begin{pmatrix} 0 & 0 & 1 \\ 0 & -1 & 0 \\ 1 & 0 & 0 \end{pmatrix}$.

Transport matrices T_1 from side $1 - 2$ to side $1 - 3$, T_2 from side $2 - 3$ to side $2 - 1$ and T_3 from

ransport matrices T_1 from side 1-2 to side 1-3, T_2 from side 2-3 to side 2-1 and T_3 from side 3-1to side 3-2 (see Fig. 1) have the following form

$$\begin{array}{lcl} M_1 = T_1 & = & SH_2(Z_{201})H_1(Z_{102})L_2L_1H_2(Z_{111})L_2H_1(Z_{012})H_2(Z_{021}) \\ T_2 & = & SH_2(Z_{012})H_1(Z_{021})L_2L_1H_2(Z_{111})L_2H_1(Z_{120})H_2(Z_{210}) \\ T_3 & = & SH_2(Z_{120})H_1(Z_{210})L_2L_1H_2(Z_{111})L_2H_1(Z_{201})H_2(Z_{102}). \end{array}$$

$$M_1 = \begin{pmatrix} Z_{021}^{-1/3} Z_{102}^{1/3} Z_{111}^{-1/3} Z_{012}^{-2/3} Z_{201}^{2/3} & Z_{021}^{-1/3} Z_{102}^{1/3} (Z_{111}^{-1/3} + Z_{111}^{2/3}) Z_{102}^{1/3} Z_{201}^{2/3} & Z_{021}^{2/3} Z_{102}^{1/3} Z_{111}^{2/3} Z_{012}^{2/3} Z_{201}^{2/3} \\ -Z_{021}^{-1/3} Z_{102}^{-1/3} Z_{111}^{-1/3} Z_{012}^{-2/3} Z_{201}^{-1/3} & -Z_{021}^{-1/3} Z_{102}^{-1/3} Z_{111}^{-1/3} Z_{012}^{1/3} Z_{201}^{-1/3} & 0 \\ Z_{021}^{-1/3} Z_{102}^{-2/3} Z_{111}^{-1/3} Z_{012}^{-2/3} Z_{201}^{-1/3} & 0 \end{pmatrix},$$

Finally, $M_2 = T_2^{-1}$. We can easily factorize M_2 in the product of elementary matrices noting that $S^{-1} = (-1)^{n-1}S$, $H_k(t)^{-1} = H_k(t^{-1}) = SH_{n-k}(t)S$, $L_k^{-1} = \mathrm{Id}_n - E_k = SL_{n-k}^{\mathrm{T}}S$, where L_j^{T} is the transpose of matrix L_i . Then,

$$\begin{array}{lcl} M_2 & = & H_2(Z_{210})^{-1}H_1(Z_{120})^{-1}L_2^{-1}H_2(Z_{111})^{-1}L_1^{-1}L_2^{-1}H_1(Z_{021})^{-1}H_2(Z_{012})^{-1}S^{-1} \\ & = & SH_1(Z_{210})SSH_2(Z_{120})SSL_1^{\rm T}SSH_1(Z_{111})SSL_2^{\rm T}SSL_1^{\rm T}SSH_2(Z_{021})SSH_1(Z_{012})SS(-1)^{n-1} \end{array}$$

$$= (-1)^{n-1} S H_1(Z_{210}) H_2(Z_{120}) L_1^{\mathrm{T}} H_1(Z_{111}) L_2^{\mathrm{T}} L_1^{\mathrm{T}} H_2(Z_{021}) H_1(Z_{012})$$

$$= S^{\mathrm{T}} H_1(Z_{210}) H_2(Z_{120}) L_1^{\mathrm{T}} H_1(Z_{111}) L_2^{\mathrm{T}} L_1^{\mathrm{T}} H_2(Z_{021}) H_1(Z_{012}).$$

To obtain normalized quantum transport matrices we expand all entries of classical transport matrix M_i in the sum of monomials $m_j(Z_\alpha)$ and replace all m_j by the corresponding Weyl form ${}^{\bullet}m_j{}^{\bullet}$. For instance, the (1,2)-entry of quantum M_1 becomes

$$(M_1)_{12} = {}^{\bullet}Z_{021}^{-1/3}Z_{102}^{1/3}Z_{111}^{-1/3}Z_{102}^{1/3}Z_{201}^{2/3} {}^{\bullet} + {}^{\bullet}Z_{021}^{-1/3}Z_{102}^{1/3}Z_{111}^{2/3}Z_{102}^{1/3}Z_{201}^{2/3} {}^{\bullet}$$

In Section 2.5 we generalize this construction to non-normalized quantum transport matrices defined for more general class of planar quivers.

Example 2.7. A toy example is the one in which all Z_{α} are the units. Matrix entries then just count numbers of monomials entering the corresponding matrix elements $a_{i,j} \in (-1)^{i+1} \mathbb{Z}_{\geq 0}[[Z_{\alpha}^{\pm 1}]]$. Then, for the M_1 matrix, we have the following representation:

$$M_{1} = \begin{pmatrix} 1 & 2 & 1 \\ -1 & -1 & 0 \\ 1 & 0 & 0 \end{pmatrix}, \quad \begin{pmatrix} 1 & 3 & 3 & 1 \\ -1 & -2 & -1 & 0 \\ 1 & 1 & 0 & 0 \\ -1 & 0 & 0 & 0 \end{pmatrix}, \text{ etc,}$$

$$(2.8)$$

that is, $(M_1)_{ij} = (-1)^{i+1} \binom{n-i}{j}$ for PGL_n . We introduce the antidiagonal unit matrix $|S| = (\delta_{i,n+1-j})_{i,j=1}^n$ (to distinguish it from $S_{ij} = (-1)^{i+1} \delta_{i,n+1-j}$).

For M_2 we have

$$M_2 = M_1^2 = \begin{pmatrix} 0 & 0 & 1 \\ 0 & -1 & -1 \\ 1 & 2 & 1 \end{pmatrix}, \quad \begin{pmatrix} 0 & 0 & 0 & 1 \\ 0 & 0 & -1 & -1 \\ 0 & 1 & 2 & 1 \\ -1 & -3 & -3 & -1 \end{pmatrix}, \text{ etc}$$
 (2.9)

A riddle-thirsty reader can check the following relations between these matrices:

$$M_1^2 = M_2 = (-1)^{n+1} |S| \cdot M_1 \cdot |S|, \quad M_1^3 = (-1)^{n+1} [|S| \cdot M_1]^2 = (-1)^{n+1} I$$

$$M_1^{\mathrm{T}} M_2 = \mathbb{A} = \begin{pmatrix} 1 & 3 & 3 \\ 0 & 1 & 3 \\ 0 & 0 & 1 \end{pmatrix}, \begin{pmatrix} 1 & 4 & 6 & 4 \\ 0 & 1 & 4 & 6 \\ 0 & 0 & 1 & 4 \\ 0 & 0 & 0 & 1 \end{pmatrix}, \text{ etc}$$
 (2.10)

that is
$$(\mathbb{A})_{ij} = \binom{n}{j-i}$$
.

2.5 Quantum transport matrices and Fock-Goncharov coordinates

In this section we describe how quantized transport matrices are expressed in terms of quantized Fock-Goncharov parameters.

Remark 2.8. See [14] for description of quantum algebra of loop functions and [18] for detailed description of quantum cluster algebras and its unitary representations. Non-normalized quantum boundary measurements were introduced in the same way and studied by G.Schrader and A.Shapiro in [40].

In the quantization of $\mathcal{P}_{PGL_n,\Sigma}$ the quantized Fock-Goncharov variables form a quantum torus $\Upsilon^{\frac{1}{n}}$ with commutation relation described by the quiver shown on Fig. 8. Vertices of the quiver label quantum Fock-Goncharov coordinates Z_{α} (we use Greek letters to indicate barycentric labels) while the arrows encode commutation relations: if there are m arrows from vertex α to β then $Z_{\beta}Z_{\alpha} = q^{-2m}Z_{\alpha}Z_{\beta}$. Dashed arrow counts

as m=1/2. In particular, a solid arrow from Z_{α} to Z_{β} implies $Z_{\beta}Z_{\alpha}=q^{-2}Z_{\alpha}Z_{\beta}$, a dashed arrow from Z_{α} to Z_{β} implies $Z_{\beta}Z_{\alpha}=q^{-1}Z_{\alpha}Z_{\beta}$, and, for the future use, a double arrow from Z_{α} to Z_{β} means $Z_{\beta}Z_{\alpha}=q^{-4}Z_{\alpha}Z_{\beta}$. Vertices not connected by an arrow commute.

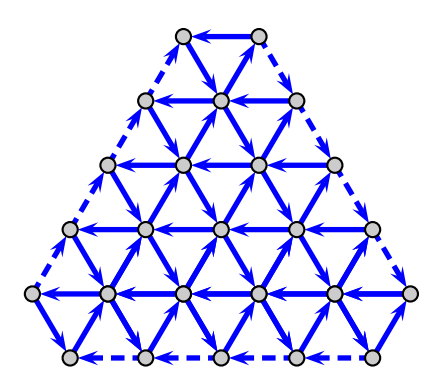


Fig. 8. The quiver of Fock-Goncharov parameters in the triangle $\Sigma_{0,1,3}$ parametrizing $\mathcal{P}_{PGL_6,\Sigma}$; note that the vertices (600), (060), and (006) are excluded.

Consider the following planar oriented graph G in the disk dual to the quiver above. Label vertices on the left, on the right and on the bottom sides from 1 to n as shown on Figure 9. Now barycentric indices label the vertices of the quiver which correspond to the faces of the dual oriented graph. Vertices of the new dual graph are colored black and white depending on whether there are two or one incoming arrows. Faces of G are equipped with q-commuting weights Z_{α} . We add also three face weights $Z_{n,0,0}$, $Z_{0,n,0}$, and $Z_{0,0,n}$ with commutation relations:

$$\begin{split} Z_{n,0,0}Z_{n-1,1,0} &= q^{-1}Z_{n-1,1,0}Z_{n,0,0}, \ Z_{n,0,0}Z_{n-1,0,1} = qZ_{n-1,0,1}Z_{n,0,0} \\ Z_{0,n,0}Z_{1,n-1,0} &= qZ_{1,n-1,0}Z_{0,n,0}, \ Z_{0,n,0}Z_{0,n-1,1} = q^{-1}Z_{0,n-1,1}Z_{0,n,0} \\ Z_{0,0,n}Z_{1,0,n-1} &= q^{-1}Z_{1,0,n-1}Z_{0,0,n}, \ Z_{0,0,n}Z_{0,1,n-1} = qZ_{0,1,n-1}Z_{0,0,n} \end{split}$$

All the remaining variables not explicitly mentioned above commute with $Z_{n,0,0}, Z_{0,n,0}, Z_{0,0,n}$.

Any maximal oriented path in the dual graph connects a vertex on the right side 1-2 of the triangle either with a vertex of the left side 1-3 or with a vertex on the bottom side 2-3. We assign to every oriented path $\pi: j \leadsto i'$ from the right side to the left side or to the bottom side $\pi: j \leadsto i''$ the quantum weight

$$w(\pi) = \prod_{\substack{\text{face } \alpha \text{ lies to the} \\ \text{right of the path } \pi}} Z_{\alpha}$$

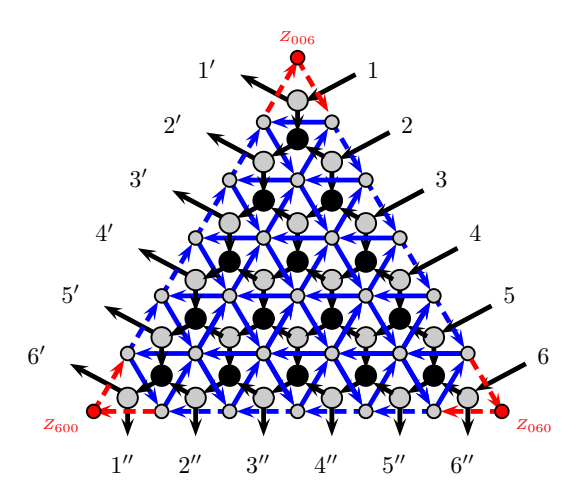


Fig. 9. The plabic graph G dual to the quiver of Fock-Goncharov parameters for $\mathcal{P}_{PGL_6,\Sigma_{0,1,3}}$. Face weights $Z_{600}, Z_{060}, Z_{006}$ (colored red) are added forming extended PGL_6 -quiver.

Definition 2.9. We define two $n \times n$ non-normalized quantum transition matrices

$$(\mathcal{M}_1)_{ij} = \sum_{\substack{\text{directed path } \pi: j \sim i'\\ \text{from right to left}}} w(\pi) \quad \text{and} \quad (\mathcal{M}_2)_{i,j} = \sum_{\substack{\text{directed path } \pi: j \sim i''\\ \text{from right to bottom}}} w(\pi).$$

Note that each \mathcal{M}_1 is a lower-triangular matrix and \mathcal{M}_2 is an upper-triangular matrix.

In section 7 we generalize this definition. Let Γ be a planar oriented graph in the rectangle with no sources or sinks inside (see Fig 36), m univalent boundary sinks on the left labeled 1 to m top to bottom and n univalent boundary sources on the right labelled 1 to n top to bottom. All arcs of Γ are oriented right to left, in particular, G has no oriented cycles. Note that this condition is in particular satisfied by the plabic graph G (see Fig 9) considered as a graph with n sources and 2n sinks. Indeed, we can redraw G in a rectangle such that the right side of the triangle becomes the right vertical side of the rectangle while union of the left and the bottom sides becomes the left side of the triangle.

Faces of Γ are equipped with q-commuting weights Z_{α} whose commutation relations are governed by the plabic graph (see Section 7 for details). In the same way as for the case of triangle shown in Figure 9, we define weight of the maximal oriented path π from a source a to a sink b in Γ as

$$w(\pi) = \prod_{\substack{\text{face } \alpha \text{ lies to the} \\ \text{right of the path } \pi}} Z_{\alpha} . \tag{2.11}$$

Then, for all $1 \le a \le m, \ 1 \le b \le n$ the entry (a,b) of a $m \times n$ non-normalized transport matrix is given by the formula

$$[\mathcal{M}]_{ab} = \sum_{\text{directed path } \pi: b \leadsto a} w(\pi). \tag{2.12}$$

Lemma 7.16 implies that the matrix \mathcal{M} satisfies the quantum R-matrix relation $\mathcal{R}_m(q) \stackrel{1}{\mathcal{M}} \otimes \stackrel{2}{\mathcal{M}} = \stackrel{2}{\mathcal{M}} \otimes \stackrel{1}{\mathcal{M}} \mathcal{R}_n(q)$, where $\mathcal{R}_k(q)$ is a $k^2 \times k^2$ matrix

$$\mathcal{R}_{k}(q) = \sum_{1 \leq i, j \leq k} \stackrel{1}{e}_{ii} \otimes \stackrel{2}{e}_{jj} + (q-1) \sum_{1 \leq i \leq k} \stackrel{1}{e}_{ii} \otimes \stackrel{2}{e}_{ii} + (q-q^{-1}) \sum_{1 \leq j < i \leq k} \stackrel{1}{e}_{ij} \otimes \stackrel{2}{e}_{ji}$$
(2.13)

Here, the superindices 1 and 2 means the order of spaces in the tensor product (1 means the left factor, 2 means the right one) while the order of spaces means the order of factors in the each coordinate of the tensor

product. For instance,
$$\begin{pmatrix} a \\ b \end{pmatrix} \otimes \begin{pmatrix} c^2 d \end{pmatrix} = \begin{pmatrix} ac & ad \\ bc & bd \end{pmatrix}$$
 while $\begin{pmatrix} c^2 d \end{pmatrix} \otimes \begin{pmatrix} a \\ b \end{pmatrix} = \begin{pmatrix} ca & da \\ cb & db \end{pmatrix}$.

Note that \mathcal{R}_k has the following properties

$$\mathcal{R}_k^{-1}(q) = \mathcal{R}_k(q^{-1}), \qquad \mathcal{R}_k(q) - \mathcal{R}_k^{\mathrm{T}}(q^{-1}) = (q - q^{-1})P_k,$$
 (2.14)

where P_k is the standard permutation matrix $P_k := \sum_{1 \leq i,j \leq k} \stackrel{1}{e_{ij}} \otimes \stackrel{2}{e_{ji}}$. Note that the total transposition of $\mathcal{R}_k(q)$ results in interchanging the space labels $1 \leftrightarrow 2$. In Sec. 8 we show that this algebra remains valid also in the case of a planar directed network with loops.

In Fig. 9 we have an example of a directed network with 6 sources and 12 sinks. Adding face weights Z_{600} , Z_{060} , Z_{060} supplied with "natural" commutation relations $Z_{600}Z_{501} = qZ_{501}Z_{600}$ and $Z_{600}Z_{510} = q^{-1}Z_{510}Z_{600}$, etc., we obtain extended PGL_6 -quiver and graph Γ in the rectangle with n=6 sources and 2n=12 sinks; then \mathcal{M} has a block matrix form $\mathcal{M}=\begin{pmatrix} \mathcal{M}_1\\ \mathcal{M}_2 \end{pmatrix}$ in which we let \mathcal{M}_1 be the upper $n\times n$ block and \mathcal{M}_2 be the lower $n\times n$ block. We want to show that Lemma 7.16 implies the following commutation relations for \mathcal{M}_1 and \mathcal{M}_2 :

$$\mathcal{R}_n(q)\overset{1}{\mathcal{M}}_i \otimes \overset{2}{\mathcal{M}}_i = \overset{2}{\mathcal{M}}_i \otimes \overset{1}{\mathcal{M}}_i \mathcal{R}_n(q), \quad i = 1, 2, \tag{2.15}$$

and

$$\stackrel{1}{\mathcal{M}}_{1} \otimes \stackrel{2}{\mathcal{M}}_{2} = \stackrel{2}{\mathcal{M}}_{2} \otimes \stackrel{1}{\mathcal{M}}_{1} \mathcal{R}_{n}(q).$$
(2.16)

Let now indices i, j run from 1 to n. We rewrite the above matrix $\mathcal{R}_{2n}(q)$ as

$$\mathcal{R}_{2n}(q) = \sum_{1 \le i,j \le n} \frac{1}{e_{ii}} \otimes \frac{2}{e_{jj}} + (q-1) \sum_{1 \le i \le n} \frac{1}{e_{ii}} \otimes \frac{2}{e_{ii}} + (q-q^{-1}) \sum_{1 \le j < i \le n} \frac{1}{e_{ij}} \otimes \frac{2}{e_{ji}}$$

$$+ \sum_{1 \le i,j \le n} \frac{1}{e_{n+i,n+i}} \otimes \frac{2}{e_{n+j,n+j}} + (q-1) \sum_{1 \le i \le n} \frac{1}{e_{n+i,n+i}} \otimes \frac{2}{e_{n+i,n+i}}$$

$$+ (q-q^{-1}) \sum_{1 \le j < i \le n} \frac{1}{e_{n+i,n+j}} \otimes \frac{2}{e_{n+j,n+i}}$$

$$+ \sum_{1 \le i,j \le n} \frac{1}{e_{i+i}} \otimes \frac{2}{e_{n+j,n+j}}$$

$$+ \sum_{1 \le i,j \le n} \frac{1}{e_{n+i,n+i}} \otimes \frac{2}{e_{j,j}} + (q-q^{-1}) \sum_{1 \le i,j \le n} \frac{1}{e_{n+i,j}} \otimes \frac{2}{e_{j,n+i}}$$

In the first two lines we immediately recognize $\mathcal{R}_n(q)$ in two diagonal $n \times n$ blocks of $\mathcal{R}_{2n}(q)$: the relations for the pair of first indices (i,j) and (n+i,n+j) generate (2.15) for \mathcal{M}_1 and \mathcal{M}_2 respectively; setting (i,n+j), which corresponds to the fourth line, we obtain just a unit matrix in the left-hand side thus producing relation (2.16), whereas in the case (n+i,j) (the fifth line), we have the equation

$$\mathring{\mathcal{M}}_2 \otimes \mathring{\mathcal{M}}_1 + (q - q^{-1}) P_n \mathring{\mathcal{M}}_1 \otimes \mathring{\mathcal{M}}_2 = \mathring{\mathcal{M}}_1 \otimes \mathring{\mathcal{M}}_2 \mathcal{R}_n(q).$$

We first push the permutation operator P_n through the \mathcal{M} -matrix product interchanging the labels of spaces in the tensor product and then use the identity $(q-q^{-1})P_n = \mathcal{R}_n(q) - \mathcal{R}_n^{\mathrm{T}}(q^{-1})$ obtaining

$$\mathring{\mathcal{M}}_2 \otimes \mathring{\mathcal{M}}_1 + \mathring{\mathcal{M}}_1 \otimes \mathring{\mathcal{M}}_2(\mathcal{R}_n(q) - \mathcal{R}_n^{\mathrm{T}}(q^{-1})) = \mathring{\mathcal{M}}_1 \otimes \mathring{\mathcal{M}}_2 \mathcal{R}_n(q),$$

or

$$\overset{1}{\mathcal{M}}_{2} \otimes \overset{2}{\mathcal{M}}_{1} = \overset{2}{\mathcal{M}}_{1} \otimes \overset{1}{\mathcal{M}}_{2} \mathcal{R}_{n}^{\mathrm{T}}(q^{-1}),$$

which is just another form of writing relation (2.16). This accomplishes the proof of relations 2.15 and 2.16. Now, in order to eliminate extra variables $Z_{n,0,0}$, $Z_{0,n,0}$ and $Z_{0,0,n}$ we normalize the matrices \mathcal{M}_i , i=1,2 by multiplying them by corresponding special functions. Namely, we multiply the matrix \mathcal{M}_1 by D_1^{-1} , where $D_1 = \prod_{k=1}^n \left[\prod_{i+j=n-k} \left[Z_{i,j,k}\right]^{k/n}\right]^{\bullet}$ is the quantum function (6.10) commuting with all elements of \mathcal{M}_1 . Note that, $Z_{0,0,n}$ commutes with D_1 and all entries of \mathcal{M}_1 . Moreover, $Z_{0,0,n}$ enters in the first power into all monomial summands of any matrix entry of \mathcal{M}_1 and also into D_1 . Therefore we conclude that any entry of $D_1^{-1}\mathcal{M}_1$ is independent of $Z_{0,0,n}$. Similarly, we multiply \mathcal{M}_2 by $D_1^{-1}D_2^{-1}$ where $D_2 = \tau^2 D_1$ is the similar element that starts with the variable $Z_{n,0,0}$. These multiplications preserve the form of relations (2.15) and their only effect on (2.15) is the appearance of the constant factor in the R-matrix in the right-hand side (this is because D_1 commutes with \mathcal{M}_1 , and ${}^{\bullet}D_1^{-1}D_2^{-1}{}^{\bullet}$ commutes with \mathcal{M}_2 ; only D_1 and D_2 do not commute. We now define the *normalized quantum transport* matrices of the *standard PGL_n-quiver*:

Definition 2.10. Normalized quantum transport matrices for the quantum space $\mathcal{P}_{PGL_n,\Sigma}$ are defined by the following expressions

$$T_1 = QS\mathcal{M}_1D_1^{-1}, T_2 = \tau(T_1) \text{ and } T_3 = \tau^2(T_1)$$

$$M_1 = T_1 = QS\mathcal{M}_1D_1^{-1}, M_2 = (T_2)^{-1} = QS\mathcal{M}_2 • D_1^{-1}D_2^{-1} • \text{ and } M_3 = T_3$$

where $Q = \text{diag}\{q^{\frac{1-n}{2n}-j+1}\}_{j=[1,n]}$ and S is defined in 2.4. They are quantizations of the classical normalized transport matrices 2.2. Abusing notations, we use T_i and M_i for both classical and quantum normalized transport matrices.

Remark 2.11. Since D_1 commutes with any Z_{α} entering \mathcal{M}_1 we have $QS\mathcal{M}_1D_1^{-1} = QS^{\bullet}\mathcal{M}_1D_1^{-1}$. Similarly, $QS\mathcal{M}_2 \bullet D_1^{-1} D_2^{-1} \bullet = QS \bullet \mathcal{M}_2 D_1^{-1} D_2^{-1} \bullet .$

Entries of M_i are neither Weyl-ordered symmetric operators nor they are positive definite. We can note however that each entry of M_i is a symmetric positive-definite operator multiplied by $\pm q^{\alpha}$ with a rational α .

Note that

$$\overset{1}{Q}\otimes\overset{2}{Q}\mathcal{R}_n(q)=\mathcal{R}_n(q)\overset{1}{Q}\otimes\overset{2}{Q}$$
 for any diagonal matrix Q

or taking transposition and noting that $\stackrel{1}{Q} \otimes \stackrel{2}{Q}$ is invariant under transposition

$$\overset{1}{Q} \otimes \overset{2}{Q} \mathcal{R}_n^{\mathrm{T}}(q) = \mathcal{R}_n^{\mathrm{T}}(q) \overset{1}{Q} \otimes \overset{2}{Q}$$

and

$$\overset{1}{S} \otimes \overset{2}{S} \mathcal{R}_n(q) = \mathcal{R}_n^{\mathrm{T}}(q) \overset{1}{S} \otimes \overset{2}{S}$$
 for any antidiagonal matrix S .

We have therefore proved the following theorem.

Theorem 2.12. The normalized quantum transport matrices M_1 and M_2 (see Definition 2.10) satisfy the relations

$$R_n^{\mathrm{T}}(q) \stackrel{1}{M}_i \otimes \stackrel{2}{M}_i = \stackrel{2}{M}_i \otimes \stackrel{1}{M}_i R_n(q), \quad i = 1, 2, \dots$$

$$\stackrel{1}{M}_1 \otimes \stackrel{2}{M}_2 = \stackrel{2}{M}_2 \otimes \stackrel{1}{M}_1 R_n(q)$$

where

$$R_n(q) = q^{-1/n} \left[\sum_{i,j} \frac{1}{e_{ii}} \otimes e_{jj}^2 + (q-1) \sum_{i} \frac{1}{e_{ii}} \otimes e_{ii}^2 + (q-q^{-1}) \sum_{i>j} \frac{1}{e_{ij}} \otimes e_{ji}^2 \right]$$
(2.17)

is the quantum trigonometric R-matrix

Remark 2.13. Relations 2.15 and 2.16 and Theorem 2.12 were independently proved by G.Schrader and A.Shapiro [41].

Theorem 2.14. The normalized quantum transport matrices T_i (see Definition 2.10) satisfy the quantum groupoid relation

$$T_1T_2T_3 = \operatorname{Id}$$
.

Remark 2.15. Recalling $M_1 = T_1$, $M_2 = T_2^{-1}$, $M_3 = T_3$ we have

$$M_3M_1=M_2.$$

Proof. The product $(QS)^{-1}T_3T_1$ is given by the following double sum over directed paths:

$$[(QS)^{-1}T_3T_1]_{ij} = \sum_{k=1}^n (-1)^k q^{\frac{1-n}{2n}-k+1} \sum_{\text{paths } k \to i} : \prod Z_\alpha : (\tau^2(D_1))^{-1} \sum_{\text{paths } j \to k} : \prod Z_\beta : D_1^{-1}, \tag{2.18}$$

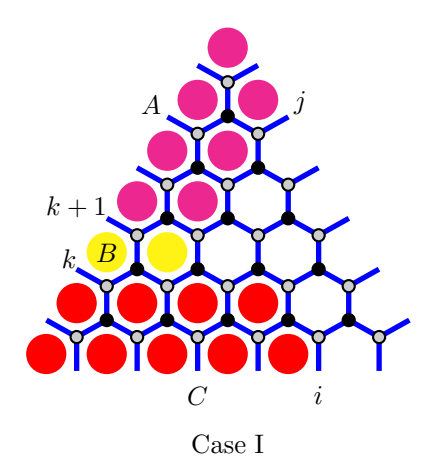
where the second sum is taken over all oriented path connecting vertex j to k (see Figure "Case I" below) where orientations of edges are shown in the Figure 9 while orientations of all non-vertical edges in the first sum are reversed compared to the Figure 9 and $\tau^2(D_1) = D_2$.

Recall again that D_1 commutes with all elements of \mathcal{M}_1 . Therefore, (2.18) equals

$$D_2^{-1} \sum_{k=1}^n (-1)^{k-1} q^{\frac{1-n}{2n} - k + 1} \sum_{\text{paths } k \to i} \prod_{j \to k} Z_{\alpha} \sum_{\text{paths } j \to k} \prod_{j \to k} Z_{\beta} D_1^{-1}$$
(2.19)

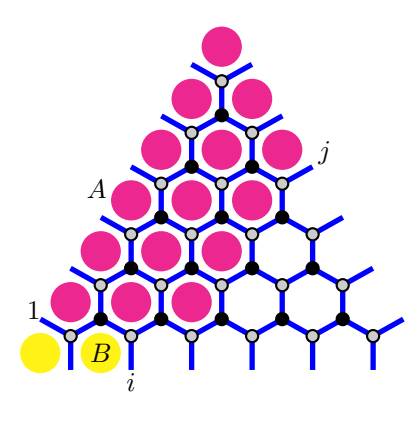
We now consider the pattern in the figure below. We do not indicate arrows on edges recalling that all paths in T_1 go from right to left and from top to bottom whereas all paths in T_3 go from left to right and from top to bottom. A continuous consecutive sequence of edges either directed alternatingly to the left downwards and to the left upwards or directed alternatingly to the right downwards and to the right upwards (located on the same horizontal level) and attached to the left side of triangle of hexagons in Fig. Case I is called a horizontal leg (see, for example, the interval of top (or bottom) edges of yellow hexagons B in Fig. Case I).

Two paths: $j \to k$ from T_1 and $k \to i$ from T_3 share the common horizontal leg; if we remove this leg then the remaining part of the union of $j \to k$ and $k \to i$ is a path that first goes from right to left and top to bottom, then (in a general Case I) has the leftmost vertical edge, then goes from left to right and top to bottom. In a very special Case II, the path does not have the last part; this happens only for k=1 and only if the last horizontal part of the path $j \to k = 1$ is strictly longer than the shared horizontal leg



In Case I, given a path $j \to k$ encompassing the regions A and B and a path $k \to i$ encompassing the region C we have the corresponding path $j \to k+1$ encompassing the regions A and the path $k+1 \to i$ encompassing the regions B and C. These pairs of paths are in bijection being the only two possible combinations of paths having the same union of domains $A \cup B \cup C$. Contributions from these two pairs of paths have opposite signs and since commutation relations and definition of normal ordering imply ${}^{\bullet}CB^{\bullet} = q^{\frac{1}{2}} {}^{\bullet}C^{\bullet\bullet}B^{\bullet}$ and ${}^{\bullet}BA^{\bullet} = q^{-\frac{1}{2}} {}^{\bullet}B^{\bullet\bullet}A^{\bullet}$ we obtain $CB^{\bullet,A} = q C^{\bullet,B}A^{\bullet}$ and these contributions are mutually canceled in the sum (2.18).

The only pairs of paths $(j \to k+1, k+1 \to i)$ that do not have counterparts are those for which the region C is absent (Case II):



Case II

In this case, ${}^{\bullet}B^{\bullet}$ commutes with ${}^{\bullet}A^{\bullet}$ and therefore ${}^{\bullet}B^{\bullet}A^{\bullet}={}^{\bullet}BA^{\bullet}$, k is necessarily equal to 1, and after removing the common leg, all these pairs of paths are in bijection with single paths going from right to left and top to bottom and encompassing the regions A and B; note that these paths are exactly paths constituting the matrix M_2 . So the sum in (2.19) just gives

$$q^{\frac{1}{2n}}D_2^{-1}\left(\sum_{\text{paths }j\to i} \Box Z_{\alpha}\right) D_1^{-1}$$

$$(2.20)$$

Note that the weight w(P) of any path P from j to i is a monomial which contains only one variable Z_{00n} not commuting with D_2^{-1} . Therefore, $D_2^{-1}w(P) = q^{2\langle D_2^{-1}, w(P) \rangle}w(P)D_2^{-1} = q^{-\frac{1}{n}}w(P)D_2^{-1}$. Since the same

commutation relation holds for any path weight, it holds for their sum also and we rewrite (2.20) as

$$q^{-\frac{1}{2n}} \left(\sum_{\text{paths } j \to i} \mathbf{1} \prod Z_{\alpha} \right) D_2^{-1} D_1^{-1} = \left(\sum_{\text{paths } j \to i} \mathbf{1} \prod Z_{\alpha} \right) \mathbf{1} D_2^{-1} D_1^{-1} = \sum_{\text{paths } j \to i} \mathbf{1} \left(\prod Z_{\alpha} \right) D_2^{-1} D_1^{-1}$$
(2.21)

because $D_2^{-1}D_1^{-1} = q^{\frac{1}{2n}} D_2^{-1}D_1^{-1}$ and $D_2^{-1}D_1^{-1}$ commutes with any $\prod Z_{\alpha}$ from the sum. The right hand side of (2.21) coincides with the corresponding element of M_2 (after multiplication of both sides by QS on the left). We have therefore proved that $T_3T_1=M_2 \;\; \Box$

Note that we shall present in §7.2 the second proof of the groupoid property using quantum Grassmannian.

Remark 2.16. The semiclassical limit of Theorem 2.12 statement reads

$$\{ \stackrel{1}{M}_{1} \otimes \stackrel{2}{M}_{2} \} = \stackrel{2}{M}_{2} \otimes \stackrel{1}{M}_{1} \left(-\frac{1}{n} \stackrel{1}{I} \otimes \stackrel{2}{I} + r_{n} \right)$$

where

$$r_n = \sum_{i} e_{ii}^1 \otimes e_{ii}^2 + 2 \sum_{i>j} e_{ij}^1 \otimes e_{ji}^2$$
 (2.22)

is the semiclassical r-matrix. Equivalently,

$$\{(M_1)_{ab}, (M_2)_{cd}\} = -\frac{1}{n}(M_1)_{ab}(M_2)_{cd} + (M_1)_{ad}(M_2)_{cb}\theta(b-d), \quad \theta(x) = \begin{cases} 2, & \text{if } x > 0, \\ 1, & \text{if } x = 0, \\ 0, & \text{if } x < 0. \end{cases}$$

Remark 2.17. For the trigonometric R-matrix (2.17) the quantum relation

$$R_n^T(q)\stackrel{1}{M}_i\otimes \stackrel{2}{M}_i = \stackrel{2}{M}_i\otimes \stackrel{1}{M}_iR_n(q)$$

has an equivalent form of writing

$$\stackrel{1}{M}_{i} \otimes \stackrel{2}{M}_{i} R_{n}^{T}(q) = R_{n}(q) \stackrel{2}{M}_{i} \otimes \stackrel{1}{M}_{i} \text{ for } i = 1, 2.$$

Both these relations generate the same quantum algebra on elements of the matrices M_1 and M_2 and have the same semiclassical limit

$$\{(M_i)_{ab}, (M_i)_{cd}\} = (M_i)_{ad}(M_i)_{cb}(\theta(b-d) - \theta(a-c)) \quad i = 1, 2, \ \theta(x) = \begin{cases} 2, & \text{if } x > 0, \\ 1, & \text{if } x = 0, \\ 0, & \text{if } x < 0. \end{cases}$$

Example 2.18. For n=3 transport matrices are computed in Example 2.6. Direct computations show

$$\stackrel{1}{M_1} \otimes \stackrel{2}{M_2} = \stackrel{2}{M_2} \otimes \stackrel{1}{M_1} R_3(q),$$

where

$$R_3(q) = q^{-1/3} \begin{pmatrix} q & 0 & 0 & 0 & 0 & 0 & 0 & 0 & 0 \\ 0 & 1 & 0 & 0 & 0 & 0 & 0 & 0 & 0 \\ 0 & 0 & 1 & 0 & 0 & 0 & 0 & 0 & 0 \\ \hline 0 & q - q^{-1} & 0 & 1 & 0 & 0 & 0 & 0 & 0 \\ 0 & 0 & 0 & 0 & q & 0 & 0 & 0 & 0 \\ 0 & 0 & 0 & 0 & 0 & 1 & 0 & 0 & 0 \\ \hline 0 & 0 & 0 & 0 & 0 & 0 & 1 & 0 & 0 \\ 0 & 0 & 0 & 0 & 0 & q - q^{-1} & 0 & 1 & 0 \\ 0 & 0 & 0 & 0 & 0 & 0 & 0 & 0 & q \end{pmatrix}$$

Similarly, for both i = 1, 2, we have $R_3^T(q)M_i \otimes M_i = M_i \otimes M_i R_3(q)$. Direct computations show that in this example Theorem 2.14 also holds

Goldman brackets and commutation relations between transport matrices

To obtain a full-dimensional (without zero entries) form of transport matrices we define transport matrices along more general paths.

Namely, let $\mathbb{O} = (O, \mathbb{M})$ be a disk O with four marked boundary points $\mathbb{M} = \{A, B, D, C\}$ in clockwise order, $(\Delta ABC, \Delta BCD)$ be a triangulation of O and we also assume clockwise orientation of all triangle sides inside every triangle. The space $\mathcal{P}_{PGL_n,\mathbb{O}}$ coincides with the space of quadruple of complete flags (one flag assigned to each marked point) and pinnings (one pinning for every interval of \mathbb{O} between marked points.

A snake inside a triangle determines a projective basis as explained above. Each oriented side of triangulation determines such a snake and a corresponding projective basis in \mathbb{C}^n . Fix a clockwise orientation of both triangles. We use the following agreement: if a side of a triangulation is common for two adjacent triangles then the orientation of a side determines one adjacent triangle whose orientation is compatible with the orientation of the side. For instance, the oriented side BC determines the unique snake from B to C inside triangle $\triangle ABC$, while the side CB is associated with the snake from C to B inside triangle ΔBCD , with corresponding projective basis chosen in each case.

Subtriangulation of $\mathbb O$ has n-1 nodes p_1,\ldots,p_{n-1} on the side BC and we denote the corresponding Fock-Goncharov parameters by Z_{p_j} . Factor every Z_{p_j} into a product $Z_{p_j}=Z_{p_j}^{\Delta ABC}\cdot Z_{p_j}^{\Delta BCD}$. Parameters $Z_{p_j}^{\Delta ABC}$ define a pinning of the side BC in the triangle ΔABC while parameters $Z_{p_j}^{\Delta BCD}$ define a pinning of the side CB in the triangle ΔBCD .

Gluing sides of two distinct triangles and multiplying corresponding parameters is called in [26] an amalgamation procedure. By an amalgamation procedure, the transition matrix $\hat{T}_{BC\leftarrow CB}$ from basis \mathbf{b}_{CB} to \mathbf{b}_{BC} is the product $\widehat{T}_{BC \leftarrow CB} = H_{in}^{BC} \cdot S \cdot H_{out}^{CB}$ where $H_{in}^{BC}(H_{out}^{CB})$ are diagonal matrices defined in terms of the Fock-Goncharov parameters on the side BC (CB, correspondingly) by Formula 2.5(2.4) and S is introduced in Definition 2.4. This allows to define transport matrix for any pair of oriented sides as transition matrix for the pair of corresponding bases; the matrix S acts by changing the orientation of the corresponding side. Let $\widehat{T}_{BC\leftarrow AB}$ be a transport in $\triangle ABC$ from side AB to \widehat{BC} . Pay attention that the sides are oriented and the order of endpoints in side notation matters. Similarly, $\hat{T}_{CB\leftarrow DC}$ is a transport matrix in ΔBCD from DC to CB. Note that $\hat{T}_{DC\leftarrow CB} = \hat{T}_{CB\leftarrow DC}^{-1}$. Then, we define a transport $\hat{T}_{DC\leftarrow AB}$ from AB to DC as $\hat{T}_{DC\leftarrow AB} = \hat{T}_{DC\leftarrow CB}\hat{T}_{CB\leftarrow BC}\hat{T}_{BC\leftarrow AB} = \hat{T}_{CB\leftarrow DC}\hat{T}_{CB\leftarrow BC}\hat{T}_{BC\leftarrow AB}$. Similarly, $\hat{T}_{BD\leftarrow AB} = \hat{T}_{BD\leftarrow CB}\hat{T}_{CB\leftarrow BC}\hat{T}_{BC\leftarrow AB}$.

Finally, to obtain transport matrix $T_{CD\leftarrow BA}$ from one boundary interval BA to another boundary interval CD we need to precompose and postcompose $T_{CD\leftarrow BA}$ with diagonal matrices determined by the pinnings on boundary intervals BA and CD, $T_{CD\leftarrow BA} = H_{out}^{CD} \hat{T}_{CD\leftarrow BA} H_{in}^{BA}$.

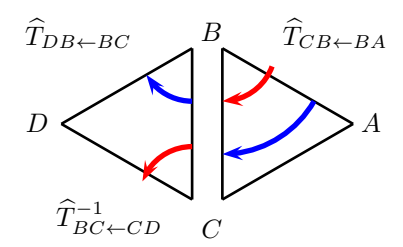


Fig. 10. Disk with four marked points.

To describe the quantum case, we split each quantum Fock-Goncharov parameter (or quantum cluster parameter) on the side BC into a product of two, one inside triangle $\triangle ABC$ the other inside triangle $\triangle BCD$. The quantum parameters in triangle $\triangle ABC$ commute with those of triangle $\triangle BCD$, so the product of two Weyl-ordered monomials is itself a Weyl-ordered monomial, in which we perform an amalgamation of variables on the side BC. Due to the double action of the matrix S, the amalgamation of boundary (frozen) variables in neighbor triangles respects the surface orientation, so, we amalgamate pairwise variables on the sides BC of the two triangles ordered in the same direction, from B to C. After the amalgamation, we unfreeze the obtained new variables. Therefore, in a network on a surface obtained as a union of several triangles, the Weyl ordering of weights of any path that does not go through any given triangle more than once is the product of Weyl orderings of weights inside each triangle.

It was explicitly demonstrated in Proposition 4.2 of [40] that the elements of non-normalized quantum transport matrices defined by such Weyl ordering are preserved by a special type of quantum mutations at a 4-valent quiver vertex with alternating incoming and outgoing arrows (we include mutations of amalgamated variables as well as mutations of variables in the interior of triangles). This implies, in particular, that the corresponding normalizing factor stays invariant. Let us explain this in more details on the example of an PGL_3 parallelogram composed out of two extended PGL_3 -quivers. We perform the chain of mutations and in the Figure 11 we paint black the quiver vertices at which mutations occur at the given step; if the corresponding mutations commute (for vertices not connected by an edge) then, for the brevity of presentation, we perform the corresponding mutations simultaneously; dotted lines indicate splitting into triangles in the original and resulting quivers:

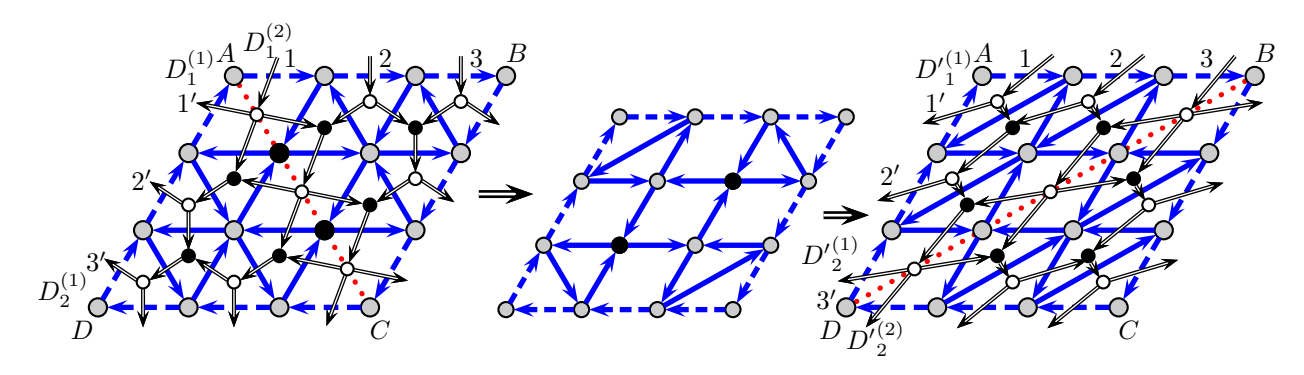


Fig. 11. The chain of mutations that leads to a flip of triangulation

We perform mutations for non-normalized cluster variables and the corresponding transport matrices. Note, for example, that frozen variables at the corners of the parallelogram are not changed by this sequence of mutations, likewise all elements of a non-normalized transport matrix since all mutations correspond to Postnikov's moves of type M1.

In the first and last quivers we indicate by double directed arrows the dual networks defining the corresponding transport matrices $T_{i',j}$. Since all cluster mutations correspond to Postnikov's moves of type M1, elements of these transport matrices remain invariant under each move/mutation.

According to [40], for any planar acyclic network, defining quantum non-normalized transport matrix elements $(\widehat{T}_{DA\leftarrow AB})_{i',j}$ by formula (2.12) (see also, Fig. 10), all these elements are preserved by Postnikov moves of type M1; these moves correspond to mutations of cluster variables at four-valent vertices.

Consider a network and the dual quiver amalgamated from two GL_n (nonnormalized) Fock–Goncharov networks with the corresponding transport matrices $\mathcal{M}_1^{(1)}$ and $\mathcal{M}_1^{(2)}$. The total non-normalized transport matrix is then $\widehat{T}_{DA\leftarrow AB}=\mathcal{M}_1^{(1)}\mathcal{M}_1^{(2)}$. We now normalize each $\mathcal{M}_1^{(i)}$, i=1,2, by $D_1^{(i)}$ and consider the product of normalized matrices. Using the fact that all matrix elements of both $\mathcal{M}_1^{(1)}$ and $\mathcal{M}_1^{(2)}$ commute with both $D_1^{(1)}$ and $D_1^{(2)}$ we observe that

$$[D_1^{(1)}]^{-1} \mathcal{M}_1^{(1)} [D_1^{(2)}]^{-1} \mathcal{M}_1^{(2)} = [D_1^{(1)} D_1^{(2)}]^{-1} T.$$

All quantum transport matrix elements of the network T' obtained after a sequence of mutations/M1 Postnikov moves coincide with the corresponding matrix elements in the network T before normalization,

$$T'_{i',j} = \mathcal{M}'_1 = T_{i',j}.$$

We do not mutate the normalizing factor; we compute the normalization factor for T' obtained after the complete sequence of mutations corresponding to a MCG transformation and compare it with the the normalizing factors in the original network.

The normalizing factor for T' is $D_1'^{(1)}$ (as in the previous case, all $T'_{i',j}$ commute with $D_1'^{(1)}$. It therefore remains only to show that

$$D_1^{\prime(1)} = D_1^{(1)} D_1^{(2)}$$

Consider $[D_1^{\prime(1)}]^n$ and $[D_1^{(1)}D_1^{(2)}]^n$. Both expressions are Weyl-ordered products of integer powers of $T_{i',i}$ —the diagonal elements of the transport matrices. All these diagonal elements are monomials in cluster variables

being therefore automatically positive-definite, and their fractional powers are the corresponding products of fractional powers of Z-variables. Since all Z-variables have homogeneous commutation relations, the only possible mismatch between $D_1^{\prime(1)}$ and $D_1^{(1)}D_1^{(2)}$ could be a power of q, but since both expressions, being Weyl-ordered, are self-adjoint and $q^{\alpha\star}=q^{-\alpha}$, $\alpha=0$ and we come to the desired equality.

The matrix $T_{i',j}$ is lower-triangular in the first and in the last quiver, and its determinant, which is the product of elements $T_{i',i}$, is equal $\left(D_1^{(1)}D_1^{(2)}\right)^n$ in the left quiver and is equal $D_1^{(1)}$ in the right quiver. So, we have that $\left(D_1^{(1)}D_1^{(2)}\right)^n = \left(D_1^{(1)}\right)^n$. It implies $D_1^{(1)}D_1^{(2)} = D_1^{(1)}$ because all operators in the last equality are positive definite self-adjoint. We similarly obtain the second relation $D_1^{(2)} = D_2^{\prime(1)}D_2^{\prime(2)}$, so all elements of the corresponding normalized transport matrices are preserved by flips of "big" triangles.

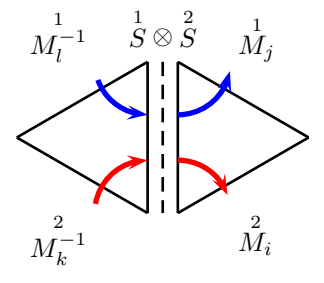
We now show that the commutation relations from Theorem 2.12 together with the groupoid condition (Theorem 2.14) imply the commutativity relations and Goldman brackets.

Theorem 3.1. Consider a triangle decomposition of any surface $\Sigma_{g,s,n}$. Then for two normalized quantum transport matrices $T_{1,3}$ and $T_{2,4}$ corresponding to graph-simple paths in this triangle decomposition with distinct starting edges ("windows") 1,2,3,4 and such that paths $1 \rightarrow 3$ and $2 \rightarrow 4$ has a single intersection, commutation relations of Theorem 2.12 induce the quantum Goldman relation

$$q^{-1/n}T_{1,3}T_{2,4} - q^{1/n}T_{2,4}T_{1,3} = (q^{-1} - q)T_{1,4}T_{2,3},$$

where the quantum transport matrices $T_{1,4}$ and $T_{2,3}$ correspond to disjoint paths obtained by a natural resolution of the intersection; moreover, $T_{1,4}$ and $T_{2,3}$ mutually commute.

Proof. We begin with the pattern in the figure below. In both (left and right) triangles the dashed line plays the role of side 2-3 in Fig. 6.



We use the identities

$$M_{l}^{-1} \otimes M_{k}^{-1} = R_{n}(q)M_{k}^{-1} \otimes M_{l}^{-1}$$

$$M_{j}^{-1} \otimes M_{i}^{-1} = M_{i} \otimes M_{j} (R_{n}^{-1}(q))^{T}$$

$$R_{n}(q)S \otimes S = S \otimes SR_{n}^{T}(q),$$

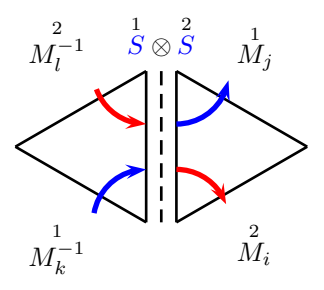
where the last identity holds for any antidiagonal matrix S whose elements commutes with all elements of quantum torus.

We then have

$$\begin{split} & [\overset{1}{M_{j}}\overset{1}{S}\overset{1}{M_{l}^{-1}}] \otimes [\overset{2}{M_{i}}\overset{2}{S}\overset{2}{M_{k}^{-1}}] = \overset{2}{M_{i}} \otimes \overset{1}{M_{j}} \left(R_{n}^{-1}(q)\right)^{\mathrm{T}}\overset{1}{S} \otimes \overset{2}{S}R_{n}(q)\overset{2}{M_{k}^{-1}} \otimes \overset{1}{M_{l}^{-1}} \\ = & \overset{2}{M_{i}} \otimes \overset{1}{M_{j}}\overset{1}{S} \otimes \overset{2}{S}R_{n}^{-1}(q)R_{n}(q)\overset{2}{M_{k}^{-1}} \otimes \overset{1}{M_{l}^{-1}} = [\overset{2}{M_{i}}\overset{2}{S}\overset{2}{M_{k}^{-1}}] \otimes [\overset{1}{M_{j}}\overset{1}{S}\overset{1}{M_{l}^{-1}}], \end{split}$$

so two transport matrices corresponding to nonintersecting paths commute. This is consistent with the quantum mapping class group transformations: flipping BC edge separates the paths $AB \to BD$ and $AC \to CD$ into two adjacent triangles.

Consider now the case of two *intersecting* paths (we consider a single intersection inside a quadrangle).



We then have

$$\begin{split} q^{-1/n}[M_{j}\overset{1}{S}M_{k}^{-1}] \otimes [M_{i}\overset{2}{S}M_{l}^{-1}] - q^{1/n}[M_{i}\overset{2}{S}M_{l}^{-1}] \otimes [M_{j}\overset{1}{S}M_{k}^{-1}] \\ = & M_{i} \otimes M_{j}\overset{1}{S} \otimes \overset{2}{S}[q^{-1/n}R_{12}^{-1}(q) - q^{1/n}R_{12}^{\mathrm{T}}(q)]M_{k}^{-1} \otimes M_{l}^{-1} \\ = & (q^{-1}-q)M_{i}\overset{2}{\otimes} M_{j}\overset{1}{S} \otimes \overset{2}{S}P_{n}M_{k}^{-1} \otimes M_{l}^{-1} = (q^{-1}-q)M_{i}\overset{2}{S}M_{k}^{-1} \otimes M_{j}\overset{1}{S}M_{l}^{-1}P_{n}. \end{split}$$

The second equality follows from total transposition of the basic relation (2.14) (with accounting for $P_n^{\rm T} = P_n$). So we have a quantum Goldman relation

$$q^{-1/n}$$
 $= (q^{-1} - q)$ P_n

with P_n the permutation matrix. In the semiclassical limit with $q = e^{\pi i \hbar}$ (where $\hbar = b^2$) the term linear in \hbar gives rise to the Goldman bracket for SL_n [25].

Let a polygon be triangulated into collection of triangles containing triangle ΔABC , let EF be another side of triangulation different from sides of ΔABC , let γ be a path connecting EF to AB crossing any side of triangulation at most once and crossing neither AC nor BC (see Figure 12). Denote by $T_{\gamma} = T_{BA \leftarrow EF}$ the composition of transport matrices along the path γ , define normalized transport matrices $M_1 = T_{AB \leftarrow CA}^{-1} ST_{\gamma}$, $M_2 = T_{BC \leftarrow AB} ST_{\gamma}.$

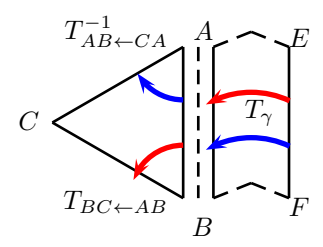


Fig. 12. $M_1 = T_{CA \leftarrow AB}ST_{BA \leftarrow EF}, M_2 = T_{BC \leftarrow AB}ST_{BA \leftarrow EF}.$

Theorem 3.2. The normalized transport matrices M_1 and M_2 in Fig. 12 satisfy the commutation relations

(i)
$$M_1 \otimes M_2 = M_2 \otimes M_1 R_n(q)$$

(iii)
$$M_2^{-1} M_{BC \leftarrow CA} M_1 = 1$$
.

Proof. The first two relations (i) and (ii) are simple corollaries of the respective two relations in (2.16) and (2.15). Relation (iii) is the quantum groupoid condition (2.14) proved earlier. Another proof will be given in Section 7.2 Now we show how to derive relation (i) from (2.16). The proofs of the other two are similar.

Consider a transport matrix corresponding to a path not passing twice through the same triangle. It is given by the matrix product $M_{i_{m-1}}^{(m-1)}S\cdots SM_{i_2}^{(2)}SM_{i_1}^{(1)}=T_{BA\leftarrow EF}$ where $i_k=1,2$ and variables of $M_{i_k}^{(k)}$ and $M_{i_p}^{(p)}$ commute for distinct k and p. Every such product satisfies the relation $R_n^{\mathrm{T}}(q)^{\frac{1}{T}} \otimes T^{\frac{2}{T}} = T^{\frac{2}{T}} \otimes T^{\frac{1}{T}} R_n(q)$. Then,

General algebras of transport matrices in an ideal triangle decomposition of $\Sigma_{g,s,p}$ —a genus g Riemann surface with s holes and p > 0 marked points on the hole boundaries are governed by a quantum version of the Fock-Rosly Poisson algebra [20] also considered in [11].

Solving reflection equation via transition matrices

In this section, we consider a special combination of non-normalized quantum transition matrices \mathcal{M}_1 and \mathcal{M}_2 from Definition 2.9:

$$\mathbb{A}^{\hbar} := \mathcal{M}_{1}^{\mathsf{T}} \mathcal{M}_{2}. \tag{4.1}$$

Note that the transposition in the quantum case is formal: the quantum ordering is preserved, only matrix elements are permuted. Also, since both $\mathcal{M}_1^{\mathrm{T}}$ and \mathcal{M}_2 are upper-triangular matrices, the matrix \mathbb{A}^{\hbar} is automatically upper-triangular.

Remark 4.1. The matrix \mathbb{A}^{\hbar} is defined as a matrix with quantum entries; we denote by \mathbb{A} a (semi-)classical

Theorem 4.2. The matrix $\mathbb{A}^{\hbar} = \mathcal{M}_{1}^{T} \mathcal{M}_{2}$ (Equation (4.1)) satisfies the quantum reflection equation

$$\mathcal{R}_{n}(q)\mathbb{A}^{\hbar}\mathcal{R}_{n}^{\mathbf{t}_{1}}(q)\mathbb{A}^{\hbar} = \mathbb{A}^{\hbar}\mathcal{R}_{n}^{\mathbf{t}_{1}}(q)\mathbb{A}^{\hbar}\mathcal{R}_{n}(q)$$

with the trigonometric R-matrix (2.13), where $\mathcal{R}_n^{t_1}(q)$ is a partially transposed (w.r.t. the first space) Rmatrix.

Note that, since two R-matrices (2.13) and (2.17) differ only by a constant multiple, we can use any of them in the relation in the theorem.

The proof is a short direct calculation that uses only R-matrix relations (2.15) and (2.16). Note that transposing (2.16) with respect to the first space, we obtain

$$\overset{1}{\mathcal{M}_{1}^{\mathrm{T}}} \otimes \overset{2}{\mathcal{M}_{2}} = \overset{2}{\mathcal{M}_{2}} \mathcal{R}_{n}^{\mathrm{t}_{1}}(q) \overset{1}{\mathcal{M}_{1}^{\mathrm{T}}}$$

and the total transposition of relation (2.15) gives

$$\overset{1}{\mathcal{M}_{1}^{\mathrm{T}}} \otimes \overset{2}{\mathcal{M}_{1}^{\mathrm{T}}} \mathcal{R}_{n}^{\mathrm{T}}(q) = \mathcal{R}_{n}^{\mathrm{T}}(q) \overset{2}{\mathcal{M}_{1}^{\mathrm{T}}} \otimes \overset{1}{\mathcal{M}_{1}^{\mathrm{T}}}.$$

However, since the total transposition of $\mathcal{R}_n^{\mathrm{T}}(q)$ is equivalent to interchanging indices $1 \leftrightarrow 2$ of spaces in the direct product, we can equivalently write this relation as

$$\mathcal{M}_{1}^{\mathrm{T}} \otimes \mathcal{M}_{1}^{\mathrm{T}} \mathcal{R}_{n}(q) = \mathcal{R}_{n}(q) \mathcal{M}_{1}^{\mathrm{T}} \otimes \mathcal{M}_{1}^{\mathrm{T}},$$

that is, R-matrix relations have the same form for both \mathcal{M}_i and $\mathcal{M}_i^{\mathrm{T}}$.

Note that $\mathcal{M}_2 \mathcal{R}_n^{t_1}(q) \mathcal{M}_1^{\mathrm{T}} = \mathcal{M}_1^{\mathrm{T}} \mathcal{M}_2$. Indeed, let us obtain this formula out of the defining relation $\mathcal{M}_1 \mathcal{M}_2 = \mathcal{M}_2 \mathcal{M}_1 \mathcal{R}_n$. First, we interchange indices of spaces $1 \leftrightarrow 2$, which results in the similar expression with fully transposed R-matrix: $\mathcal{M}_1 \mathcal{M}_2 = \mathcal{M}_2 \mathcal{M}_1 \mathcal{R}_n^{\mathrm{T}}$. Second, we perform the transposition in the second space; note that this transposition does not affect the quantum space, so the order of operators remains the same. On the left-hand side we merely obtain $\mathcal{M}_1^{\mathrm{T}} \mathcal{M}_2$, whereas on the right-hand side we must take into account that components of the classical R-matrix lying in the second space must be interchanged with components of \mathcal{M}_1 and components of R-matrix lying in the first space commute with \mathcal{M}_1 , so the order of their multiplication with \mathcal{M}_1 is irrelevant. Altogether, this can be written as $\left[\mathcal{M}_1 \mathcal{R}_n^{\mathrm{T}}\right]^{t_2} = \left[\mathcal{R}_n^{\mathrm{T}}\right]^{t_2} \mathcal{M}_1^{\mathrm{T}} = \mathcal{R}_n^{t_1} \mathcal{M}_1^{\mathrm{T}}$, which produces the desired equality.

Hence.

$$\begin{split} & \mathcal{R}_n(q) \overset{1}{\mathcal{M}}_1^{\mathrm{T}} \bigg(\overset{1}{\mathcal{M}}_2 \mathcal{R}_n^{\mathrm{t}_1}(q) \overset{2}{\mathcal{M}}_1^{\mathrm{T}} \bigg) \overset{2}{\mathcal{M}}_2 = \bigg(\mathcal{R}_n(q) \overset{1}{\mathcal{M}}_1^{\mathrm{T}} \overset{2}{\mathcal{M}}_1^{\mathrm{T}} \bigg) \overset{1}{\mathcal{M}}_2 \overset{2}{\mathcal{M}}_2 = \overset{2}{\mathcal{M}}_1^{\mathrm{T}} \overset{1}{\mathcal{M}}_1^{\mathrm{T}} \bigg(\mathcal{R}_n^{\mathrm{T}}(q) \overset{1}{\mathcal{M}}_2 \overset{2}{\mathcal{M}}_2 \bigg) \\ = & \overset{2}{\mathcal{M}}_1^{\mathrm{T}} \bigg(\overset{1}{\mathcal{M}}_1^{\mathrm{T}} \overset{2}{\mathcal{M}}_2 \bigg) \overset{1}{\mathcal{M}}_2 \mathcal{R}_n(q) = \overset{2}{\mathcal{M}}_1^{\mathrm{T}} \overset{2}{\mathcal{M}}_2 \mathcal{R}_n^{\mathrm{t}_1}(q) \overset{1}{\mathcal{M}}_1^{\mathrm{T}} \overset{1}{\mathcal{M}}_2 \mathcal{R}_n(q), \end{split}$$

which completes the proof.

Our claim is that, in a semi-classical limit, the coordinates Z_{α} parameterize Poisson leaves of \mathcal{A} . Bondal [2] demonstrated that dimensions of these leaves are dictated by the Jordan form of the matrix $\Omega := \mathbb{A}\mathbb{A}^{-T}$, which undergoes adjoint transformations $\Omega \to B\Omega B^{-1}$ under the standard groupoid transformation of the matrix \mathbb{A} . Whereas we do not intend to perform a complete analysis of dimensions of the corresponding symplectic leaves, note that in the case where all eigenvalues of Ω are distinct, corresponding symplectic leaves have maximum dimension. Theorem 1 in [12] explicitly expresses eigenvalues of Ω as special monomials of Casimirs C_k (see (5.3)) of \mathcal{A} -quiver; all these eigenvalues are distinct for Casimirs determined by X_{α} in a general position. Therefore, we can conclude that the image of the map from the space of parameters Z_{α} to \mathcal{A} intersects any maximal symplectic leave, and since the map is Poisson the image contains the whole symplectic leave as well.

Let X be a Poisson variety with a Poisson bracket $\{,\}$. Recall that a collection of functions $f_i \in C^{\infty}(X,\mathbb{R})$ is called log-canonical if $\{f_i,f_j\}=c_{ij}f_if_j$ for some constants $c_{ij}\in\mathbb{R}$. A log-canonical collection $\{f_1,\ldots f_{dim X}\}$ is called a log-canonical coordinate system if functions f_i are functionally independent. If X is an affine algebraic variety with an algebraic Poisson bracket which possesses a log-canonical collection of regular functions then according to [32] Darboux coordinate system consisting of meromorphic functions does not exist, and log-canonical coordinates are regular coordinates such that the Poisson bracket takes a simple form.

We thus conclude that collection of Fock-Goncharov parameters Z_{α} provide a log-canonical coordinate representation for operators satisfying the reflection equation. Moreover all matrix elements of \mathbb{A} are Laurent polynomials with positive coefficients of Z_{α} and q. In particular, positive integers in equation (2.10) count numbers of monomials in the corresponding Laurent polynomials.

By construction of normalized quantum transport matrices in Sec. 2.5, all matrix elements of \mathcal{M}_1 and \mathcal{M}_2 are Weyl-ordered. For $\left(\mathbb{A}^{\hbar}\right)_{ij} = \sum\limits_{k=i}^{j} \left(\mathcal{M}_1\right)_{ki} \left(\mathcal{M}_2\right)_{kj}$ we obtain that for i < j, $\left(\mathcal{M}_1\right)_{ki}$ commutes with $\left(\mathcal{M}_2\right)_{kj}$ (a path contribution to $\left(\mathcal{M}_1\right)_{ki}$ equals Weyl ordering of a product of all parameters Z_{α} above the path while the a path contribution to $\left(\mathcal{M}_2\right)_{kj}$ equals to the Weyl ordering of a product of all Z_{α} below, therefore the set of Z_{α} contributing to $\left(\mathcal{M}_1\right)_{ki}$ is disjoint from the set contributing to $\left(\mathcal{M}_2\right)_{kj}$ for i < j and any element from one set commutes with any element of the second set), so the corresponding products are automatically Weyl-ordered,

$$\left(\mathbb{A}^{\hbar}\right)_{ij} = \sum_{k=i}^{j} \left(\mathcal{M}_{1}\right)_{ki} \left(\mathcal{M}_{2}\right)_{kj} \left(\mathcal{M}_{2}\right)_{kj}$$

For i=j, $\left(\mathbb{A}^{\hbar}\right)_{ii}=\left(\mathcal{M}_{1}\right)_{ii}\left(\mathcal{M}_{2}\right)_{ii}$ since the remaining terms of the sum vanish. Moreover, there is a unique path contributing to $(\mathcal{M}_{1})_{ii}$ and a unique path contributing to $(\mathcal{M}_{2})_{ii}$ and these paths have exactly one common starting half-edge. This implies that $(\mathcal{M}_{1})_{ii}(\mathcal{M}_{2})_{ii}=q^{-1}(\mathcal{M}_{2})_{ii}(\mathcal{M}_{1})_{ii}$ implying $(\mathcal{M}_{1})_{ii}(\mathcal{M}_{2})_{ii}=q^{1/2}(\mathcal{M}_{1})_{ii}(\mathcal{M}_{2})_{ii}$. Therefore,

$$\left(\mathbb{A}^{\hbar}\right)_{ii} = \left(\mathcal{M}_{1}\right)_{ii} \left(\mathcal{M}_{2}\right)_{ii} = q^{-1/2} \bullet \left(\mathcal{M}_{1}\right)_{ii} \left(\mathcal{M}_{2}\right)_{ii} \bullet$$

This explains the appearance of $q^{-1/2}$ factors on the diagonal of the quantum matrix \mathbb{A}^{\hbar} (see (1.9), [8]).

Corollary 4.3. Entries a_{ij}^{\hbar} of \mathbb{A}^{\hbar} for i < j are symmetric operators.

Proof. Quantized Fock-Goncharov parameters Z_{α} can be represented as self-adjoint unbounded operators acting on a dense subspace \mathbb{H} of a Hilbert space $L^2(\mathbb{R}^d)$ with a positive spectrum (see, [18, 26]). In particular any (rational) power of Z_{α} is self-adjoint and the Weyl ordering of any monomial of self-adjoint operators is self-adjoint and, therefore, a_{ij}^{\hbar} is an unbounded symmetric operator on \mathbb{H} because $(\mathcal{M}_1)_{ki}$ and $(\mathcal{M}_2)_{kj}$ are Weyl orderings of monomials in rational power of Z_{α} 's.

Remark 4.4. Although spectral theory of operators a_{ij}^{\hbar} is beyond the scope of this paper, we have a strong evidence that these operators are essentially self-adjoint: their spectra are $[2, \infty)$, and their von Neumann index is presumably zero, so we can conjecture that they admit self-adjoint extensions.

As usual we call a function on a Poisson variety X a Casimir function or simply a Casimir if it Poisson commute with any other function on X. If the algebra of functions on X is quantized to some operator algebra then Casimirs become operators which commute with any other operator, a quantization of a function on X. In particular, quantizing algebra of functions on A_n we notice that all Weyl-ordered products of (rational powers of) Z_{α}^{h} are self-adjoint and the whole classical algebra of functions on A_n is generated by polynomials in these rational powers of Z_{α} 's, Casimir operators commute with any such Weyl product, are monomial in Z_{α} , and we may always assume that all Casimirs are taken to be self-adjoint operators.

We have that ${}^{\bullet}(\mathcal{M}_1)_{ii}(\mathcal{M}_2)_{ii}{}^{\bullet} = \prod_{j=1}^{i} K_j$, where K_j are quantizations of special Casimirs (5.2) of the \mathcal{A}_n -quiver introduced in the next section.

To obtain a full-dimensional (not upper-triangular) form of the matrix \mathbb{A}_{gen} let us consider adjoint action by any transport matrix:

Theorem 4.5. Any matrix $\mathbb{A}^{\hbar}_{gen} := M_{\gamma}^{T} S^{T} \mathcal{D} \mathbb{A}^{\hbar} \mathcal{D} S M_{\gamma}$, where M_{γ} is a normalized quantum transport matrix satisfying commutation relations of Theorem 2.12 such that its elements commute with those of $\mathbb{A}^{\hbar} = \mathcal{M}_{1}^{T} \mathcal{M}_{2}$ and \mathcal{D} is any diagonal matrix whose entries commute with each other and with all entries of M_{γ} and \mathbb{A}^{\hbar} , satisfies the quantum reflection equation of Theorem 4.2.

The proof is again a direct computation; note also that if we represent $\mathbb{A}^{\hbar} = \mathcal{M}_{1}^{T} \mathcal{M}_{2}$, then $\mathcal{M}'_{1} = \mathcal{M}_{1} \mathcal{D} S M_{\gamma}$ and $\mathcal{M}'_{2} = \mathcal{M}_{2} \mathcal{D} S M_{\gamma}$ satisfy commutation relations (2.15) and (2.16) and $\mathbb{A}^{\hbar}_{gen} := \mathcal{M}'_{1}^{T} \mathcal{M}'_{2}$ then satisfy the quantum reflection equation.

In the semiclassical limit the quantum reflection relation (Theorem 4.2) leads to a Poisson bracket on the set of the matrices that are represented as a product $\mathcal{M}_1^T \mathcal{M}_2$. By Theorem 4.2 the push forward of the Poisson bracket on the moduli space of pinnings $\mathcal{P}_{PGL_n,\Sigma}$ induces a Poisson bracket on the set of matrices factorizable as $\mathcal{M}_1^T \mathcal{M}_2$ that is an open subset \mathcal{F} in the space \mathcal{B} of nondegenerate upper-triangular matrices. It is well known [9] that \mathcal{A}_n is a Poisson subvariety of \mathcal{F} . We show in Section 5.1 that the set \mathcal{A}_n of unipotent matrices is obtained from \mathcal{F} by fixing the values of Casimirs $K_i = 1, i = 1 \dots n-1$ defined by Equation 5.2.

Summarizing, we obtain the following result.

Corollary 4.6. The Poisson bracket on $\mathcal{P}_{PGL_n,\Sigma}$ induces canonical Poisson structure (1.6) on the space of unipotent upper triangular matrices \mathcal{A}_n .

5 The quiver for an upper-triangular \mathbb{A} and the braid-group action

In this section we consider classical commutative ring of functions on the set \mathcal{A}_n of upper-triangular matrices and commutative Fock-Goncharov parameters equipped with the corresponding Poisson brackets. We first construct the quiver corresponding to the log-canonical coordinates on \mathcal{A}_n and, second, present the braid-group action on \mathcal{A}_n via chains of mutations in the newly constructed quiver. We would like to notice that the quasi-cluster braid group action on the transport matrices and therefore on the framed moduli space \mathcal{P}_{PGL_n} was constructed in [26]. However, our construction seems to be different.

5.1 A_{∞} -quiver

In this section we will show that the classical space \mathcal{A}_n can be described as a Poisson submanifold \mathcal{U} in the Poisson cluster variety with \mathcal{A}_n -quiver (see definition below). In this section we assume that classical matrices M_i and \mathcal{M}_i have commutative entries.

Let us have a closer look on the structure of matrix entries of the product $(\mathbb{A})_{ij} := (\mathcal{M}_1^T \mathcal{M}_2)_{i,j} = \sum_k (\mathcal{M}_1)_{ki} (\mathcal{M}_2)_{kj}$. All monomials contributing to $(\mathcal{M}_1)_{ki}$ contain the same factor $\prod_{i=1}^k Z_{i,0,n-i}$ and all monomials contributing to $(\mathcal{M}_2)_{k,j}$ contain the same factor $\prod_{i=1}^k Z_{n-i,i,0}$, so the dependence of all elements of $(\mathbb{A})_{ij}$ on the frozen variables $Z_{i,0,n-i}$ and $Z_{n-i,i,0}$ is via their pairwise products, and we therefore amalgamate these variables pairwise thus obtaining a single new variable

$$\bar{Z}_i := Z_{i,0,n-i} Z_{n-i,i,0}, \quad i = 1, \dots, n-1.$$
 (5.1)

This results in a "twisted" pattern shown in Fig. 22.

Theorem 4.2 states that the map from the Poisson space of Fock-Goncharov parameters of PGL_n -quiver to the space of the upper triangular matrices is Poisson. In particular, all Casimir functions of PGL_n -quiver (Lemma 6.1) remain Casimirs with respect to the induced Poisson bracket on the upper triangular matrices. They are addressed in what follows as "original Casimir functions". Explicit monomial forms of $\lfloor \frac{n}{2} \rfloor$ generators of the ring of Casimirs for PGL_n quiver are described in details in Section 6.1.

As a result of the amalgamation procedure we obtain new quiver which admits additionally n-1 new independent Casimirs depicted in Fig. 23 (see Lemma 6.5): Note that each of the new Casimirs K_i is again a monomial expression

$$K_{i} := Z_{0,i,n-i}^{2} \prod_{j=1}^{i-1} Z_{j,i-j,n-i} \bar{Z}_{i} \prod_{j=1}^{n-i-1} Z_{j,i,n-i-j},$$

$$(5.2)$$

which contains exactly one square of one of the frozen variable $Z_{0,i,n-i}$, and we have exactly one such Casimir per every frozen variable $Z_{0,i,n-i}$. Notice that the jth diagonal element $(\mathbb{A})_{ii} := (\mathcal{M}_1^T \mathcal{M}_2)_{ii} = (\mathcal{M}_1)_{ii}(\mathcal{M}_2)_{ii} = \prod_{j=1}^i K_j$. In particular, setting all $K_j = 1$ we obtain a unipotent upper-triangular matrix \mathbb{A} .

Theorem 5.1. The collection of Fock-Goncharov parameters Z_{abc} , a+b+c=n, $1 \le a, b, c \le n-2$ and \bar{Z}_i , $i=1,\ldots,n-1$ equipped with the log-canonical Poisson bracket

$$\{Z_{abc}, Z_{a'b'c'}\} = \lambda(a, b, c; a', b', c') Z_{abc} Z_{a'b'c'},$$

$$-\{\bar{Z}_k, Z_{abc}\} = \{Z_{abc}, \bar{Z}_k\} = \mu(a, b, c; k) Z_{abc} \bar{Z}_k,$$

$$\{\bar{Z}_k, \bar{Z}_{k'}\} = \nu(k; k') \bar{Z}_k \bar{Z}_{k'},$$

$$\{1, \quad \text{if } a' = a - 1, b' = b, c' = c + 1, \text{ or } a' = a, b' = b + 1, c' = c - 1, \text{ or } a' = a + 1, b' = b - 1, c' = c;$$

$$-1, \quad \text{if } a' = a + 1, b' = b, c' = c - 1, \text{ or } a' = a, b' = b - 1, c' = c + 1, \text{ or } a' = a - 1, b' = b + 1, c' = c;$$

$$0, \quad \text{otherwise};$$

$$\mu(a, b, c; k) = \mu_{\pi^{1}}(a, b, c; k) + \mu_{\pi^{1}}(a, b, c; k),$$

$$\mu(a,b,c;k) = \mu_{*1*}(a,b,c;k) + \mu_{**1}(a,b,c;k),$$

$$\mu_{*1*}(a,b,c;k) = \begin{cases} 1, & \text{if } k = a+1, b=1; \\ -1, & \text{if } k = a, b=1; \\ 0, & \text{otherwise} \end{cases} \text{ and } \mu_{**1}(a,b,c;k) = \begin{cases} -1, & \text{if } k = b, c=1; \\ 1, & \text{if } k = b+1, c=1; \\ 0, & \text{otherwise}; \end{cases}$$

$$\text{and } \nu(k,k') = \begin{cases} 1, & \text{if } k = k'+1 \text{ or } k = n-1, k'=1; \\ -1, & \text{if } k' = k+1 \text{ or } k=1, k'=n-1; \\ 0, & \text{otherwise}. \end{cases}$$
form the low consideration of coordinates on the cases of uninotent unner triangular and the law considerations of the case of uninotent unner triangular and the case of uninotent unner triangu

form the log-canonical system of coordinates on the space of unipotent upper triangular matrices A_n with respect to the canonical Poisson bracket (1.6).

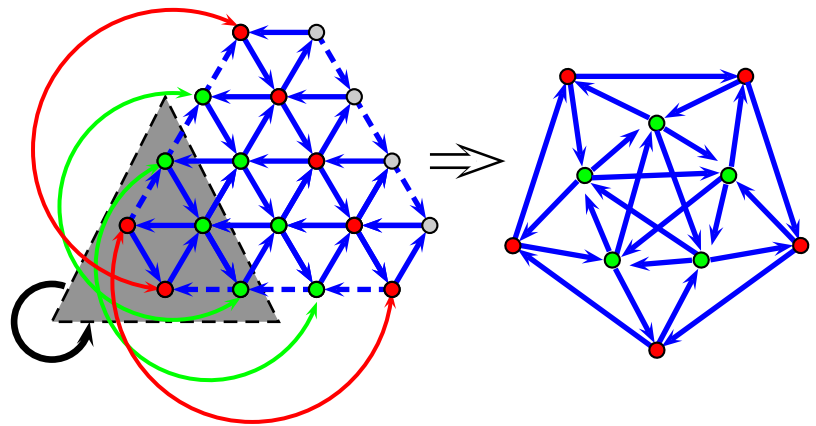
Remark 5.2. The entries a_{ij} of unipotent upper triangular $\mathbb{A} \in \mathcal{A}_n$ are expressed through Z_{abc} and \bar{Z}_i as a sum of weights of paths, where the paths entering in the sum and their weights are explained on Figure 16; each weight is a product of $Z_{abc}^{\pm \frac{1}{2}}$ and $\bar{Z}_i^{\pm \frac{1}{2}}$.

Proof. Let us change the system of coordinates in \mathcal{A}_n replacing $Z_{0,i,n-i}$ by $(K_i)^{1/2}$. Note that K_i is a Weyl ordering of positive essentially self-adjoint operators Z_{abc} , hence a positive essentially self-adjoint operator. Therefore, its positive self-adjoint fractional power is uniquely defined. Clearly, it is nondegenerate change of coordinates. Fixing values $K_i = 1$ leads to a Poisson submanifold \mathcal{A}_n . Elements Z_{0bc} , b+c=n are

dependent of all other Fock-Goncharov parameters through equations $K_i = 1$, elements $Z_{i,0,n-i}$ and $Z_{n-i,i,0}$ enter $\mathbb{A} = \mathcal{M}_1^{\mathrm{T}} \mathcal{M}_2$ only pairwise as described by (5.1). We noted already that all Fock-Goncharov parameters parametrize symplectic leaves of A_n . Comparing dimension of A_n with the number of parameters left after removing $Z_{0,i,n-i}$ and replacing pair $(Z_{k,0,n-k},Z_{n-k,k,0})$ by Z_k we can conclude that \bar{Z}_i , $i=1\ldots n-1$ and $Z_{a,b,c}$, a > 0 form log-canonical coordinate system on A_n .

It is straightforward to check that expressions in Theorem 5.1 for the Poisson bracket of pair of functions from the union $\{Z_{abc}\} \cap \{Z_k\}$ correspond to the quiver obtained by the following construction.

Poisson bracket on A_n is described by a quiver obtained from PGL_n -quiver by the following steps. First, we remove vertices corresponding to frozen variables $Z_{0,i,n-i}$. Second, we glue vertices $Z_{k,0,n-k}$ and $Z_{n-k,k,0}$ into the vertex Z_k and then unfreeze it. Note that the connected part of the resulting quiver, which we call the A_n -quiver, contains only unfrozen variables. A most symmetric way of vizualizing this quiver is to "cut out" the half-sized triangle located in the left-lower corner, then reflect this small triangle through the diagonal passing through its left-lower corner preserving the incidence relations for arrows in the both parts of the quiver, then glue pairwise the amalgamated variables $Z_{k,0,n-k}$ and $Z_{n-k,k,0}$. Example of the amalgamation operations for \mathcal{A}_5 is shown below.



Note each of $\lfloor n/2 \rfloor$ original Casimirs of the PGL_n -quiver gives rise to the corresponding Casimir element of the A_n -quiver

$$C_k = \bar{Z}_k \prod_{i=1}^{n-k-1} Z_{k,i,n-k-i} \bar{Z}_{n-k} \prod_{j=1}^{k-1} Z_{n-k,j,k-j},$$
(5.3)

and in figures representing A_n -quivers, cluster variables of sites of the same color contribute (all in power one) to the same Casimir. We present the A_n -quivers for n=3,4,5,6 in Fig. 13 where we indicate [n/2] independent Casimir elements depicted in Fig. 24.

Since all Casimirs of $\mathbb{A} \in \mathcal{A}_n$ are generated by λ -power expansion terms for $\det(\mathbb{A} + \lambda \mathbb{A}^T)$ (see, [3]) and by $C_1, \ldots, C_{\lfloor n/2 \rfloor}$, we automatically obtain the following result

Lemma 5.3. The coefficient of λ^k of $\det(\mathbb{A} + \lambda \mathbb{A}^T)$ is a function $P_k(C_1, \dots, C_{\lfloor n/2 \rfloor})$, where C_i are Casimirs of the A_n -quiver.*

Remark 5.4. In the cases n=3 and n=4, the constructed quivers are those of geometric systems: these cases admit three-valent fat-graph representations in which \mathcal{X} -cluster variables are identified with (exponentiated) Thurston shear coordinates z_{α} enumerated by edges of the corresponding graphs, and nontrivial commutation relations are between variables on adjacent edges; for n=3 and n=4 these graphs are the relative spines of Riemann surfaces $\Sigma_{1,1}$ and $\Sigma_{1,2}$ depicted in Fig. 14; the Laurent polynomials for entries of A coincide up to a linear change of log-canonical variables with the expressions obtained by identifying these entries with geodesic functions corresponding to closed paths on these graphs; for more details and for the explicit construction of geodesic functions, see [6], [8]. Note here that, likewise all $a_{i,j}$ constructed in this paper, all geodesic functions for all surfaces $\Sigma_{g,s}$ are positive Laurent polynomials of $e^{z_{\alpha}/2}$.

 $^{{}^*}P_k$ are polynomial functions whose explicit expressions were found in [13].

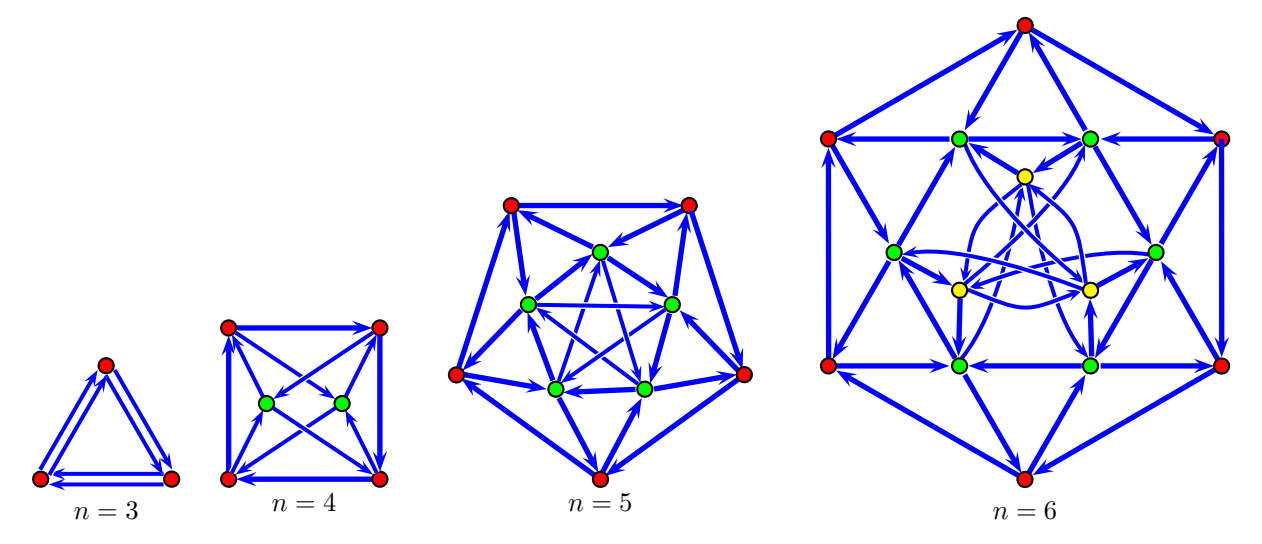


Fig. 13. A_n -quivers for n = 3, 4, 5, 6.

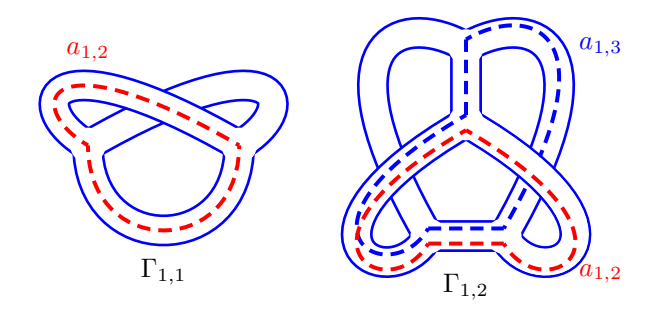


Fig. 14. Fat graphs $\Gamma_{1,1}$ and $\Gamma_{1,2}$ corresponding to the respective quivers for A_3 and A_4 . We indicate closed paths that produce elements $a_{1,2} \in \mathbb{A} \in \mathcal{A}_3$ and $a_{1,2}$ and $a_{1,3}$ of $\mathbb{A} \in \mathcal{A}_4$. For example, setting all $Z_{\alpha} = 1$ for simplicity and using formulas from [6] for the corresponding geodesic functions we obtain $a_{1,2} = \operatorname{tr}(LR) = 3$ in \mathcal{A}_3 and $a_{1,2} = \operatorname{tr}(LLR) = 4$ and $a_{1,3} = \operatorname{tr}(LLRR) = 6$ in \mathcal{A}_4 , where $L = \begin{bmatrix} 1 & 0 \\ 1 & 1 \end{bmatrix}$ and $R = \begin{bmatrix} 1 & 1 \\ 0 & 1 \end{bmatrix}$ are matrices of the respective left and right turns of paths occuring at three-valent vertices of a spine. It is easy to see that the above $a_{i,j}$ coincide with those in Example 2.7.

5.2 Braid-group action through mutations

Our second major goal in this paper is to find a representation of the braid-group action from Sec. 1.2 in terms of cluster mutations of the A_n -quiver. In this section we find cluster expressions of generators of braid group action on the classical space A_n . It is well-known that for \mathbb{A} belonging to a specific symplectic leaf in A_n its matrix elements $a_{i,j}$ are identified with the geodesics functions. In this leaf, braid-group transformations correspond to Dehn twists along geodesics corresponding to geodesic functions $a_{i,i+1}$ on $\Sigma_{g,s}$ (n=2g+s) and s=1,2). We know that every Dehn twist on a Riemann surface $\Sigma_{g,s}$ is a sequence of cluster mutations since it can be presented as a chain of mutations of shear variables on edges of the corresponding spine $\Gamma_{q,s}$. Whereas, for n=3 and n=4, generic symplectic leaves in \mathcal{A}_n are geometric and the corresponding mutation sequences are identical, for larger n the generic symplectic leaves become essentially different and we have to reinvent a braid group action. Knowing the answer for n=3 and 4 helps in guessing the answer for a general n. We begin with the example of A_5 -quiver:

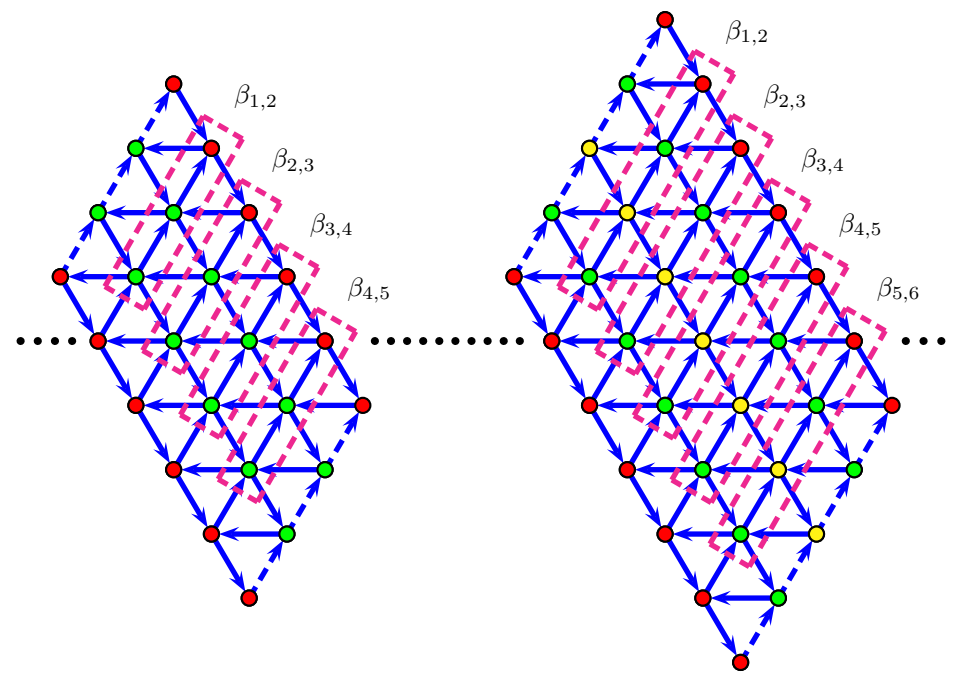
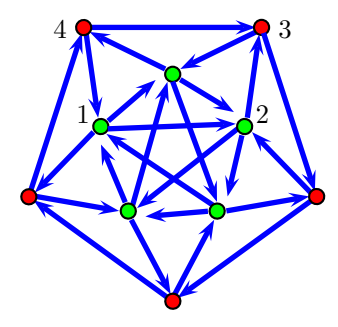


Fig. 15. The braid-group action represented on the union of two triangles, each of which is the copy of the A_n -quiver, for n=5 and 6. The dotted line indicates the line of the triangle gluing. Dashed blocks enclose cluster variables sequences of mutations at which produce elementary braid-group transformation $\beta_{i,i+1}$: every such sequence commences with mutating the lowest element inside a box (corresponding to a six-valent vertex), then its upper-right neighbor and so on until we reach the upper element, mutate it, and repeat mutations at all inner elements in the reverse order. So, every such braid-group transformation is produced by a sequence of 2n-5 mutations in the corresponding A_n -quiver.



The following chain of mutations $\beta_{3,4} = \mu_1 \mu_2 \mu_3 \mu_2 \mu_1 = S_{3,4}$ preserves the form of the original quiver with the interchanged vertices 3 and 4, where μ_i is a mutation at vertex i.

A convenient way to represent a set of elementary braid-group transformations for a general A_n quiver is the process schematically depicted in Fig. 15 below: we take another copy of the triangle representing the quiver, reflect it and glue the resulting triangle to the original one along the bottom side of the latter in a way that amalgamated variables on the sides of two triangles match and the colored vertices representing Casimir elements are stretched along SE diagonals. The sequences of mutations corresponding to elementary generating elements $\beta_{i,i+1}$ of the braid groups are indicated in the figure.

Before presenting the result of the braid-group transformation, we describe contributions of cluster variables located at sites of the A_n -quiver to a normalized element $a_{i,j} \in \mathbb{A}$ with i < j. (Note that this normalization is different from the one we applied to obtain M_i from \mathcal{M}_i .) Before normalization this element is homogeneous in frozen cluster variables $\rho_k \equiv Z_{0,k,n-k}$ and is proportional to the product $\prod_{k=0}^i \rho_k^2 \prod_{l=i+1}^j \rho_l$. We normalize this element by dividing it by the product $\prod_{k=0}^{i} K_k \prod_{l=i+1}^{j} K_l^{1/2}$ of Casimirs (5.2) thus eliminating the dependence of \mathbb{A} on ρ_i . This normalization changes the powers in which cluster variables enter sums over paths. We have eight domains in total in the leftmost part of Fig. 16: let us describe two of them. In the domain labeled "a,"

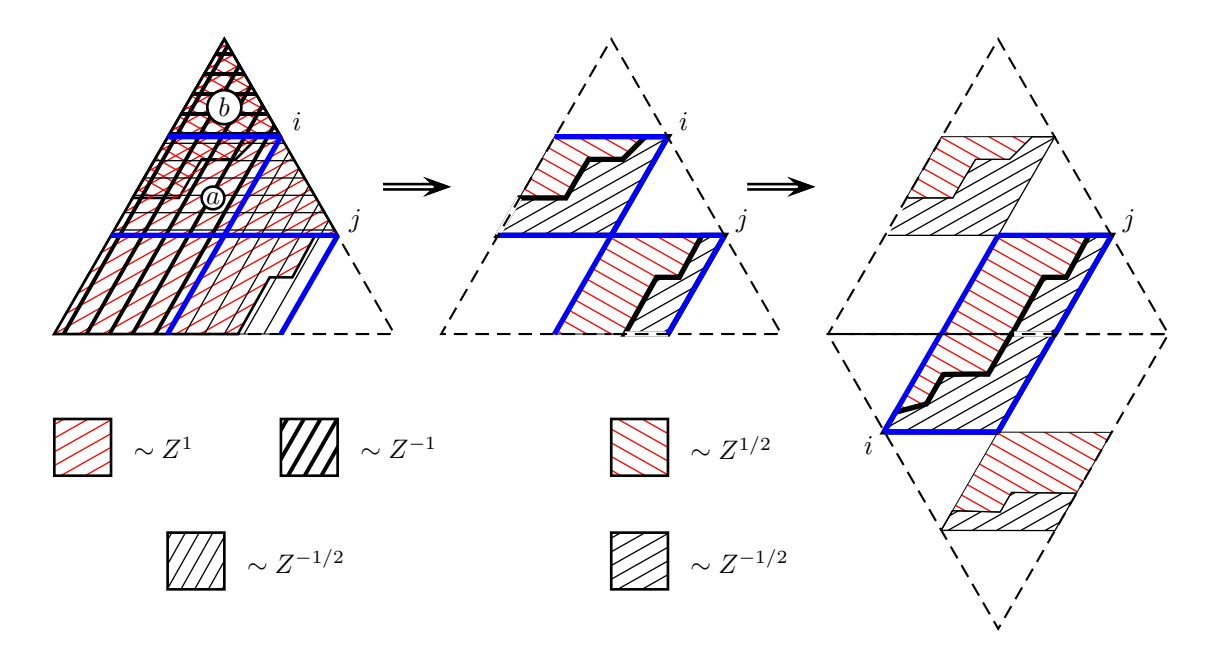


Fig. 16. Paths contributing to $a_{i,j}$ in the glued A_n -quivers. In the left picture we indicate contributions of cluster variables of PGL_n quiver into a normalized element $a_{i,j}$: we schematically draw two paths: the upper path corresponds to $(M_1)_{ki}$ and the lower path corresponds to $(M_2)_{kj}$. All cluster variables above the first path enter in power two and all variables between two path enter with power one into a nonnormalized expression; we then normalize it by the products of cluster variables entering the product of Casimirs $\prod_{k=0}^{i} K_k \prod_{l=i+1}^{j} K_l^{1/2}$. The resulting pattern is presented in the middle picture: cluster variables enter with powers 1/2 or -1/2 and variables from empty areas do not contribute. In the rightmost figure we take another copy of the A_n -quiver and attach it as in Fig. 15; two domains in the original triangle then constitute a parallelogram with a continuous path joining its opposite vertices.

nonnormalized variables enter with power 1 and each of them enters exactly one Casimir K_k with $k \leq i$ and one Casimir K_l with $i+1 \le l \le j$, so the normalization decreases the power by 3/2 and the total power with which these variables enter the normalized element is -1/2. In the uppermost domain labeled "b," every element enters with power two into a nonnormalized sum over paths and it enters two Casimirs K_k with $k \leq i$, so the normalization add power -2 and the total power is zero. We indicate powers by different hatchings, which overlap in the figure on the left; the resulting powers -1/2, 0, and 1/2 are indicated in the middle figure.

We then glue two copies of the PGL_n triangle in the rightmost part of Fig. 16: the union of two domains containing cluster variables contributing into the normalized element $a_{i,j}$ is then a parallelogram with sides of positive lengths j-i and n+i-j, and in order to obtain the element $a_{i,j}$ we have to take a sum over all paths inside this parallelogram starting at the vertex of the dual lattice located "beyond" NE vertex j and terminating at the vertex of the dual lattice located "beyond" SW vertex i (a standard exercise in combinatorics is that we have exactly $\binom{n}{i-i}$ such paths, cf. toy Example 2.7).

In the more detailed picture (Fig. 17), we indicate a part of the directed network inside which we take a sum over paths from j to i contributing to $a_{i,j}$ (an example of such path is shown in light green color in the Figure 17); all contributing cluster variables are confined inside the corresponding parallelogram. All cluster variables inside the parallelogram and above a path contribute with power one to the nonnormalized matrix entry. Normalization correction (as explained above) changes the power of each cluster variable above the path and inside the parallelogram to 1/2. Similarly, all cluster variables inside the parallelogram and below the path enter with the power -1/2. All variables outside the parallelogram do not contribute.

We now explore how cluster variables transform under chains of mutations $\beta_{i,i+1}$. Recall that mutation μ_Z transforms any variable Y at the head of an outgoing solid arrow $Z \to Y$ as $Y \mapsto Y(1+Z)$, and at the head of outgoing double arrow $Z \Rightarrow Y$ as $Y \mapsto Y(1+Z)^2$ whereas a variable X joined to Z by an incoming solid arrow, $Z \leftarrow X$, transforms as $X \to X(1+Z^{-1})^{-1}$, and for incoming double arrow, $Z \leftarrow X$, we have $X \to X(1+Z^{-1})^{-2}$. Finally, $\mu_Z(Z) = Z^{-1}$ and quiver mutation is standard ([21]).

Before formulating the general statement, let us consider an example of such a quiver transformation for PGL_5 . In this case we have a sequence of five consecutive mutations depicted in Fig. 18.

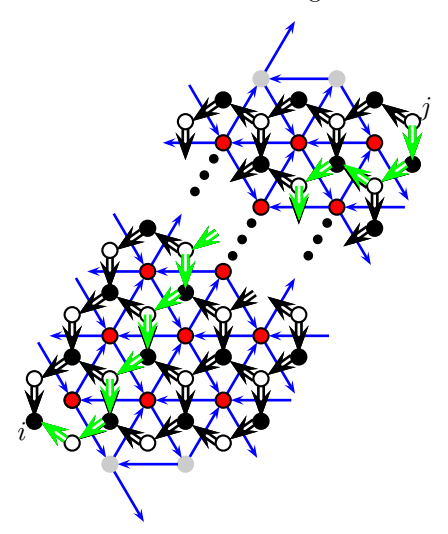


Fig. 17. More detailed path weight: all cluster variables inside the drawn parallelogram and above a light green path enter with the power 1/2 and all cluster variables inside the parallelogram and below the path enter with the power -1/2. All variables outside the parallelogram do not contribute.

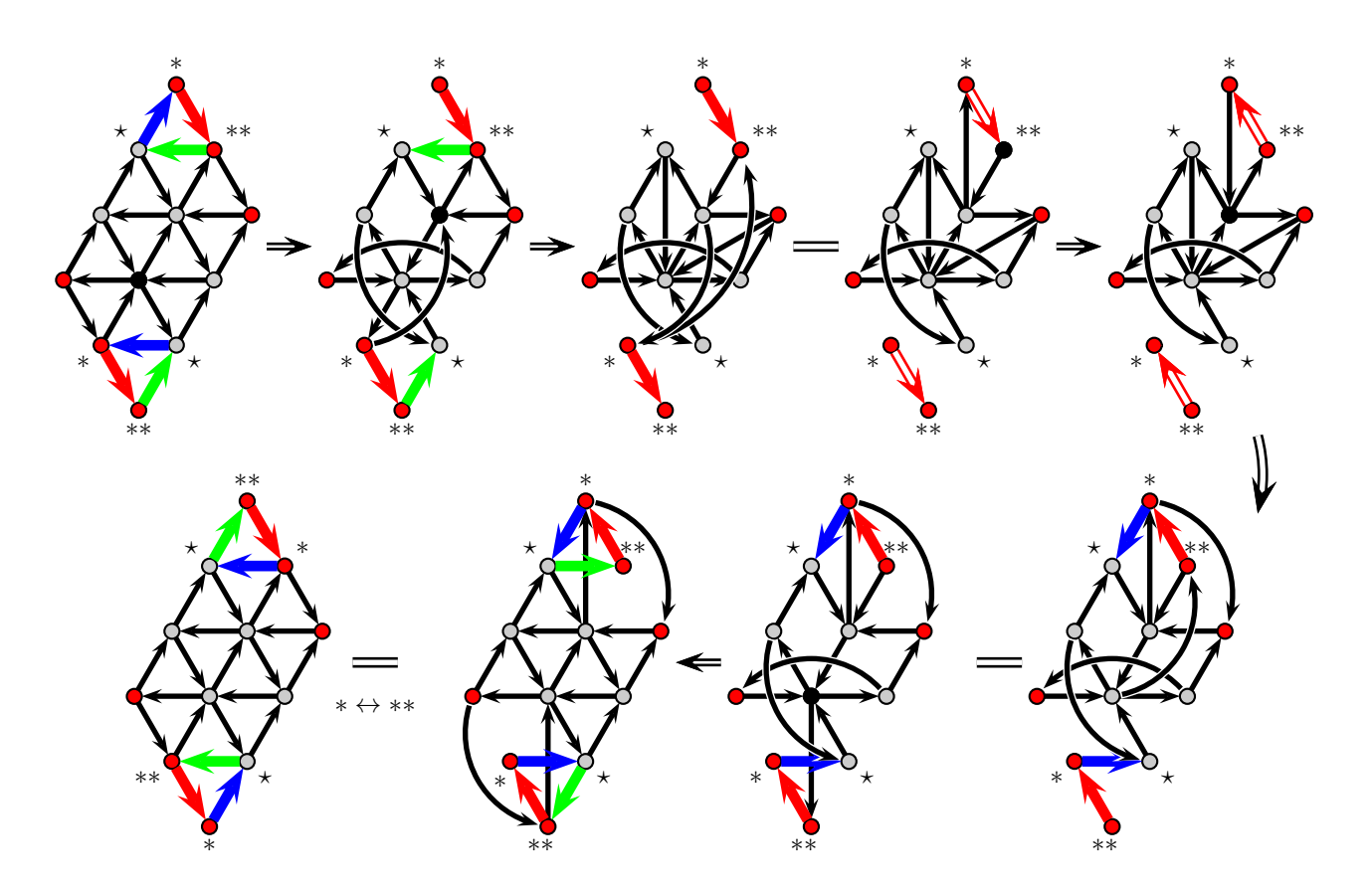


Fig. 18. The sequence of mutations producing a braid-group transformation in PGL_5 case. The vertex at which mutation takes place is painted black. Three vertices labeled *, *, and ** in the bottom and top parts of the quiver are copies of the same three vertices; bold arrows connecting these vertices are two copies of the same arrow in the corresponding quiver (which has to be taken into account when doing mutations). Arrows between other vertices and between the above three vertices and the rest of vertices are summed up following standard quiver rules. Note that after the second mutation, we obtain a double arrow $* \Rightarrow **$; at the last step we interchange positions of transformed variables * and ** reconstructing the original quiver.

Fig. 19. The transformation of variables under a braid group transformation $\beta_{i,i+1}$. We indicate only variables that are transformed under the corresponding chain of mutations. Note that the cluster variables C_0 and A_r (and therefore C'_0 and A'_r) are two representatives of the same cluster variable taken from two different fundamental domains; we use different letters to denote the same cluster variable only for making formulas in this section uniform.

Till the end of this section we let r = n - 3 for brevity. Consider the following sequence of mutations $\beta = \mu_{B_1} \dots \mu_{B_r} \mu_{S_2} \mu_{B_r} \dots \mu_{B_2} \mu_{B_1}$ (see Fig. 19). The net result of this chain of mutations is shown on the right hand side of Fig. 19. Note that the resulting quiver is isomorphic to the original one when all the mutated variables except S_1 and S_2 retain their positions, while the boundary variables S_1 and S_2 are permuted.

Lemma 5.5. In the notation of Fig. 19, cluster variables transform as follows (recall that for brevity we set r := n - 3):

$$B'_{k} = B_{k} \frac{\eta_{k+2}}{\eta_{k}}, \ k = 1, \dots, r; \quad A'_{k} = A_{k} \frac{\eta_{k+1}}{\eta_{k+2}}, \ k = 0, \dots, r-1; \quad C'_{k} = C_{k} \frac{\eta_{k+1}}{\eta_{k+2}}, \ k = 1, \dots, r;$$

$$A'_{r} = C'_{0} = A_{r} \frac{\eta_{n+1}\eta_{1}}{\eta_{2}}; \quad S'_{1} = \frac{S_{1}S_{2}^{2}B_{1} \cdots B_{r}}{\eta_{r+1}\eta_{1}}; \quad S'_{2} = \frac{\eta_{2}}{S_{2}B_{1} \cdots B_{r}},$$

where

$$\eta_{r+2} = 1, \quad \eta_{r+1} = 1 + S_2, \quad \eta_r = 1 + S_2 + S_2 B_r,
\eta_{r-1} = 1 + S_2 + S_2 B_r + S_2 B_r B_{r-1}, \dots, \quad \eta_1 = 1 + S_2 + \dots + S_2 B_r \dots B_1.$$
(5.4)

Proof. The proof of Lemma 5.3 is a long but straightforward calculation during which we may observe a regular pattern moving along the strip of cluster variables affected by this chain of mutations: first in one direction, then in opposite direction reconstructing in its reverse motion the original quiver with transformed variables at vertices. The chain of quiver mutations is illustrated on Figure 18. Using the structure of quivers in the mutation sequence the transformation of formulas for cluster variables is straightforward.

Note first that Casimirs (5.3) of the A_n -quiver are invariant under the transformation in Lemma 5.5. This immediately follows from the equalities

$$A'_k B'_k C'_{k-1} = A_k B_k C_{k-1}, \ k = 2, \dots, r-1,$$

 $A'_1 B'_1 A'_r B'_r C'_r = A_1 B_1 A_r B_r C_r,$

and
$$S_1'S_2'A_0'C_r' = S_1S_2A_0C_r.$$
 (5.5)

We now formulate the main statement

Theorem 5.6. The cluster transformations in Lemma 5.5 generate the braid-group transformations for entries $a_{i,j}$ of the (classical) matrix A.

Proof. The pivotal calculation is the transformation of quantities η_k defined in (5.4) under transformations in Lemma 5.5. Let us denote by \mathcal{G} the non-normalized transport matrix corresponding to matrix A. First, let us compute the (non-normalized) element $G_{i,i+1}$ of \mathcal{G} :

$$G_{i,i+1} := \eta_1 + S_2 B_r \cdots B_1 S_1 = 1 + S_2 + S_2 B_r + \cdots + S_2 B_r \cdots B_1 + S_2 B_r \cdots B_1 S_1. \tag{5.6}$$

Then, after mutation sequence $\beta_{i,i+1}$, we obtain

$$\begin{split} &\eta_k' = 1 + S_1' + S_1'B_r' + S_1'B_r'B_{r-1}' + \dots + S_1'B_r'B_{r-1}' \dots B_k' \\ &= 1 + \frac{S_1S_2^2B_r \dots B_1}{\eta_{r+1}\eta_1} \left(1 + \frac{B_r}{\eta_r} + B_rB_{r-1} \frac{\eta_{r+1}}{\eta_r\eta_{r-1}} + \dots + B_rB_{r-1} \dots B_k \frac{\eta_{r+1}}{\eta_{k+1}\eta_k} \right) \\ &\text{(note that } 1 + B_r/\eta_r = (1 + S_2)(1 + B_r)/\eta_r = \eta_{r+1}(1 + B_r)/\eta_r) \\ &= 1 + \frac{S_1S_2^2B_r \dots B_1}{\eta_1} \left(\frac{1 + B_r}{\eta_r} + \frac{B_rB_{r-1}}{\eta_r\eta_{r-1}} + \dots + \frac{B_rB_{r-1} \dots B_k}{\eta_{k+1}\eta_k} \right) \\ &\left(\text{note that } \frac{1 + B_r}{\eta_r} + \frac{B_rB_{r-1}}{\eta_r\eta_{r-1}} = \frac{1}{\eta_r\eta_{r-1}} \left((1 + B_r)(1 + S_2 + S_2B_r + S_2B_rB_{r-1}) + B_rB_{r-1} \right) \\ &= \frac{1}{\eta_r\eta_{r-1}} (1 + B_r + B_rB_{r-1})\eta_r = \frac{1 + B_r + B_rB_{r-1}}{\eta_{r-1}} \right) \\ &= \dots = 1 + \frac{S_1S_2B_r \dots B_1}{\eta_1} \frac{1 + B_r + B_rB_{r-1} + \dots + B_rB_{r-1} \dots B_k}{\eta_k} \\ &= 1 + \frac{S_1S_2B_r \dots B_1(\eta_k - 1)}{\eta_1\eta_k} = \frac{G_{i,i+1}}{\eta_1} - \frac{S_1S_2B_r \dots B_1}{\eta_1\eta_k}. \end{split}$$

We therefore obtain that

$$\eta_k' = \frac{G_{i,i+1}}{\eta_1} - \frac{S_1 S_2 B_r \cdots B_1}{\eta_1 \eta_k}, \ k = 1, \dots, r+2, \tag{5.7}$$

and

$$G'_{i,i+1} = \eta'_r + S'_1 B'_r B'_{r-1} \cdots B'_1 S'_2 = \frac{G_{i,i+1}}{\eta_1}.$$
 (5.8)

We consider several cases of matrix entries a_{ij} ; the rest we leave for the reader. Note, first, the relations for triples of the cluster variables:

$$A'_{k-1}B'_kC'_k = A_{k-1}B_kC_k, \ k = 1, \dots, r, \text{ and } S'_1S'_2A'_r = S_1S_2A_r.$$
 (5.9)

In particular, these relations imply that the total product of all cluster variables is conserved.

For all elements $a_{i,j}$ we take into account their normalization by taking the sum over paths weighted by products of cluster variables (in power one) inside the corresponding parallelogram and above the path and dividing this sum by the product of all cluster variables inside the parallelogram taken with power 1/2.

We begin with the element

$$a_{i,i+1} = (S_2 B_r \cdots B_1 S_1)^{-1/2} G_{i,i+1}.$$

Since $S_1'B_r'\cdots B_1'S_2' = S_2B_r\cdots B_1S_1\eta_1^{-2}$ we have that

$$a'_{i,i+1} = (S'_1 B'_r \cdots B'_1 S'_2)^{-1/2} G'_{i,i+1} = a_{i,i+1},$$

so, as expected, this element is preserved by the braid-group transformation $\beta_{i,i+1}$.

We next consider an arbitrary element $a_{l,m}$ with $(l,m) \neq (i,i+1)$. Note first that the normalizing factor for any such element is a product of triples of cluster variables (5.9) taken either in powers 1/2 or zero; since all these triples are preserved by the transformation, all such factors are invariant under the transformation. It suffices therefore to consider a nonnormalized sum over paths contributing to $a_{l,m}$. Consider a contribution of cluster variables to paths that enter the pattern in Fig. 19 from the right between elements C_{p-1} and C_p and exit from the left between elements A_{k-1} and A_{k-2} (with $k \leq p$). This path may cross the "B-line" anywhere between B_{k-1} and B_p and we have to take a sum over all possible variants. The corresponding contribution therefore has the form

$$\Pi'_{k,p} = C'_p C'_{p+1} \cdots C'_m \times \left[\eta'_k - \eta'_{p+1} \right] \times S'_2 A'_m A'_{m-1} \cdots A'_{k-1}
= \eta_{p+1} C_p C_{p+1} \cdots C_m \times \frac{S_1 S_2 B_r \cdots B_1}{\eta_1 \eta_k \eta_{p+1}} (\eta_k - \eta_{p+1}) \times \frac{\eta_1 \eta_k}{S_2 B_r \cdots B_1} A_m \cdots A_{k-1}
= C_p C_{p+1} \cdots C_m (\eta_k - \eta_{p+1}) S_1 A_m \cdots A_{k-1} = \Pi_{k,p},$$

so all these elements are preserved, as well as all normalizing factors, and $a'_{l,m} = a_{l,m}$. Consider now

$$\begin{split} a'_{i,i+2} = & \left(A'_r \cdots A'_0 S'_1 B'_r \cdots B'_1 \right)^{-1/2} \left[\eta'_{r+2} + A'_r \eta'_{r+1} + A'_r A'_{r-1} \eta'_r + \cdots + A'_r A'_{r-1} \cdots A'_0 \eta'_1 \right] \\ = & \left(S_1 A_r \cdots A_0 S_2^2 B_r^2 \cdots B_1^2 \eta_2^{-2} \right)^{-1/2} \left[1 + A_r \frac{\eta_{r+1} \eta_1}{\eta_2} \left(\frac{G_{i,i+1}}{\eta_1} - \frac{S_1 S_2 B_r \cdots B_1}{\eta_1 \eta_{r+1}} \right) + \cdots \right. \\ & + \left. \left(A_r \cdots A_k \right) \frac{\eta_{k+1} \eta_1}{\eta_2} \left(\frac{G_{i,i+1}}{\eta_1} - \frac{S_1 S_2 B_r \cdots B_1}{\eta_1 \eta_{k+1}} \right) + \cdots + \left(A_r \cdots A_0 \right) \frac{\eta_1 \eta_1}{\eta_2} \left(\frac{G_{i,i+1}}{\eta_1} - \frac{S_1 S_2 B_r \cdots B_1}{\eta_1 \eta_1} \right) \right] \\ = & \left[\frac{1 + A_r \eta_{r+1} + \cdots + A_r A_{r-1} \cdots A_0 \eta_1}{(A_r \cdots A_0 S_2 B_r \cdots B_1)^{1/2}} \cdot \frac{G_{i,i+1}}{(S_2 B_r \cdots B_1 S_1)^{1/2}} - \frac{1 + S_1 + S_1 A_r + \cdots + S_1 A_r \cdots A_0}{(S_1 A_r \cdots A_0)^{1/2}} \right] \\ = & a_{i,i+2} a_{i,i+1} - a_{i+1,i+2}. \end{split}$$

Next,

$$\begin{split} a'_{i-1,i+1} = & \left(B'_r \cdots B'_1 S'_2 C'_r \cdots C'_0 \right)^{-1/2} \left(1 \cdot \left(G'_{i,i+1} - \eta'_{r+2} \right) + C'_r (G'_{i,i+1} - \eta'_{r+1}) \right. \\ & + C'_r C'_{r-1} (G'_{i,i+1} - \eta'_r) + \cdots + C'_r \cdots C'_0 (G'_{i,i+1} - \eta'_1) \right) \\ = & \frac{1}{(C_r \cdots C_0 S_2)^{1/2}} \left(1 + C_r + C_r C_{r-1} + \cdots + C_r C_{r-1} \cdots C_1 + C_r C_{r-1} \cdots C_1 C_0 \eta_{r+1} \right) \\ = & \frac{1}{(C_r \cdots C_0 S_2)^{1/2}} \left(1 + C_r + C_r C_{r-1} + \cdots + C_r C_{r-1} \cdots C_1 + C_r C_{r-1} \cdots C_1 C_0 (1 + S_2) \right) = a_{i-1,i}. \end{split}$$

Proving the rest of relations we leave to the reader. \square

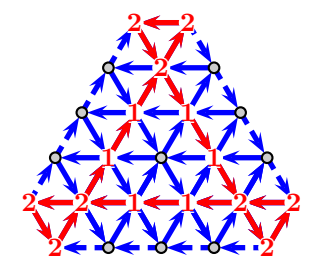
6 Casimirs

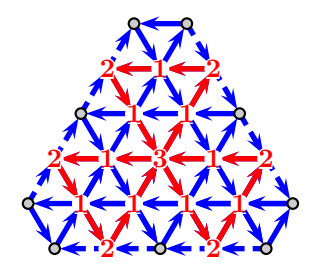
In this section, we derive complete sets of Casimirs for all relevant (sub)varieties of cluster Poisson varieties related to regular quivers associated to PGL_n and \mathcal{A}_n systems. All Casimirs in consideration are obtained as a finite product of (rational) powers of Fock-Goncharov parameters Z_{ijk} shown on the Figures below (red quiver vertices carry contributing parameters, red numbers show the corresponding powers). All proofs are direct calculations: to show that a given monomial is Casimir one can check that the total number of incoming minus the total number of outgoing arrows weighted by the rational powers connecting any given vertex of quiver with all vertices of the support of the monomial is zero, independence follows from the fact that vectors of exponents of Casimirs are independent whereas their completeness follows from the known answers for dimensions of symplectic leaves (see [3]). Finally, to obtain quantum Casimirs by a quantization of a Casimir monomial $\prod_{\alpha} Z_{\alpha}^{r_{\alpha}}$ we need to take the Weyl ordering $\prod_{\alpha} Z_{\alpha}^{r_{\alpha}}$. This fact follows immediately from the commutation relation $\prod_{\alpha} Z_{\alpha}^{r_{\alpha}} Z_{\beta} = q^{\sum_{\alpha} r_{\alpha} \alpha, \beta} Z_{\beta} \prod_{\alpha} Z_{\alpha}^{r_{\alpha}} Z_{\alpha}^{r_{\alpha}}$ with any Fock-Goncharov parameter Z_{β} . Note that for any Casimir $\prod_{\alpha} Z_{\alpha}^{r_{\alpha}}$ the value $\prod_{\alpha} Z_{\alpha}^{r_{\alpha}} Z_{\alpha}^{r_{\alpha}}$ the value $\prod_{\alpha} Z_{\alpha}^{r_{\alpha}} Z_{\alpha}^{r_{\alpha}}$ went of this section we consider only semi-classical Casimir functions in commutative variables unless explicitly mentioned otherwise.

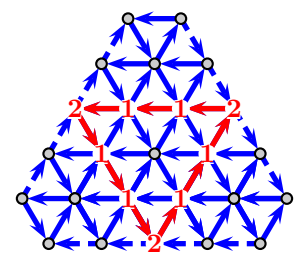
6.1 The full-rank PGL_n -quiver

Lemma 6.1. The complete set of Casimir operators for the full-rank PGL_n -quiver are $\lfloor \frac{n}{2} \rfloor$ products of cluster variables depicted in the figure below for the example of PGL_6 : numbers at vertices indicate the power with

which the corresponding variable comes into the product; all nonnumbered variables have power zero. All Casimirs correspond to closed broken-line paths in the PGL_n -quiver with reflections at the boundaries (the "frozen" variables at boundaries enter the product with powers two, powers of non-frozen variables can be 0,1,2, and 3, and they count how many times the path goes through the corresponding variable. The total Poisson dimension of the full-rank quiver is therefore $\frac{(n+2)(n+1)}{2} - 3 - \lfloor \frac{n}{2} \rfloor$.





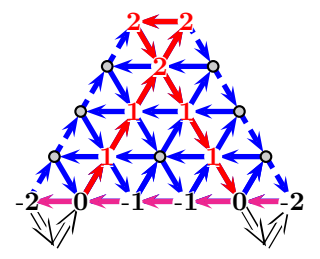


Three central elements of the full-rank quiver for PGL_6 .

Remark 6.2. All Casimir operators from Lemma 6.1 remain Casimirs for the full-rank GL_n -quiver obtained by adding three more cluster variables at the corners of the triangle (the variables $Z_{6,0,0}$, $Z_{0,6,0}$, and $Z_{0,0,6}$ in Fig. 25). If we include these three corner variables into the quiver, we have to add one more Casimir operator which is the product of all frozen (non-corner) variables along all three boundaries of the PGL_n -quiver taken in power one and the product of three corner variables taken in power three.

For completeness, we also present Casimirs for a reduced quiver in which we eliminate one of the three sets of frozen variables. The remaining n(n+1)/2-1 variables are those parameterizing, say, the transport matrix M_1 (for M_2 we have to remove another set of frozen variables). In this case, every Casimir of the full-rank quiver has its counterpart in the reduced quiver except the element that is represented by a triangle-shaped path in the full-rank quiver (such an element exists only for even n), which has no counterpart.

Lemma 6.3. The complete set of Casimir operators for the reduced PGL_n -quiver are $\left\lfloor \frac{n-1}{2} \right\rfloor$ products of cluster variables depicted in Fig. 21 for the example of PGL_6 : numbers at vertices indicate the power with which the corresponding variable comes into the product; all nonnumbered variables have power zero. All Casimirs correspond, as in Fig. 20, to closed broken-line paths in the corresponding full-rank quiver with reflections at the boundaries (the "frozen" variables at boundaries enter the product with powers two), but now the path is split into two parts separated by two reflections at the side of the triangle that corresponds to the erased frozen variables; these two parts enter with opposite signs; the corresponding Casimir therefore contains cluster variables in both positive and negative powers. As in the case of full-rank quiver, these powers count (with signs) how many times the path goes through the corresponding variable). The total Poisson dimension of the reduced PGL_n -quiver is therefore $\frac{n(n+1)}{2} - 1 - \lfloor \frac{n-1}{2} \rfloor$.



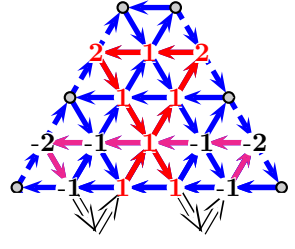


Fig. 21. Two central elements of the reduced quiver for PGL_6 . Every element of the complete quiver in Fig. 20 has its counterpart in the reduced quiver except the third element.

In our construction below, an important role is played by the additional Casimir that appears if we add the variable (0,0,6) at the summit of the triangle corresponding to a reduced quiver. In this case, besides the Casimirs in Lemma 6.3, we have one more central element D described in the following statement.

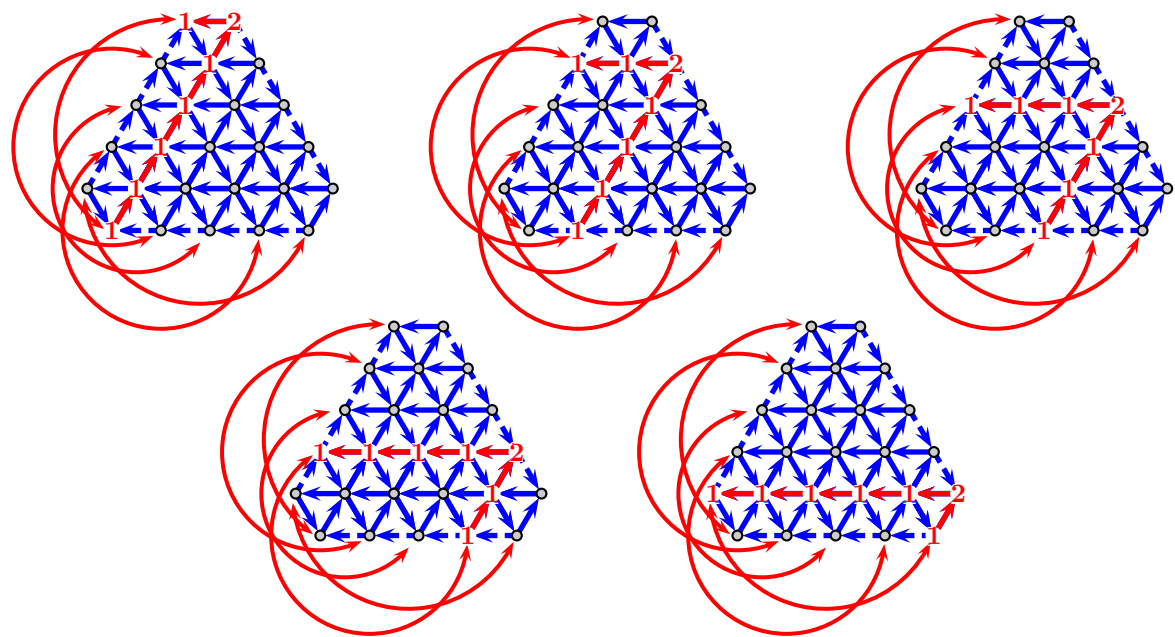


Fig. 23. Five new central elements of the main quiver for PGL_6 due to amalgamation. (We use these central elements to set all diagonal elements of the upper-triangular matrix $\mathbb{A} = M_1^{\mathrm{T}} M_2$ to be the unities.)

Lemma 6.4. The complete set of Casimirs for the reduced PGL_n -quiver with added the ("frozen") cluster variable (0,0,n) comprises all Casimirs described in Lemma 6.3 plus the element D_1 given by the following formula. Let us enumerate the plabic weights $Z_{i,j,k}$ as in Fig. 25 by three nonnegative integers (i,j,k) with i + j + k = n. Then the element

$$D_1 = \prod_{k=1}^{n} \left[\prod_{i+j=n-k} \left[Z_{i,j,k} \right]^{k/n} \right]$$
 (6.10)

is central for the subset of $Z_{i,j,k}$ with k>0. Moreover, the only elements that have nonzero homogeneous commutation relations with D_1 are $Z_{n,0,0}$ and $Z_{0,n,0}$.

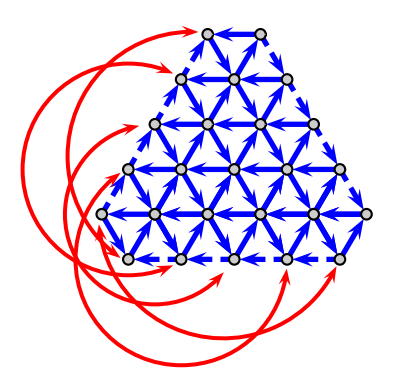


Fig. 22. The amalgamation of the quiver corresponding to the triangle $\Sigma_{0,1,3}$ (The example in the figure corresponds to PGL_6).

Casimirs for the upper-triangular matrices

Entries of the matrix $\mathbb{A} := \mathcal{M}_1^{\mathrm{T}} \mathcal{M}_2$ depend on all variables of the PGL_n -quiver, but due to the transposition, two sets of the frozen variables become amalgamated, that is, only their products appear in the entries of the matrix A. We explicitly show this amalgamation in Fig. 22.

It is easy to see that all Casimirs from Lemma 6.1 remain Casimirs in the amalgamated quiver (just four, or two, depending on the Casimir element, frozen variables become pairwise amalgamated). More, this amalgamation results in the appearance of n-1 new Casimirs; in Sec. 5 we have used these new Casimirs to eliminate the dependence of A on remaining n-1 frozen variables: diagonal entries of $\mathbb{A}=\mathcal{M}_1^T\mathcal{M}_2$ are

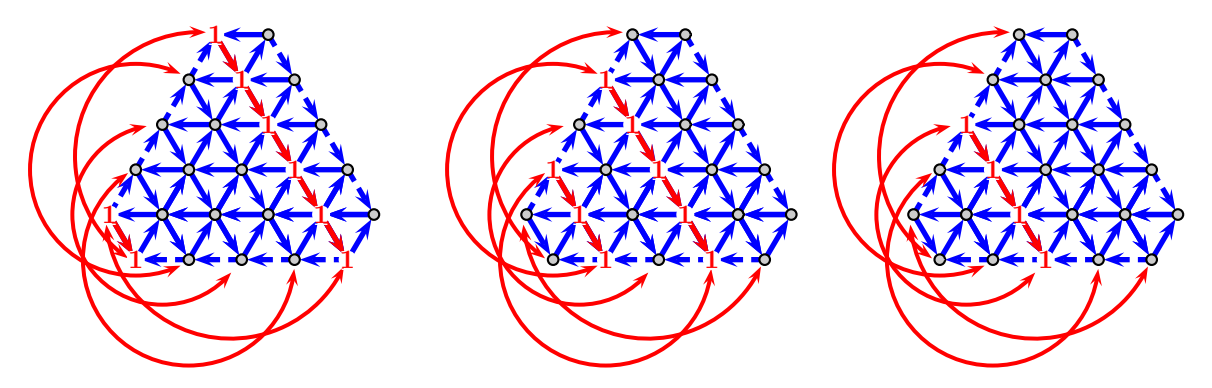


Fig. 24. Three remaining central elements of the full-rank quiver for PGL_6 after amalgamation and setting the diagonal elements of \mathbb{A} equal to unities.

particular products of these Casimirs in classical case and $q^{-1/2}$ multiplied by a product of such Casimirs in the quantum case , and we adjust the values of these Casimirs to make all diagonal elements of \mathbb{A} equal to the unities in the classical case and $q^{-1/2}$ in the quantum case (recall that all quantum Casimirs are assumed to be self-adjoint operators).

Lemma 6.5. The complete set of central elements for the amalgament quiver in Fig. 22 comprises n-1 new Casimirs depicted in Fig. 23 for the case of PGL_6 and $\left|\frac{n}{2}\right|$ central elements (products of old Casimirs with the new ones) depicted in Fig. 24.

Quantum Grassmannian and measurement maps

Non-normalized quantum transport matrices

We add additional vertices labelled (n,0,0),(0,n,0) and (0,0,n) to the quiver of Fock-Goncharov parameters Z_{abc} and construct dual planar bicolored (plabic) graph G (Figure 9). Then, we define non-normalized quantum transport matrices \mathcal{M}_1 and \mathcal{M}_2 as quantization of boundary measurement matrices of graph G introduced by Postnikov in [37]. Namely, we assign to every path P connecting a source of G to a sink a quantum weight w(P)that is element of the quantum torus Υ . We define the boundary measurement between source p and sink q as $\mathcal{M}_{pq} = \sum_{\text{path } P: p \leadsto q}$ w(P). Finally, note that G has n sources and 2n sinks, we organize boundary measurements

 \mathcal{M}_{pq} into $2n \times n$ matrix that we divide into two $n \times n$ matrices \mathcal{M}_1 and \mathcal{M}_2 .

Vertices of G are colored into black and white color as follows: a black vertex has two incoming arrows and one outgoing, while a white vertex has two outgoing and one incoming arrows.

We equip faces of Figure 25 with weights Z_{α} associated with the corresponding vertices of graph Figure 8. We define the quantum weight of a maximal oriented path in G by formula 2.11 (see Fig.25).

Example 7.1. Consider the triangular network of PGL_3 (Fig. 26)

Normalized quantum transport matrices have the following form:

$$M_{1} = \begin{pmatrix} q_{6}^{\frac{1}{6}} : (Z_{021}Z_{111})^{-\frac{1}{3}} Z_{102}^{\frac{1}{3}} Z_{012}^{-\frac{2}{3}} Z_{201}^{\frac{2}{3}} : & q_{6}^{\frac{1}{6}} : Z_{021}^{-\frac{1}{3}} (Z_{102}Z_{102})^{\frac{1}{3}} (Z_{111}^{-\frac{1}{3}} + Z_{111}^{\frac{2}{3}}) Z_{201}^{\frac{2}{3}} : & q_{6}^{\frac{1}{6}} : (Z_{102}Z_{012})^{\frac{1}{3}} (Z_{021}Z_{111}Z_{201})^{\frac{2}{3}} : \\ -q^{-\frac{5}{6}} : (Z_{021}Z_{102}Z_{111}Z_{201})^{-\frac{1}{3}} Z_{012}^{\frac{2}{3}} : & -q^{-\frac{5}{6}} : (Z_{021}Z_{102}Z_{111}Z_{201})^{-\frac{1}{3}} Z_{012}^{\frac{1}{3}} : & 0 \\ q^{-\frac{11}{6}} : (Z_{021}Z_{111}Z_{201})^{-\frac{1}{3}} (Z_{102}Z_{012})^{-\frac{2}{3}} : & 0 \end{pmatrix}.$$

$$M_1 = QSD_1^{-1}\mathcal{M}_1$$
, where $D_1 = {}^{\bullet}Z_{021}^{\frac{1}{3}}Z_{102}^{\frac{2}{3}}Z_{111}^{\frac{1}{3}}\frac{\mathbf{Z}_{003}}{\mathbf{Z}_{012}}Z_{201}^{\frac{2}{3}}{}^{\bullet}$ and

$$\mathcal{M}_{1} = \begin{pmatrix} \mathbf{Z}_{003}^{\bullet} & 0 & 0 \\ \mathbf{Z}_{003}^{\bullet} Z_{102}^{\bullet} & \mathbf{Z}_{012}^{\bullet} Z_{003}^{\bullet} Z_{102}^{\bullet} & 0 \\ \mathbf{Z}_{003}^{\bullet} Z_{102}^{\bullet} & \mathbf{Z}_{012}^{\bullet} Z_{003}^{\bullet} Z_{102}^{\bullet} & 0 \\ \mathbf{Z}_{003}^{\bullet} Z_{102}^{\bullet} & \mathbf{Z}_{012}^{\bullet} Z_{003}^{\bullet} Z_{102}^{\bullet} & \mathbf{Z}_{021}^{\bullet} Z_{012}^{\bullet} Z_{201}^{\bullet} \end{pmatrix}$$

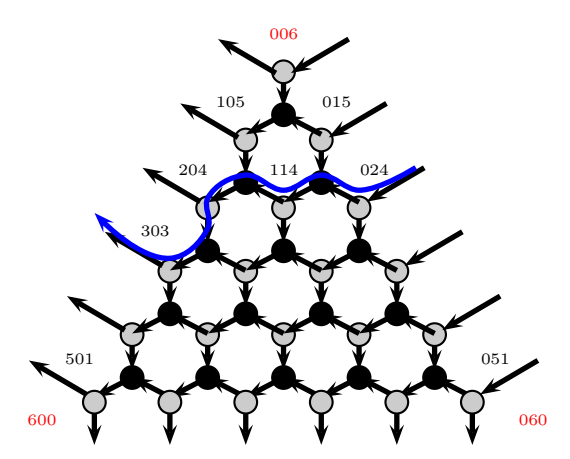


Fig. 25. Face and path weights of G. Faces are labeled by indices $i, j, k \in \mathbb{Z}$, i+j+k=6, the corresponding Fock-Goncharov face weight is denoted by Z_{ijk} . The weight w(P) of the blue path P is $w(P) = 2 C_{024} Z_{015} Z_{114} C_{006} Z_{105} Z_{204} Z_{303}$. Note that corner faces do not carry Fock-Goncharov variables and don't contribute to the normalized transport matrices M_1 and M_2 . However, they do contribute toward non-normalized transport matrices M_1 and M_2 .

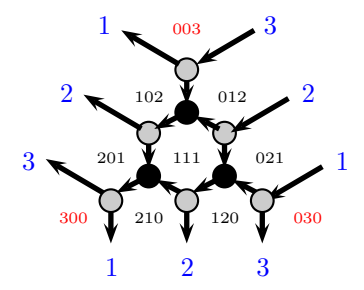


Fig. 26. Face and path weights of G_{PGL_3} . Triples $i, j, k \in \mathbb{Z}$, i + j + k = 3 label faces.

Similarly,

$$M_{2} = \begin{pmatrix} 0 & 0 & q^{\frac{1}{6}:}(Z_{210}Z_{111}Z_{012})^{\frac{1}{3}}(Z_{120}Z_{021})^{\frac{2}{3}:} \\ 0 & -q^{-5/6}:(Z_{210}Z_{111}Z_{012})^{\frac{1}{3}}(Z_{120}Z_{021})^{-\frac{1}{3}:} & -q^{-\frac{5}{6}:}(Z_{210}Z_{111}Z_{012})^{\frac{1}{3}}Z_{120}^{\frac{2}{3}}Z_{021}^{\frac{2}{3}:} \\ q^{-\frac{11}{6}:}(Z_{210}Z_{111}Z_{012})^{-\frac{2}{3}}(Z_{120}Z_{021})^{-\frac{1}{3}:} & q^{-\frac{11}{6}:}Z_{210}^{-\frac{2}{3}}(Z_{111}^{-\frac{2}{3}}Z_{111}^{\frac{2}{3}}Z_{120}^{\frac{2}{3}}Z_{021}^{-\frac{1}{3}:} & q^{-\frac{11}{6}:}Z_{210}^{-\frac{2}{3}}(Z_{111}Z_{012})^{\frac{1}{3}}Z_{120}^{-\frac{1}{3}}Z_{021}^{\frac{2}{3}:} \end{pmatrix}$$

$$M_{2} = QS^{\bullet} D_{1}^{-1} D_{2}^{-1 \bullet} \mathcal{M}_{2}, \text{ where } D_{2} = \mathcal{Z}_{300}Z_{201}^{2/3}Z_{102}^{1/3}Z_{102}^{1/3}Z_{210}^{1/3}Z_{111}^{1/3}Z_{120}^{1/3} \bullet = \tau(D_{1}) \text{ and}$$

$$\mathcal{M}_{2} = \begin{pmatrix} \mathcal{Z}_{003}Z_{300}Z_{201}Z_{102}^{\bullet}, & \mathcal{Z}_{003}Z_{300}(1+Z_{111})Z_{012}Z_{201}Z_{102}^{\bullet}, & \mathcal{Z}_{003}Z_{300}Z_{210}Z_{111}Z_{012}Z_{201}Z_{102}^{\bullet}, \\ 0 & \mathcal{Z}_{003}Z_{300}Z_{210}Z_{210}Z_{210}Z_{210}Z_{210}Z_{211}Z_{201}Z_{102}^{\bullet}, \\ 0 & \mathcal{Z}_{003}Z_{300}Z_{210}Z_{210}Z_{210}Z_{211}Z_{211}Z_{201}Z_{102}^{\bullet}, \\ \mathcal{Z}_{003}Z_{300}Z_{210}Z_{210}Z_{210}Z_{211}Z_{211}Z_{201}Z_{102}^{\bullet}, \\ \mathcal{Z}_{003}Z_{300}Z_{210}Z_{210}Z_{210}Z_{211}Z_{211}Z_{201}Z_{102}^{\bullet}, \\ \mathcal{Z}_{003}Z_{300}Z_{210}Z_{210}Z_{210}Z_{211}Z_{211}Z_{201}Z_{102}^{\bullet}, \\ \mathcal{Z}_{003}Z_{300}Z_{210}Z_{210}Z_{210}Z_{211}Z_{211}Z_{201}Z_{102}^{\bullet}, \\ \mathcal{Z}_{003}Z_{300}Z_{210}Z_{210}Z_{210}Z_{211}Z_{211}Z_{201}Z_{201}Z_{102}^{\bullet}, \\ \mathcal{Z}_{003}Z_{300}Z_{210}Z_{210}Z_{210}Z_{210}Z_{210}Z_{210}Z_{210}Z_{210}^{\bullet}Z_{201}Z_{102}^{\bullet}, \\ \mathcal{Z}_{003}Z_{300}Z_{210}Z_{210}Z_{210}Z_{210}Z_{210}Z_{210}Z_{210}Z_{210}Z_{201}Z_{102}^{\bullet}, \\ \mathcal{Z}_{003}Z_{300}Z_{210}Z_{210}Z_{210}Z_{210}Z_{210}Z_{210}Z_{210}Z_{210}Z_{210}^{\bullet}Z_{210}^{\bullet}Z_{210}^{\bullet}, \\ \mathcal{Z}_{003}Z_{000$$

Notice that both \mathcal{M}_1 and \mathcal{M}_2 are non-normalized quantum transport matrices of network shown on Figure 26.

7.2 Quantum Grassmannian and proofs of Theorems 2.12 and 3.2

We now prove Theorems 2.12 and 3.2 utilizing the notion of plabic graphs introduced by Postnikov in [37].

Following [37] we call a *planar network* an embedded in the disk D oriented graph with trivalent vertices inside D (which are neither sources nor sinks) and univalent sources and sinks on the boundary ∂D (sources are

separated from sinks) and whose faces are equipped with weights. We assume that the both sets of boundary vertices: the set of sources and the set of sinks are nonempty. An example of such planar network N is drawn on Figure 27 in rectangle R with sources on the right side and sinks on the left side.

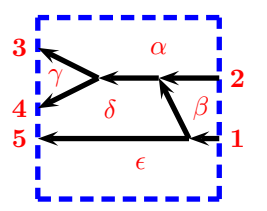


Fig. 27. Network N in rectangle R.

Denote by Faces(N) the set of faces of network N. Faces in Figure 27 are labelled by Greek letters, namely, $Faces(N) = \{\alpha, \beta, \gamma, \delta, \epsilon\}$. Represent Faces(N) as a disjoint union of two subsets Faces(N) = $Faces_B(N) \stackrel{.}{\cup} Faces_I(N)$ where $Faces_B(N)$ contains all faces adjoined to the boundary ∂D and $Faces_I(N)$ contains the faces which are not adjoined to ∂D . In Figure 27, $Faces(N) = Faces_B(N) = \{\alpha, \beta, \gamma, \delta, \epsilon\}$, $Faces_I(N) = \emptyset$. Consider the integer lattice $\hat{\Lambda}$ which is a free abelian group whose generators are elements of Faces(N) and vector space $\tilde{V} = \mathbb{Q} \otimes \tilde{\Lambda}$. We equip $\tilde{\Lambda}$ with the integer skew-symmetric form \langle , \rangle as described below. Note that the form on $\tilde{\Lambda}$ induces a form on \tilde{V} which we will also denote as $\langle \ , \ \rangle$.

Definition 7.3. [37] A planar bicolored graph, or simply a plabic graph is a planar (undirected) graph G, without orientations of edges, such that each boundary vertex b_i is incident to a single edge and all internal vertices are colored either black or white. A perfect orientation of a plabic graph is a choice of orientation of its edges such that each black internal vertex v is incident to exactly one edge directed away from v; and each white v is incident to exactly one edge directed towards v. A plabic graph is called perfectly orientable if it has a perfect orientation.

Let us transform the oriented graph G of network into plabic graph G^{pl} by coloring inner vertices of G into black and white colors according to the rule: black vertex has two incoming arcs and one outgoing; white vertex has one incoming and two outgoing. We forget boundary sources and sinks so that any arcs connecting inner vertex to the boundary one becomes a half-arc (see Fig. 29). For a plabic graph G^{pl} we define an oriented dual graph $(G^{pl})^*$ as follows. Vertices of $(G^{pl})^*$ are faces of G^{pl} . For every black and white vertex x of G^{pl} we define 3 arcs of $(G^{pl})^*$ that cross half-edges attached to x in counterclockwise direction if x is black and clockwise direction if x is white (see Fig. 28).



Fig. 28. Dashed blue arcs are edges of the dual graph $(G^{pl})^*$ around black and white vertex of G^{pl} .

For $\theta, \phi \in Faces(N)$ let $\#(\theta \to \phi)$ denote the number of arcs from θ to ϕ in $(G^{pl})^*$. The skew-symmetric form $\langle \ , \ \rangle$ on $\tilde{\Lambda}$ is defined by the formula

$$\langle \theta, \phi \rangle = \frac{1}{2} \left(\#(\theta \to \phi) - \#(\phi \to \theta) \right). \tag{7.11}$$

Example 7.4. The plabic graph and its dual for the network Fig. 27 are shown on the Fig. 29.

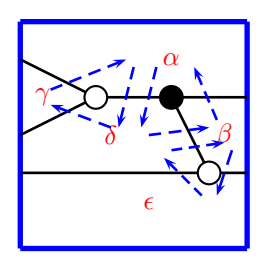


Fig. 29. Arcs of plabic graph G^{pl} corresponding to network N on Fig. 27 are black solid lines; arcs of its dual $(G^{pl})^*$ are dashed blue arrows. Then, $\langle \alpha, \beta \rangle = -1/2, \langle \alpha, \delta \rangle = 1, \langle \alpha, \gamma \rangle = -1/2, \langle \beta, \epsilon \rangle = 1/2, \langle \beta, \delta \rangle = -1, \langle \gamma, \delta \rangle = -1/2, \langle \delta, \epsilon \rangle = -1/2$.

Let \mathbb{Z} -lattice $\tilde{\Lambda}$ be generated as an abelian group by elements of Faces(N) equipped with the skewsymmetric integer form $\langle \ , \ \rangle$, $\tilde{\Upsilon}$ be the corresponding quantum torus, and $(\tilde{\Upsilon})^{1/n}$ be the quantum torus corresponding to $\frac{1}{n}\tilde{\Lambda}$. It is well-known that a quantum torus is an Øre domain [1] and we denote by the $\tilde{\mathcal{F}}$ the corresponding non-commutative fraction field.

Set $\sigma = \sum_{\theta \in Faces(N)} \theta \in \frac{1}{n}\tilde{\Lambda}$. Let V be the quotient space $V = \tilde{V}/\sigma$ and $\Lambda = \tilde{\Lambda}/\sigma$ be the induced integer lattice in V. Note that σ lies in the kernel of the skew-symmetric form and its push forward to V is well-defined. Abusing notation we will use $\langle \ , \ \rangle$ for the induced skew-symmetric form on V. Dual lattice $\Lambda^* = \operatorname{Hom}(\Lambda, \mathbb{Z})$.

We construct quantum torus Υ ($\Upsilon^{1/n}$) associated with the lattice $\Lambda(\frac{1}{n}\Lambda)$. Observe that Z_{σ} belongs to the center $Z(\Upsilon^{1/n})$ and $Z_{\sigma}-1$ can be factored as $(Z_{\sigma}^{\frac{1}{n}}-1)((Z_{\sigma}^{\frac{1}{n}})^{n-1}+(Z_{\sigma}^{\frac{1}{n}})^{n-2}+\cdots+1)$. Define the non-commutative localization $\mathcal{F}=\Psi^{-1}\Upsilon^{1/n}$ where Ψ is a complement in $\Upsilon^{1/n}$ to the minimal two-sided ideal containing all zero divisors. Elements of \mathcal{F} can be written as elements of $\tilde{\mathcal{F}}$ modulo the relation $Z_{\sigma} = 1$.

It was mentioned in the proof of Corollary 4.3 that every face weight $Z_{\alpha} \in \tilde{\mathcal{F}}$ corresponding to a face $\alpha \in Faces(N)$ is a self-adjoint operator in $L^2(\mathbb{R}^d)$ having a continuous spectrum $(0,\infty)$. Then a rational $\frac{k}{\ell}$ -power $(Z_{\alpha})^{\frac{k}{\ell}}$ is a self-adjoint operator with positive spectrum.

We call a plabic network with weights in \mathcal{F} a quantum network.

Let p be the maximal oriented path from a source i on the right to the sink j on the left of a network. Complete p to an oriented loop \tilde{p} by following path p from i to j first and then closing the loop following the piece of boundary of the rectangle in the clockwise direction from j to i.

The oriented loop \tilde{p} defines a covector $\tilde{p} \in \Lambda^*$ as follows. (We use the same notation for the loop and induced covector.) Let \mathbf{r} be a half infinite ray with starting point inside face α and directed towards infinity and q_1, \ldots, q_s be intersection points of \mathbf{r} and loop \tilde{p} , $T_{\mathbf{r}}$ be the unit direction vector of \mathbf{r} , $T_{q_i}\tilde{p}$ is the unit tangent vector to \tilde{p} at q_j . We assume that \mathbf{r} is chosen generic, i.e., for all q_j vectors $T_{\mathbf{r}}$ and $T_{q_j}\tilde{p}$ are linearly independent.

We define the intersection index $ind_{q_j}(\tilde{p}, \mathbf{r})$ of \tilde{p} and \mathbf{r} at q_j to be 1 if orientation of basis $(T_{q_j}\tilde{p}, T_{\mathbf{r}})$ coincides with counterclockwise orientation of the plane and -1 otherwise and define $\tilde{p}(\alpha) = \sum_{j=1}^{s} ind_{q_j}(\tilde{p}, \mathbf{r})$. Note that $\tilde{p}(\alpha)$ depends neither on exact position of starting point of **r** provided that the starting point varies inside the same connected component of complement to \tilde{p} nor on the particular choice of ray **r** with the same starting point. Since any face α lies entirely in some connected component of \tilde{p} we conclude that $\tilde{p}(\alpha)$ is well defined. Clearly, $\tilde{p} \in \Lambda^*$.

Assign to any path p a vector $\mathbf{v}_p = \sum_{\alpha \in Faces(N)} \tilde{p}(\alpha) \alpha \in \Lambda$. In the example in Section 2.5 where any maximal oriented path p is non-selfintersecting the vector \mathbf{v}_p is the sum of all faces to the right from the path. Set the weight w_p of the path p as $w_p = Z_{\mathbf{v}_p}$.

Let S be the set of all sources of N, F be the set of all sinks. Define for any source $a \in S$ and sink $b \in F$ a quantum boundary measurement $Meas_q(a,b) = \sum_{p:a \leadsto b} (-1)^{cross(p)} w_p$, where the sum is taken over all oriented paths p from a to b where the $crossing\ index\ cross(p)$ is the number of self-crossings of the path p. Classical boundary measurement is defined by Postnikov in [37], For the network in Section 2.5, no path is selfcrossing and $Meas_q(a,b) = \sum_{p:a \sim b} w_p$.

Let n = |S|, m = |F|. Define an $m \times n$ matrix Q_q of quantum boundary measurements as $(Q_q)_{ba} =$ $(Meas_q(a,b))_{a\in S,b\in F}$. Note that we label rows of Q_q by sinks and columns by sources of N.

In Example 27, the matrix
$$Q_q = \begin{pmatrix} Z_{\alpha+\beta} & Z_{\alpha} \\ Z_{\alpha+\beta+\gamma} & Z_{\alpha+\gamma} \\ Z_{\alpha+\beta+\gamma+\delta} & 0 \end{pmatrix}$$
. Define $(m+n) \times n$ quantum grassmannian boundary measurement matrix $Q_q^{gr}(N)$ of network N (we also

will denote it by Q_q^{gr} if it does not create a confusion). Columns of Q_q^{gr} are labelled by boundary sources

of network; rows are labelled by all boundary vertices. To describe matrix elements of \ddot{Q}_q we introduce the order of boundary vertex $b \in N$, denoted by $ord_N(b)$ (or, simply ord(b)). Enumerate all boundary vertices of N from 1 to m+n in counterclockwise direction. Let $b \in [1, m+n]$ be the index of boundary vertex. Let $\sigma(b)$ be the number of sources among boundary vertices with indices from 1 to b-1. The order is defined by the

formula $ord(b) = \begin{cases} \sigma(b), & \text{if } b \text{ is not a source;} \\ \sigma(b) + \frac{1}{2}, & \text{if } b \text{ is a source.} \end{cases}$. Let $\mathbb{J}(i) \in [1, m+n]$ be the index of ith source, $i \in [1, n]$; $\mathbb{J}: [1, n] \to [1, m+n]$ is an increasing function.

We define
$$(Q_q^{gr})_{ji} = \begin{cases} (-1)^{i+ord(j)}q^{-ord(j)} Meas_q(i,j), & \text{if } j \text{ is not a source;} \\ q^{-ord(j)}\delta(\mathbb{J}(i),j), & \text{otherwise.} \end{cases}$$

Example 7.5. In Example 27 , the matrix
$$Q_q^{gr} = \begin{pmatrix} q^{-1/2} & 0 \\ 0 & q^{-3/2} \\ -q^{-2}Z_{\alpha+\beta} & q^{-2}Z_{\alpha} \\ -q^{-2}Z_{\alpha+\beta+\gamma} & q^{-2}Z_{\alpha+\gamma} \\ -q^{-2}Z_{\alpha+\beta+\gamma+\delta} & 0 \end{pmatrix}$$
.

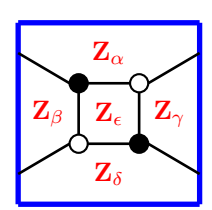
Remark 7.6. In [37] a boundary measurement map is defined as a map Meas from the space $Net_{m\times n}$ of networks with n sources, m sinks and commutative weights to Gr(n, m+n). For each $X \in \text{Net}_{m \times n}$, boundary measurements $\operatorname{Meas}(i,j)$ form an $(m+n) \times n$ matrix Q^{gr} which represents $\operatorname{Meas}(X)$. The space of $(m+n) \times n$ matrices with elements in Υ_N we denote by $\mathrm{Mat}_{(m+n)\times n}(\Upsilon_N)$ and the all invertible $n\times n$ matrices with entries from Υ_N form the group $GL_n(\Upsilon_N)$. We say that an $(m+n)\times n$ matrix $W\in \mathrm{Mat}_{(m+n)\times n}(\Upsilon_N)$ has rank n if there is an element $G \in GL_n(\Upsilon_N)$ such that $W \cdot G$ has an $n \times n$ submatrix with nonzero terms on the main diagonal and zeros everywhere else. The set of all $(m+n) \times n$ matrices of rank n is denoted by $Mat^n_{(m+n)\times n}(\Upsilon_N)$

The group $GL_n(\Upsilon_N)$ of invertible $n \times n$ matrices with entries from Υ_N acts on $\operatorname{Mat}^n_{(m+n)\times n}(\Upsilon_N)$ by the right multiplication. We define the homogeneous space $Gr_q(n, m+n)$ as the right quotient $Gr_q(n, m+n) =$ $\operatorname{Mat}_{(m+n)\times n}^n(\Upsilon_N)/GL_n(\Upsilon_N)$. For a given oriented graph embedded into disk with n sources and m sinks $n \leq m$ consider all possible networks with weights assigned to the arrows of the graph. The rank of the corresponding boundary measurement matrix does not depend on the choice of weights but depends only on the graph itself. In particular, if there is a collection of n non-crossing oriented paths connecting all n sources to some n-element subset of sinks (as on Fig.29) then the rank of any network on this graph is n. We call such graphs and associated networks maximal. In what follows, we assume that the graph N is maximal. We denote by $QNet_{m\times n}$ the space of such maximal quantum networks with n sources, m sinks and quantum weights from Υ_N . We define a quantization $\operatorname{Meas}_q: QNet_{m\times n} \to Gr_q(m,m+n)$ as the composition $QNet_{m\times n} \to Mat_{(m+n)\times n}(\Upsilon_N) \to Gr_q(n, m+n).$

Definition 7.7. Two networks are *equivalent* if they have the same boundary measurements.

Simple equivalence relations (M1-M3,R1-R3) on the space of networks ([37]) are simple local network transformations preserving boundary measurements. Please, note that in the figures below we draw the plabic graph assuming that it is equipped with a perfect orientation. Different choices of compatible perfect orientation give the same result.

The following claims generalize similar statements for commuting weights (cf [37]). Define 6 elementary moves (M1-M3), (R1-R3) as shown below.



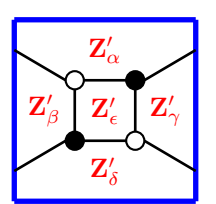


Fig. 30. Elementary move M1: $Z'_{\epsilon} = Z_{-\epsilon}$, $Z'_{\delta} = Z_{\delta} + Z_{\delta+\epsilon}$, $Z'_{\alpha} = Z_{\alpha} + Z_{\alpha+\epsilon}$, $Z'_{\beta} = \sum_{j=1}^{\infty} (-1)^{j-1} Z_{\beta+j\epsilon}$, $Z'_{\gamma} = \sum_{j=1}^{\infty} (-1)^{j-1} Z_{\beta+j\epsilon}$ $\sum_{j=1}^{\infty} (-1)^{j-1} Z_{\gamma+j\epsilon}.$

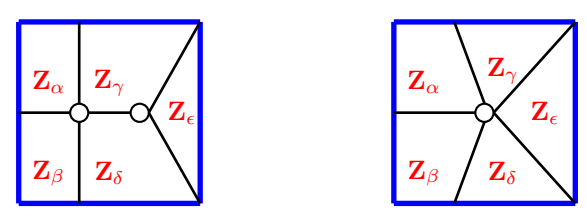


Fig. 31. Elementary move M2.

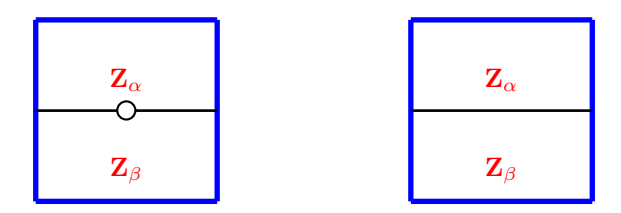


Fig. 32. Elementary move M3.

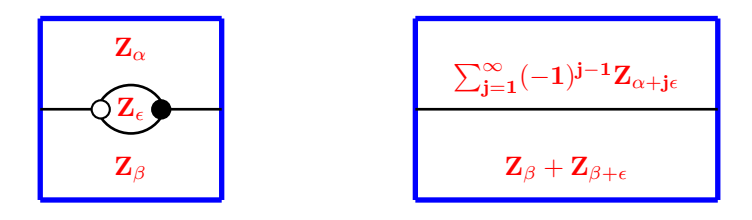


Fig. 33. Elementary move R1.

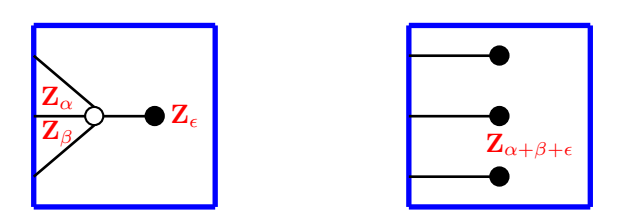


Fig. 34. Elementary move R2.

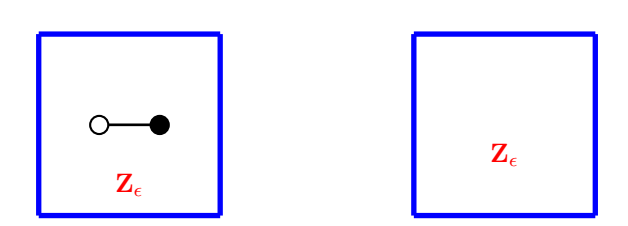


Fig. 35. Elementary move R3.

The corresponding (move) equivalence is called *quantum* (move) equivalence.

The following result extends the results of [37] to quantum networks.

Lemma 7.9. Two quantum move equivalent networks are quantum equivalent.

Proof. The proof follows [37]. Compared to the commutative case we just need to check one additional condition that elementary moves transform families of face parameters satisfying commutation relations (2.1) into families of face parameters satisfying the same relations. The cases R2.R3, M2, and M3 are evident. Let's consider M1 and R1. The case M1 is proved in [18]. We give the proof here for completeness.

We want to show that $Z'_{\alpha}, Z'_{\beta}, Z'_{\gamma}, Z'_{\delta}$ and Z'_{ϵ} q-commute. Note that $\langle \alpha, \beta + (k+1)\epsilon \rangle = \langle \alpha, \beta \rangle - (k+1) = \langle \alpha + \epsilon, \beta + k\epsilon \rangle$, hence $Z'_{\alpha}Z'_{\beta} = (Z_{\alpha} + Z_{\alpha+\epsilon})$ $\sum_{j=1}^{\infty} (-1)^{j-1} Z_{\beta+j\epsilon} = q^{\langle \alpha, \beta+\epsilon \rangle} Z_{\alpha+\beta+\epsilon}$ while $Z'_{\beta}Z'_{\alpha} = q^{-\langle \alpha, \beta+\epsilon \rangle} Z_{\alpha+\beta+\epsilon}$. Therefore, $Z'_{\beta}Z'_{\alpha} = q^{-2\langle \alpha, \beta+\epsilon \rangle} Z'_{\alpha}Z'_{\beta}$. Commutation relations for all other pairs of parameters can be checked similarly.

Different perfect orientations are in one-to-one correspondence with the almost perfect matchings (see [38]). Up to evident symmetries, there are only two essentially different almost perfect matchings and, hence, we need to check two perfect orientations. The straightforward computation shows that the elementary move M1 does not change measurements for any choice of perfect orientation.

The case R1 is similar.

Definition 7.10. ([37]) We say that a plabic network (or graph) is reduced if it has no isolated connected components and there is no network/graph in its move-equivalence class to which we can apply a reduction (R1) or (R2).

The following statements are proved in [37].

Lemma 7.11. [37] Any network is move equivalent to a *reduced* network.

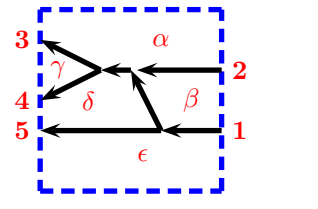
Lemma 7.12. [37] Two reduced equivalent networks are (M1-M3)-move equivalent.

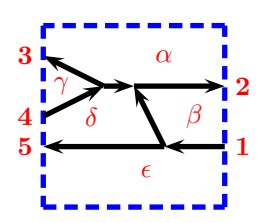
Definition 7.13. We call a maximal simple oriented path $P = (p_0, p_1, \dots, p_h), p_i \neq p_j$ for all $i \neq j$ unequivocal if there is no oriented path $(p_k, q_1, \dots, q_t, p_\ell)$ such that $q_s \neq p_r$ for all $1 \leq s \leq t$ and $0 \leq r \leq h$.

Let P be an unequivocal path in a network $N \in \text{Net}_{m,n}$. Reverse the orientation of P keeping face weights we obtain the new network N'.

Lemma 7.14. Reversing the orientation of unequivocal path P does not change quantum grassmannian measurement $\operatorname{Meas}_{a}(N') = \operatorname{Meas}_{a}(N)$.

Example 7.15. Consider networks on the Fig. 36.





Changing orientation of the path $P: \mathbf{2} \leadsto \mathbf{4}$ transforms network N on the left into network N' on the right

The corresponding quantum grassmannian measurement matrices are

$$Q_q^{gr} = \begin{pmatrix} q^{-1/2} & 0 \\ 0 & q^{-3/2} \\ -q^{-2}Z_{\alpha+\beta} & q^{-2}Z_{\alpha} \\ -q^{-2}Z_{\alpha+\beta+\gamma} & q^{-2}Z_{\alpha+\gamma} \\ -q^{-2}Z_{\alpha+\beta+\gamma+\delta} & 0 \end{pmatrix} \text{ and } \begin{pmatrix} Q_q^{gr} \end{pmatrix}' = \begin{pmatrix} q^{-1/2} & 0 \\ q^{-1}Z_{\beta} & q^{-1}Z_{\delta+\epsilon+\beta} \\ 0 & q^{-1}Z_{-\gamma} \\ 0 & q^{-3/2} \\ -q^{-2}Z_{\alpha+\beta+\gamma+\delta} & 0 \end{pmatrix}.$$

Note that
$$Q_q^{gr}C = (Q_q^{gr})'$$
, where $C = \begin{pmatrix} 1 & 0 \\ q^{1/2}Z_{\beta} & q^{1/2}Z_{\delta+\epsilon+\beta} \end{pmatrix}$.

Indeed, consider for example $(Q_q^{gr}C)_{31} = (Q_q^{gr})_{31} + q^{1/2}(Q_q^{gr})_{32}Z_{\beta} = -q^{-2}Z_{\alpha+\beta} + q^{-3/2}Z_{\alpha}Z_{\beta}$. Recall that $Z_{\alpha}Z_{\beta}=q^{-1/2}Z_{\alpha+\beta}$. Therefore, $(Q_q^{gr}C)_{31}=0=(Q_q^{gr})_{31}'$. Similarly, we can prove equalities for all the entries of these 5×2 matrices and we observe that $\mathrm{Meas}_q(N)=\mathrm{Meas}_q(N')\in\mathrm{Gr}_q(2,5)$.

Proof of Lemma 7.14. Let N' be the network obtained as a result of the change of the directions of all arrows of the simple unequivocal path P in N from a boundary vertex a to a boundary vertex b. We will denote by P^{-1} the path in N' obtained from P by orientation reversing. We assume first that the boundary vertices are labelled so that $1 \le a < b \le m + n$. Since path P is unequivocal there is only one path P from a to b, and $Q_q(a,b) = w_P$. Moreover, any other path R from s to t where both s and t are distinct from a and b has at most one common interval [V, W] with path P. The first point V (counting from s) where two paths meet has two incoming arrows and one outgoing and, hence, is colored black, the point W where two paths separate is white (see Figure 37). Similarly, any path from a to a sink different from b separates from P at a white point; any path from a sink different from a to b joins path P at a black point.

Let Q_q^{gr} be the quantum grassmannian bounded measurement matrix of the network N, $(Q_q^{gr})'$ be the quantum grassmannian boundary measurement matrix of N'. Let $F_P \subset Faces$ denote the subset of all faces to the right of the path P, $\mathbf{v}_P = \sum_{\alpha \in F_p} \alpha$. Then, $w_P = Z_{\mathbf{v}_P}$, $F_{P^{-1}} = Faces \setminus F_P$, $\mathbf{v}_{P^{-1}} = -\mathbf{v}_P$, $w_{P^{-1}} = Z_{\mathbf{v}_{P^{-1}}} = Z_{-\mathbf{v}_{P}} = (w_{P})^{-1}.$ Consider first the case $1 \le a < b$.

Let s < a < t < b in the cyclic order of the boundary vertices (see Figure 37). Observe, $w_{b \to W \to t} =$ Let s < d < t < b in the cyclic order of the boundary vertices (see Figure 31). Observe, $w_{b \to W \to t} = Z_{\alpha+\beta+\delta} = {}^{\bullet}Z_{\beta+\delta}Z_{\alpha \bullet} = {}^{\bullet}w_{a \to V \to W \to t} \cdot w_{a \to V \to W \to b}^{-} = {}^{\bullet}w_{a \to V \to W \to t} \cdot (Q'_q)_{ab} {}^{\bullet}$. Since the equality holds for any directed path from b to t, and ${}^{\bullet}(Q'_q)_{ab}(Q_q)_{ta} {}^{\bullet} = {}^{\bullet}(Q_q)_{ta}(Q_q)_{ba}^{-1} {}^{\bullet} = q^{-1/2}(Q_q)_{ta}(Q_q)_{ba}^{-1}$, we conclude that $(Q'_q)_{tb} = {}^{\bullet}(Q'_q)_{ab}(Q_q)_{ta} {}^{\bullet} = {}^{\bullet}(Q_q)_{ba}^{-1}(Q_q)_{ta} {}^{\bullet} = q^{-1/2}(Q_q)_{ta}(Q_q)_{ba}^{-1}$. Similarly, $(Q'_q)_{ab} = {}^{\bullet}(Q'_q)_{ab}(Q_q)_{bs} {}^{\bullet} = {}^{\bullet}(Q_q)_{ba}^{-1}(Q_q)_{bs} {}^{\bullet} = {}^{\bullet}(Q_q)_{bs}(Q'_q)_{tb} {}^{\bullet} = q^{1/2}(Q_q)_{bs}(Q'_q)_{tb} {}^{\bullet} = q^{1/2}(Q'_q)_{bs}(Q'_q)_{tb} {}^{\bullet} = q^{1/2}(Q'_q)_{tb} {}^$

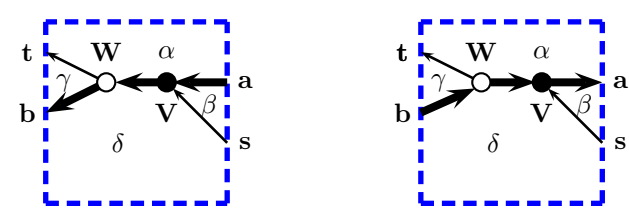


Fig. 37. Change of the orientation of the path $P : \mathbf{a} \leadsto \mathbf{b}$, s < a < t < b.

In the same way we investigate all the remaining mutual positions of s, t and $1 \le a < b$ which leads to the following matrix identity. Let $a_0 = \mathbb{J}^{-1}(a)$, f_0 be the index of source of X such that b lies between the source f_0 and $f_0 + 1$ (equivalently, $\mathbb{J}(f_0) < b < \mathbb{J}(f_0 + 1)$. Note that $a_0 \le f_0$ since a < b. Define $n \times n$ matrix C for 1 < a < b as follows

$$C_{ij} = \begin{cases} \delta_{ij}, & \text{if } i < a_0 \text{ or } i > f_0; \\ (-1)^{\lfloor |j-a_0+1/2| \rfloor} q^{1/2} (Q_q)_{ja} (Q_q)_{ba}^{-1} & \text{if } i = a_0; \\ q \delta_{i-1,j}, & \text{if } a_0 < i \le f_0. \end{cases}$$

Then, $(Q_q^{gr})' = Q_q^{gr}C$.

To study $1 \leq b < a$, note that $\left(Q_q^{gr}\right)' = Q^{gr} \cdot C$ implies $Q_q^{gr} = \left(Q_q^{gr}\right)' \cdot C^{-1}$ where C^{-1} is obtained from Cby changing the signs of the off-diagonal elements and adjusting the powers of q. More exactly, define $n \times n$ matrix C for 1 < b < a as follows

$$\widetilde{C}_{ij} = \begin{cases} \delta_{ij}, & \text{if } i \leq f_0 \text{ or } i > a_0; \\ (-1)^{\lfloor |j-a_0-1/2| \rfloor} q^{-1/2} (Q_q)_{ja} (Q_q)_{ba}^{-1} & \text{if } i = a_0; \\ q^{-1} \delta_{i+1,j}, & \text{if } f_0 < i < a_0. \end{cases}$$

This observation proves Lemma 7.14 $1 \le b < a$.

Proof. Now we will give another proof of groupoid relation (part (iii) of Theorem 3.2). Consider the network for $\mathcal{P}_{PGL_n,\Sigma}$ shown for n=6 in Figure 25. The boundary measurement matrix Q_q^{gr} has size $3n \times n$. The top $n \times n$ part $U = (Q_q^{gr})_{[1,n]}$ is the diagonal matrix with jth diagonal elements $q^{-j+\frac{1}{2}}$; the middle part of the quantum grassmannian matrix $(Q_q^{gr})_{[n+1,2n]} = q^{-n}\mathcal{M}_1S$; and the bottom part $(Q_q^{gr})_{[2n+1,3n]} = q^{-n}\mathcal{M}_2S$. Let's change the orientation of all snakelike right to left horizontal paths of the network Fig. 25. The result

is shown on the Fig. 38.

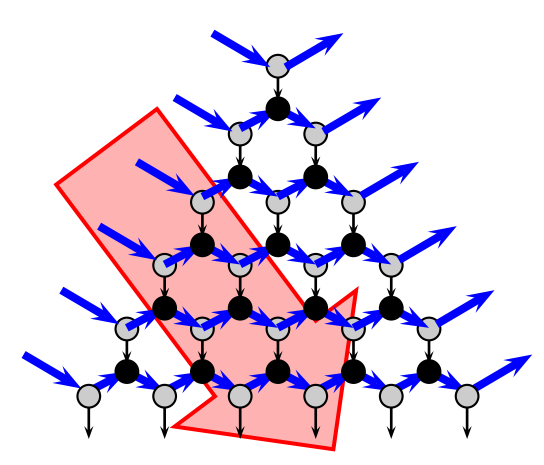


Fig. 38. This network is obtained by the simultaneous change of orientations of the snakelike horizontal bold paths (colored blue). The big arrow shows the direction of non-normalized transport matrix \mathcal{M}_3 .

The orientation change of all bold paths (see Figure 38) leads to the new quantum grassmannian measurement $(Q_q^{gr})'$. Its middle part is the submatrix $((Q_q^{gr})'_{[n+1,2n]} = U$, the bottom $n \times n$ part $((Q_q^{gr})'_{[2n+1,3n]} = q^{-n}\mathcal{M}_3S$. Using the fact that Q_q^{gr} and $(Q_q^{gr})'$ represent the same quantum grassmann element, we obtain $q^{-n}\mathcal{M}_1SC = U$, $q^{-n}\mathcal{M}_2SC = q^{-n}\mathcal{M}_3S$. Find C from the first equation: $C = S^{-1}\mathcal{M}_1^{-1}q^nU$. Substituting the expression for C into second equation we obtain $\mathcal{M}_2 = \mathcal{M}_3SU^{-1}q^{-n}\mathcal{M}_1$. Note that $US = SU^{-1}q^{-n}$, then

$$US\mathcal{M}_2 = (US\mathcal{M}_3)(US\mathcal{M}_1). \tag{7.12}$$

Recall now that $M_1 := q^{\frac{1}{2n}} U S \mathcal{M}_1 D_i^{-1}, \ M_3 := q^{\frac{1}{2n}} U S \mathcal{M}_1 D_2^{-1}, \ M_2 := q^{\frac{1}{2n}} U S \mathcal{M}_1 \bullet_0^{-1} D_2^{-1} \bullet$. Equation 7.12 implies $q^{\frac{1}{2n}} U S \mathcal{M}_2 = q^{-\frac{1}{2n}} (q^{\frac{1}{2n}} U S \mathcal{M}_3) (q^{\frac{1}{2n}} U S \mathcal{M}_1)$. Multiplying both sides by $\bullet D_1^{-1} D_2^{-1} \bullet$ on the right we obtain $M_2 = q^{-\frac{1}{2n}} (q^{\frac{1}{2n}} U S \mathcal{M}_3) (q^{\frac{1}{2n}} U S \mathcal{M}_1) \bullet_0^{-1} D_2^{-1} \bullet = q^{-\frac{1}{2n} - \frac{1}{2n}} (q^{\frac{1}{2n}} U S \mathcal{M}_3) (q^{\frac{1}{2n}} U S \mathcal{M}_1) D_1^{-1} D_2^{-1} = q^{-\frac{1}{2n} - \frac{1}{2n}} (q^{\frac{1}{2n}} U S \mathcal{M}_1) (q^{\frac{1}{2n}} U S \mathcal{M}_1) D_1^{-1} D_2^{-1} = q^{-\frac{1}{2n} - \frac{1}{2n}} (q^{\frac{1}{2n}} U S \mathcal{M}_1) (q^{\frac{1$ $q^{-\frac{1}{2n}-\frac{1}{2n}+\frac{1}{n}}(q^{\frac{1}{2n}}US\mathcal{M}_3D_1^{-1})(q^{\frac{1}{2n}}US\mathcal{M}_1)D_2^{-1}$. We conclude that $M_2=M_3M_1$.

This is clearly equivalent to the second part of Theorem 3.2
$$T_1T_2T_3 = 1$$
.

Commutation relations between face weights induce R-matrix commutation relations between entries of Q_q as described in the next lemma.

Lemma 7.16.
$$R_m \overset{1}{Q_q} \otimes \overset{2}{Q_q} = \overset{2}{Q_q} \otimes \overset{1}{Q_q} R_n$$
, where R_m, R_n are given by formula 2.13.

Proof. We will prove this statement using factorization of matrix Q_q into a product of elementary matrices. Let N_1 be a network in rectangle with m sinks on the left and n sources on the right. N_1 can be presented as a concatenation of elementary networks of two special kinds.

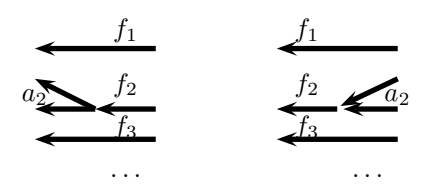


Fig. 39. Elementary forks

The boundary measurement matrix for each of the elementary piece (Fig. 39) has the form of an $m_i \times (m_i - 1)$ -matrix

$$L_{i} = \begin{pmatrix} t_{1} & 0 & \dots & 0 & 0 & \dots \\ 0 & t_{2} & \dots & 0 & 0 & \dots \\ \vdots & \ddots & 0 & 0 & \dots \\ 0 & \dots & t_{i} & 0 & 0 & \dots \\ 0 & \dots & t_{i}Z_{a_{i}} & 0 & 0 & \dots \\ 0 & \dots & 0 & t_{i+1} & 0 & \dots \\ & \dots & & \ddots \end{pmatrix}, \quad t_{1} = {}^{\bullet}Z_{f_{1}} {}^{\bullet}, \ t_{2} = {}^{\bullet}Z_{f_{1}}Z_{f_{2}} {}^{\bullet}, \ \dots$$

or an $m_i \times (m_i + 1)$ -matrix

$$U_{i} = \begin{pmatrix} t_{1} & 0 & \dots & 0 & 0 & \dots \\ 0 & t_{2} & \dots & 0 & 0 & \dots \\ \vdots & \ddots & 0 & 0 & \dots \\ \hline 0 & \dots & t_{i} & t_{i} & t_{i} Z_{a_{i}} & 0 & \dots \\ \hline 0 & \dots & 0 & 0 & t_{i+1} & \dots \\ & & & & \ddots \end{pmatrix}, \quad t_{1} = Z_{f_{1}}, \quad t_{2} = Z_{f_{1}}Z_{f_{2}}, \quad \dots$$

Therefore $Q_q = \prod_i X_i$, where $X_i = L_i$ or $X_i = U_i$ is a rectangular matrix of variable size $m_i \times m_{i+1}$ $(m_{i+1} = m_i - 1)$ in the first case and $m_{i+1} = m_i + 1$ in the second.)

Note that quantum variables from different elementary pieces commute, commutation relations between Z_{f_j} and Z_{a_i} in one elementary fork piece X_i are determined by the dual quiver. In particular, they give rise

relations for 2×1 and 1×2 matrices.

For
$$m_i = 2$$
, $m_{i+1} = 1$, let $L_i = \begin{pmatrix} a \\ b \end{pmatrix}$. Then $R_{m_i} \stackrel{1}{L_i} \otimes \stackrel{2}{L_i} = \stackrel{2}{L_i} \otimes \stackrel{1}{L_i} R_{m_{i+1}}$. Indeed,
$$\begin{pmatrix} q & 0 & 0 & 0 \\ a & 0 & 0 & 0 \end{pmatrix} \stackrel{1}{\begin{bmatrix} 1 & 2 \\ a & 0 & 0 & 0 \end{pmatrix}} \begin{pmatrix} q & 0 & 0 & 0 \\ a & 0 & 0 & 0 \end{pmatrix} \begin{pmatrix} a^2 \\ a & 0 & 0 & 0 \end{pmatrix}$$

$$\begin{pmatrix} q & 0 & 0 & 0 \\ 0 & 1 & 0 & 0 \\ 0 & q - q^{-1} & 1 & 0 \\ 0 & 0 & 0 & q \end{pmatrix} \begin{bmatrix} 1 \\ a \\ b \end{pmatrix} \otimes \begin{pmatrix} a \\ b \end{pmatrix} = \begin{pmatrix} q & 0 & 0 & 0 \\ 0 & 1 & 0 & 0 \\ 0 & q - q^{-1} & 1 & 0 \\ 0 & 0 & 0 & q \end{pmatrix} \begin{pmatrix} a^2 \\ ab \\ ba \\ b^2 \end{pmatrix} =$$

$$= \begin{pmatrix} qa^2 \\ qba \\ qab \\ qb^2 \end{pmatrix} = \left[\begin{pmatrix} a \\ b \end{pmatrix} \otimes \begin{pmatrix} a \\ b \end{pmatrix} \right] \cdot (q)$$

In a similar way, we can check relation $R_{m_i}\overset{1}{U_i}\otimes\overset{2}{U_i}=\overset{2}{U_i}\otimes\overset{1}{U_i}R_{m_{i+1}}$ for $U_i=\begin{pmatrix}a&b\end{pmatrix}$. Then,

$$R_{m_1} \overset{1}{Q_q} \otimes \overset{2}{Q_q} = R_{m_1} \prod_{i=1}^n \overset{1}{X_i} \otimes \prod_{i=1}^n \overset{2}{X_i} = R_{m_1} \overset{1}{X_1} \prod_{i=2}^n \overset{1}{X_i} \otimes \overset{2}{X_1} \prod_{i=2}^n \overset{2}{X_i} =$$

$$= \overset{2}{X_1} \otimes \overset{1}{X_1} R_{m_2} \prod_{i=2}^n \overset{1}{X_i} \otimes \prod_{i+2}^n \overset{2}{X_i} = \dots = \prod_{i=1}^n \overset{2}{X_i} \otimes \prod_{i=1}^n \overset{1}{X_i} R_{m_n} = \overset{2}{Q_q} \otimes \overset{1}{Q_q} R_{m_n}.$$

This accomplishes the proof of Lemma 7.16.

Corollary 7.17. Theorem 2.12 and Remark 2.17 follow from Lemma 7.16.

Proof. Indeed, it is enough to consider $2n \times n$ matrix B of boundary measurements of the network shown on Figure 25. Denote by \mathcal{M}_1 the top $n \times n$ block of Q_q , \mathcal{M}_2 is the bottom $n \times n$ block. Q_q satisfies R-matrix relation 7.16. Choose subset of these relations between tensor products of elements of \mathcal{M}_1 and \mathcal{M}_2 we obtain Theorem 2.12. Relations between tensor products of elements of each matrix \mathcal{M}_i give Remark 2.17.

Directed networks with cycles

In this section we generalize Lemma 7.16 to the case of planar networks containing oriented cycles and sources and sinks distributed arbitrarily along the boundary circle. The R-matrix formulation of commutation relation of elements of transport matrices is not valid for more general networks with non-separated sources and sinks. The corresponding statement is formulated in Theorem 8.3. For the case of networks with separated sources and sinks the commutation relations of Theorem 8.3 coincide with those of Lemma 7.16.

Definition 8.1. We assign to every oriented path $P: j \rightsquigarrow i$ from a source j to a sink i the quantum weight

$$w(P) = \bigcap_{\text{face } \alpha \text{ lies to the right}}^{\text{face } \alpha \text{ lies to the right}} Z_{\alpha \bullet}^{\bullet},$$

where the product is taken with repetitions,

Definition 8.2. For any planar directed network \mathcal{N} , define transport elements

$$(\alpha, a) := \sum_{\text{all paths } \alpha \sim a} (-1)^{\text{\# self-intersections}} w(P_{\alpha \sim a})$$

where the sum ranges over all paths from the source j to the sink i. This sum is finite for acyclic networks and can be infinite for networks containing cycles. In this section, we let Greek letters denote sources and Latin letters denote sinks. We draw these transport elements as simple directed paths $\alpha \to a$.

Theorem 8.3. For any planar network, we have the algebra of transport elements:

$$[(\alpha, a), (\beta, b)] = (q - q^{-1})(\alpha, b)(\beta, a);$$

$$[(\alpha, a), (\beta, b)] = 0,$$

$$[(\alpha, b), (\beta, a)] = 0,$$

$$[(\alpha, a), (\beta, b)] = 0,$$

$$[(\alpha, a), (\beta, a)] = 0,$$

$$[(\alpha, a), (\beta, b)] = 0,$$

$$[(\alpha,$$

For acyclic networks these theorem was proven above; we now consider the case of network with cycles. The proof is by induction, is rather technical and is contained in Appendix B where we treat in details only cases with four distinct sources and sinks (the first three cases in the theorem).

9 Concluding remarks

In this paper, we have found the log-canonical coordinate representation for matrices A enjoying the quantum reflection equation. We have also solved the problem of representing the braid-group action for the uppertriangular A in terms of mutations of cluster variables associated with the corresponding quiver.

In conclusion, we indicate some directions of development. The first interesting problem is to construct mutation realizations for braid-group and Serre element actions that are Poisson automorphisms in the case of block-upper triangular matrices A (the corresponding action in terms of entries of a block-upper-triangular A was constructed in [9]). We assume that it is not difficult to construct planar networks producing block-triangular transport matrices \mathcal{M}_1 and \mathcal{M}_2 enjoying the standard Poisson Lie algebra relations. Then $\mathbb{A} = \mathcal{M}_1^T \mathcal{M}_2$ will satisfy the semiclassical reflection equation.

Next, we have a conjecture that describes explicitly quantum braid group action. Namely, the kth generator of the braid group acts on every matrix element of \mathbb{A}^{\hbar} by conjugation with $U_k^{\hbar} = e^{2\pi i \ell_k^2}$ where $a_{k,k+1}^{\hbar} = 2\cosh(2\pi\hbar\ell_k)$ (see [29]). It is interesting to analyze this action in quantum cluster coordinates.

Another direction of development is to study alternative system of log-canonical coordinates based on the following semiclassical groupoid construction. Let B is a general matrix of Poisson-Lie group SL_n endowed with

Acknowledgements

The authors are grateful to Alexander Shapiro for many useful discussions and to anonymous referees for an extensive and careful work they done to improve readability of this paper. Both L.Ch. and M.S. are supported by International Laboratory of Cluster Geometry NRU HSE, RF Government grant, ag. №75-15-2021-608 dated 08.06.2021; M.S. is supported by NSF grants DMS-1702115 and DMS-2100791. M.S. would like to thank the Isaac Newton Institute for Mathematical Sciences, Cambridge, for support and hospitality during the programme "Cluster algebras and representation theory" where work on the revision of this paper was undertaken. This work was supported by EPSRC grant no EP/R014604/1.

Appendix A Standard Poisson-Lie group \mathcal{G} , its dual and induced bracket

Another description of the Poisson structure on the space of triangular forms \mathcal{A}_n as a push-forward of the standard Poisson bracket on the dual group $\mathcal{G}^* = SL_n^*$ to the set of fixed points of the natural involution was given in [2].

A reductive complex Lie group \mathcal{G} equipped with a Poisson bracket $\{\cdot,\cdot\}$ is called a <u>Poisson-Lie group</u> if the multiplication map $\mathcal{G} \times \mathcal{G} \ni (X,Y) \mapsto XY \in \mathcal{G}$ is Poisson. Denote by $\langle \ , \ \rangle$ an invariant nondegenerate form on the corresponding Lie algebra $\mathfrak{g} = Lie(\mathcal{G})$, and by ∇^R , ∇^L the right and left gradients of functions on \mathcal{G} with respect to this form defined by

$$\left\langle \nabla^R f(X), \xi \right\rangle = \frac{d}{dt} \Big|_{t=0} f(Xe^{t\xi}), \quad \left\langle \nabla^L f(X), \xi \right\rangle = \frac{d}{dt} \Big|_{t=0} f(e^{t\xi}X)$$

for any $\xi \in \mathfrak{g}$, $X \in \mathcal{G}$.

Let $\pi_{>0}$, $\pi_{<0}$ be projections of $\mathfrak g$ onto subalgebras spanned by positive and negative roots, π_0 be the projection onto the Cartan subalgebra $\mathfrak h$, and let $R=\pi_{>0}-\pi_{<0}$. The <u>standard Poisson-Lie bracket</u> $\{\cdot,\cdot\}_r$ on $\mathcal G$ can be written as

$$\{f_1, f_2\}_r = \frac{1}{2} \left(\left\langle R(\nabla^L f_1), \nabla^L f_2 \right\rangle - \left\langle R(\nabla^R f_1), \nabla^R f_2 \right\rangle \right). \tag{A.1}$$

The standard Poisson–Lie structure is a particular case of Poisson–Lie structures corresponding to quasitriangular Lie bialgebras. For a detailed exposition of these structures see, e. g., [4, Ch. 1], [39] and [44].

Following [39], let us recall the construction of the Drinfeld double. The double of \mathfrak{g} is $D(\mathfrak{g}) = \mathfrak{g} \oplus \mathfrak{g}$ equipped with an invariant nondegenerate bilinear form $\langle \langle (\xi, \eta), (\xi', \eta') \rangle \rangle = \langle \xi, \xi' \rangle - \langle \eta, \eta' \rangle$. Define subalgebras \mathfrak{d}_{\pm} of $D(\mathfrak{g})$ by $\mathfrak{d}_{+} = \{(\xi, \xi) : \xi \in \mathfrak{g}\}$ and $\mathfrak{d}_{-} = \{(R_{+}(\xi), R_{-}(\xi)) : \xi \in \mathfrak{g}\}$, where $R_{\pm} \in \text{End }\mathfrak{g}$ is given by $R_{\pm} = \frac{1}{2}(R \pm \text{Id})$. The operator $R_{D} = \pi_{\mathfrak{d}_{+}} - \pi_{\mathfrak{d}_{-}}$ can be used to define a Poisson–Lie structure on $D(\mathcal{G}) = \mathcal{G} \times \mathcal{G}$, the double of the group \mathcal{G} , via

$$\{f_1, f_2\}_D = \frac{1}{2} \left(\left\langle \left\langle R_D(\nabla^L f_1), \nabla^L f_2 \right\rangle \right\rangle - \left\langle \left\langle R_D(\nabla^R f_1), \nabla^R f_2 \right\rangle \right\rangle \right), \tag{A.2}$$

where ∇^R and ∇^L are right and left gradients with respect to $\langle \langle \cdot, \cdot \rangle \rangle$. The diagonal subgroup $\{(X, X) : X \in \mathcal{G}\}$ is a Poisson–Lie subgroup of $D(\mathcal{G})$ (whose Lie algebra is \mathfrak{d}_+) naturally isomorphic to $(\mathcal{G}, \{\cdot, \cdot\}_r)$.

The group \mathcal{G}^* whose Lie algebra is \mathfrak{d}_- is a Poisson-Lie subgroup of $D(\mathcal{G})$ called the dual Poisson-Lie group of \mathcal{G} . The Poisson bracket $\{\cdot,\cdot\}_D$ induces the Poisson bracket on \mathcal{G}^* .

For $\mathcal{G} = SL_n$ the dual group $\mathcal{G}^* = \{(X_+, Y_-)\} \in B_+ \times B_-$ satisfying the additional relation $\pi_0(X_+)\pi_0(Y_-) = \text{Id}$ where $B_+(B_-) \subset SL_n$ are Borel subgroups of nondegenerate upper (lower) triangular matrices.

The involution $\iota_{\mathcal{G}^*}: \mathcal{G}^* \to \mathcal{G}^*$ takes (X_+, Y_-) to (Y_-^t, X_+^t) .

The subgroup \mathcal{U}_+ of unipotent upper triangular matrices is embedded diagonally in \mathcal{G}^* . The embedding $\epsilon: \mathcal{U}_+ \hookrightarrow \mathcal{G}^*$ maps $X \in \mathcal{U}_+$ to (X, X). The image $\epsilon(\mathcal{U}_+)$ is the set of fixed points of involution $\iota_{\mathcal{G}^*}$.

The image $\epsilon(\mathcal{U}_+)$ is not a Poisson subvariety of \mathcal{G}^* however the Dirac reduction induces the Poisson bi-vector Π (1.4) on U_{+} .

To remind the definition of Dirac reduction we consider a subvariety X of a Poisson variety $(V, \{\cdot, \cdot\}_{PB})$ defined by constraints $\phi_i = const.$ The second class constraints are constraints ϕ_a whose Poisson brackets with at least one other constraint do not vanish on the constraint surface.

Define matrix U with entries $U_{ab} = \{\phi_a, \phi_b\}_{PB}$. Note that U is always invertible.

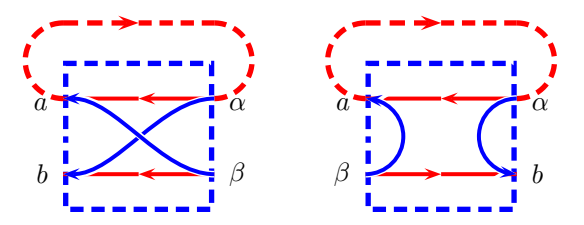
Then, Dirac bracket of functions f and g on X is

$$\{f,g\}_{DB} = \{f,g\}_{PB} - \sum_{a,b} \{f,\tilde{\phi}_a\}_{PB} U_{ab}^{-1} \{\tilde{\phi}_b,g\}_{PB},$$

see [27] for details.

Appendix B Proof of Theorem 8.3

We consider all possible cases corresponding to the situation in which we close the sink a and the (neighbour) source α . For a path (β, b) we have two possibilities:



We begin with observation that in both these cases,

$$^{\bullet}(\alpha,b)(\alpha,a)^n(\beta,a)^{\bullet} = (\alpha,b)(\alpha,a)^n(\beta,a) = (\beta,a)(\alpha,a)^n(\alpha,b),$$

where on the right we assume the natural order of the product of operators. The effect of closing the line between a and α changes the transport element from β to b: in the respective cases, we have

$$\overline{(\beta,b)} = (\beta,b) - (\beta,a)\frac{1}{1+(\alpha,a)}(\alpha,b), \text{ and } \overline{(\beta,b)} = (\beta,b) + (\beta,a)\frac{1}{1+(\alpha,a)}(\alpha,b).$$

Here and hereafter, we understand rational expressions as geometrical-progression expansions in powers of the corresponding operator. We also use the standard commutation relation formulas

$$\left[A, \frac{1}{1+B}\right] = -\frac{1}{1+B}[A, B] \frac{1}{1+B} \quad \forall A, B,$$

and use the color graphics to indicate permutations of operators in formulas of this section: a pair of operators painted red produces the factor q upon permuting these operators in the operatorial product, and a pair of operators painted blue produces a factor q^{-1} upon the corresponding permutation; pairs of operators painted

Below we have six cases of mutual distribution of sources $\{\alpha, \beta, \gamma\}$ and sinks $\{a, b, c\}$ (Note, that planarity condition requires α and a always to be neighbour), and in each such case we have two choices of transport elements: $\{(\beta, b), (\gamma, c)\}$ and $\{(\beta, c), (\gamma, b)\}$, so, altogether, we have 12 variants to be checked.

Case 1.
$$b \leftarrow \beta$$
 Variant (a): $\{\overline{(\beta,b)},\overline{(\gamma,c)}\}$.
$$c \leftarrow \gamma$$

$$\overline{[(\beta,b)},\overline{(\gamma,c)}] = \left[\left((\beta,b)-(\beta,a)\frac{1}{1+(\alpha,a)}(\alpha,b)\right),\left((\gamma,c)-(\gamma,a)\frac{1}{1+(\alpha,a)}(\alpha,c)\right)\right]$$

$$\begin{split} &= (q-q^{-1})(\beta,c)(\gamma,b) + (\gamma,a)\frac{-1}{1+(\alpha,a)}(q-q^{-1})(\beta,a)(\alpha,b)\frac{1}{1+(\alpha,a)}(\alpha,c) \\ &- (q-q^{-1})(\beta,c)(\gamma,a)\frac{1}{1+(\alpha,a)}(\alpha,b) + (\beta,a)\frac{1}{1+(\alpha,a)}(q-q^{-1})(\alpha,c)(\gamma,a)\frac{1}{1+(\alpha,a)}(\alpha,b) \\ &- (q-q^{-1})(\beta,a)\frac{1}{1+(\alpha,a)}(\alpha,c)(\gamma,b) + (\beta,a)\frac{1}{1+(\alpha,a)}(\alpha,b)(\gamma,a)\frac{1}{1+(\alpha,a)}(\alpha,c) \\ &- (\gamma,a)\frac{1}{1+(\alpha,a)}(\alpha,c)(\beta,a)\frac{1}{1+(\alpha,a)}(\alpha,b) \\ &= (q-q^{-1})\Big[(\beta,c)(\gamma,b) - (\beta,c)(\gamma,a)\frac{1}{1+(\alpha,a)}(\alpha,b) - (\beta,a)\frac{1}{1+(\alpha,a)}(\alpha,c)(\gamma,b) \\ &+ (\beta,a)\frac{1}{1+(\alpha,a)}(\alpha,c)(\gamma,a)\frac{1}{1+(\alpha,a)}(\alpha,b)\Big] \\ &+ ((q-q^{-1})-q+q^{-1})(\beta,a)\frac{1}{1+(\alpha,a)}(\alpha,c)(\gamma,a)\frac{1}{1+(\alpha,a)}(\alpha,b) \\ &= (q-q^{-1})\overline{(\beta,c)(\gamma,b)}. \end{split}$$

Variant (b): $\{\overline{(\beta,c)},\overline{(\gamma,b)}\}$

$$\begin{split} & [\overline{(\beta,c)},\overline{(\gamma,b)}] = \left[\left((\beta,c) - (\beta,a) \frac{1}{1+(\alpha,a)}(\alpha,c) \right), \left((\gamma,b) - (\gamma,a) \frac{1}{1+(\alpha,a)}(\alpha,b) \right) \right] \\ = & (\gamma,a) \frac{-1}{1+(\alpha,a)} (q-q^{-1})(\beta,a)(\alpha,c) \frac{1}{1+(\alpha,a)}(\alpha,b) + (q-q^{-1})(\gamma,a) \frac{1}{1+(\alpha,a)}(\beta,b)(\alpha,c) \\ & - (q-q^{-1})(\beta,b)(\gamma,a) \frac{1}{1+(\alpha,a)}(\alpha,c) - (q-q^{-1})(\beta,b)(\gamma,a) \frac{1}{1+(\alpha,a)}(\alpha,c) \\ & - (q-q^{-1})(\beta,a) \frac{-1}{1+(\alpha,a)}(\alpha,b)(\gamma,a) \frac{1}{1+(\alpha,a)}(\alpha,c) \\ & + (\beta,a) \frac{1}{1+(\alpha,c)}(\alpha,c)(\gamma,a) \frac{1}{1+(\alpha,a)}(\alpha,b) - (\gamma,a) \frac{1}{1+(\alpha,a)}(\alpha,b)(\beta,a) \frac{1}{1+(\alpha,a)}(\alpha,c) \\ & \text{(two last terms mutually cancelled)} \\ = & (q-q^{-1}) \left[-(\gamma,a) \frac{1}{1+(\alpha,a)}(\beta,a)(\alpha,c) \frac{1}{1+(\alpha,a)}(\alpha,b) - (\gamma,a) \left[(\beta,b), \frac{1}{1+(\alpha,a)} \right](\alpha,c) \right. \\ & + (\beta,a) \frac{1}{1+(\alpha,a)}(\gamma,a)(\alpha,b) \frac{1}{1+(\alpha,a)}(\alpha,c) \right] \end{split}$$

Case 2. $b \leftarrow \beta$ Variant (a): $\{\overline{(\beta,b)},\overline{(\gamma,c)}\}$.

 $= -(q-q^{-1})(q^{-1} + (q-q^{-1}) - q)(\gamma, a) \frac{1}{1 + (\alpha, a)}(\beta, a)(\alpha, b) \frac{1}{1 + (\alpha, a)}(\alpha, c) = 0.$

$$\begin{split} & [\overline{(\gamma,c)},\overline{(\beta,b)}] = \left[\left((\gamma,c) + (\gamma,a) \frac{1}{1+(\alpha,a)}(\alpha,c) \right), \left((\beta,b) - (\beta,a) \frac{1}{1+(\alpha,a)}(\alpha,b) \right) \right] \\ = & (\gamma,a) \frac{-1}{1+(\alpha,a)}(q-q^{-1})(\alpha,b)(\beta,a) \frac{1}{1+(\alpha,a)}(\alpha,c) \\ & - (\gamma,a) \frac{1}{1+(\alpha,a)}(\alpha,c)(\beta,a) \frac{1}{1+(\alpha,a)}(\alpha,b) + (\beta,a) \frac{1}{1+(\alpha,a)}(\alpha,b)(\gamma,a) \frac{1}{1+(\alpha,a)}(\alpha,c) = 0 \end{split}$$

Variant (b): $\{\overline{(\beta,c)},\overline{(\gamma,b)}\}.$

$$[\overline{(\gamma,b)},\overline{(\beta,c)}] = \left[\left((\gamma,b) - (\gamma,a) \frac{1}{1 + (\alpha,a)} (\alpha,b) \right), \left((\beta,c) - (\beta,a) \frac{1}{1 + (\alpha,a)} (\alpha,c) \right) \right]$$

$$= (q - q^{-1})(\gamma, a)(\beta, b) \frac{1}{1 + (\alpha, a)}(\alpha, c) + (\beta, a) \frac{-1}{1 + (\alpha, a)}(q - q^{-1})(\gamma, a)(\alpha, b) \frac{1}{1 + (\alpha, a)}(\alpha, c)$$

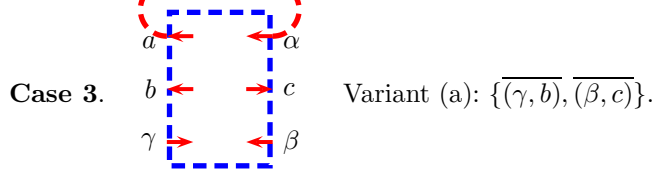
$$+ (\gamma, a) \frac{1}{1 + (\alpha, a)}(q - q^{-1})(\alpha, c)(\beta, a) \frac{1}{1 + (\alpha, a)}(\alpha, b) + (q - q^{-1})(\gamma, a) \frac{1}{1 + (\alpha, a)}(\alpha, c)(\beta, b)$$

$$+ (\gamma, a) \frac{1}{1 + (\alpha, c)}(\alpha, b)(\beta, a) \frac{1}{1 + (\alpha, a)}(\alpha, c) - (\beta, a) \frac{1}{1 + (\alpha, a)}(\alpha, c)(\gamma, a) \frac{1}{1 + (\alpha, a)}(\alpha, b)$$

$$\text{(two last terms mutually cancelled)}$$

$$= -(q - q^{-1}) \left[-(\gamma, a) \left[(\beta, b), \frac{1}{1 + (\alpha, a)} \right](\alpha, c) + (\beta, a) \frac{1}{1 + (\alpha, a)}(\gamma, a)(\alpha, b) \frac{1}{1 + (\alpha, a)}(\alpha, c) - (\gamma, a) \frac{1}{1 + (\alpha, a)}(\beta, a)(\alpha, c) \frac{1}{1 + (\alpha, a)}(\alpha, b) \right]$$

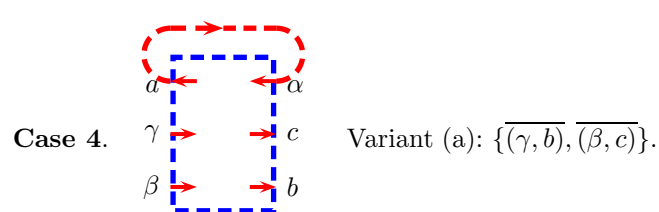
$$= (q - q^{-1}) \left((q - q^{-1}) + q^{-1} - q \right)(\gamma, a) \frac{1}{1 + (\alpha, a)}(\beta, a)(\alpha, b) \frac{1}{1 + (\alpha, a)}(\alpha, c) = 0.$$



$$\begin{split} & [\overline{(\gamma,b)},\overline{(\beta,c)}] = \left[\left((\gamma,b) - (\gamma,a) \frac{1}{1 + (\alpha,a)} (\alpha,b) \right), \left((\beta,c) + (\beta,a) \frac{1}{1 + (\alpha,a)} (\alpha,c) \right) \right] \\ & = - (q - q^{-1})(\gamma,c)(\beta,b) - (q - q^{-1})(\gamma,a)(\beta,a) \frac{1}{1 + (\alpha,a)} (\alpha,c) \\ & - (q - q^{-1})(\beta,a) \frac{-1}{1 + (\alpha,a)} (\gamma,a)(\alpha,b) \frac{1}{1 + (\alpha,a)} (\alpha,c) + (q - q^{-1})(\gamma,c)(\beta,a) \frac{1}{1 + (\alpha,a)} (\alpha,b) \\ & - (\gamma,a) \frac{1}{1 + (\alpha,a)} \frac{(\alpha,b)(\beta,a)}{1 + (\alpha,a)} \frac{1}{1 + (\alpha,a)} \frac{(\alpha,c) + (\beta,a)}{1 + (\alpha,a)} \frac{1}{1 + (\alpha,a)} (\alpha,c)(\gamma,a) \frac{1}{1 + (\alpha,a)} (\alpha,b) \\ & \text{(two last terms mutually cancelled)} \\ & = - (q - q^{-1})(\gamma,c) \left[(\beta,b) - (\beta,a) \frac{1}{1 + (\alpha,a)} (\alpha,b) \right] - (q - q^{-1})(\gamma,a) \frac{1}{1 + (\alpha,a)} (\alpha,c)(\beta,b) \\ & - (q - q^{-1})(\gamma,a) \left[(\beta,b), \frac{1}{1 + (\alpha,a)} \right] (\alpha,c) + (q - q^{-1})(\beta,a) \frac{1}{1 + (\alpha,a)} (\gamma,a)(\alpha,b) \frac{1}{1 + (\alpha,a)} (\alpha,c) \\ & = - (q - q^{-1})(\gamma,c) \left[(\beta,b) - (\beta,a) \frac{1}{1 + (\alpha,a)} (\alpha,b) \right] - (q - q^{-1})(\gamma,a) \frac{1}{1 + (\alpha,a)} (\alpha,c)(\beta,b) \\ & - (q - q^{-1}) \left((q - q^{-1}) - q \right) (\gamma,a) \frac{1}{1 + (\alpha,a)} (\beta,a)(\alpha,b) \frac{1}{1 + (\alpha,a)} (\alpha,c) \\ & = - (q - q^{-1}) \left[(\gamma,c) + (\gamma,a) \frac{1}{1 + (\alpha,a)} (\alpha,c) \right] \left[(\beta,b) - (\beta,a) \frac{1}{1 + (\alpha,a)} (\alpha,b) \right] = - (q - q^{-1}) \overline{(\gamma,c)} \overline{(\beta,b)} \end{split}$$

Variant (b): $\{\overline{(\gamma,c)},\overline{(\beta,b)}\}.$

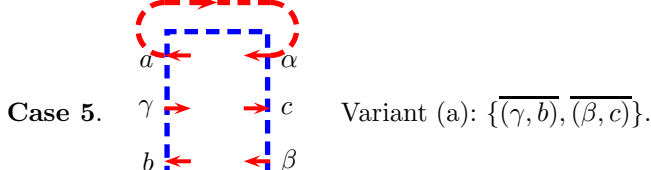
$$\begin{aligned} & [\overline{(\gamma,c)},\overline{(\beta,b)}] = \left[\left((\gamma,c) + (\gamma,a) \frac{1}{1+(\alpha,a)}(\alpha,c) \right), \left((\beta,b) - (\beta,a) \frac{1}{1+(\alpha,a)}(\alpha,b) \right) \right] \\ & = -(\gamma,a) \frac{1}{1+(\alpha,a)} (q-q^{-1})(\alpha,b)(\beta,a) \frac{1}{1+(\alpha,a)}(\alpha,c) \\ & - (\gamma,a) \frac{1}{1+(\alpha,a)} (\alpha,c)(\beta,a) \frac{1}{1+(\alpha,a)}(\alpha,b) + (\beta,a) \frac{1}{1+(\alpha,c)}(\alpha,b)(\gamma,a) \frac{1}{1+(\alpha,a)}(\alpha,c) = 0. \end{aligned}$$



$$\begin{split} & [\overline{(\gamma,b)},\overline{(\beta,c)}] = \left[\left((\gamma,b) + (\gamma,a) \frac{1}{1+(\alpha,a)}(\alpha,b) \right), \left((\beta,c) + (\beta,a) \frac{1}{1+(\alpha,a)}(\alpha,c) \right) \right] \\ = & (q-q^{-1})(\beta,a) \frac{1}{1+(\alpha,a)}(\gamma,c)(\alpha,b) - (q-q^{-1})(\gamma,c)(\beta,a) \frac{1}{1+(\alpha,a)}(\alpha,b) \\ & + (\gamma,a) \frac{1}{1+(\alpha,a)}(\alpha,b)(\beta,a) \frac{1}{1+(\alpha,a)}(\alpha,c) - (\beta,a) \frac{1}{1+(\alpha,a)}(\alpha,c)(\gamma,a) \frac{1}{1+(\alpha,a)}(\alpha,b) = 0. \end{split}$$

Variant (b): $\{\overline{(\gamma,c)},\overline{(\beta,b)}\}$

$$\begin{split} & [\overline{(\gamma,c)},\overline{(\beta,b)}] = \left[\left((\gamma,c) + (\gamma,a) \frac{1}{1+(\alpha,a)}(\alpha,c) \right), \left((\beta,b) - (\beta,a) \frac{1}{1+(\alpha,a)}(\alpha,b) \right) \right] \\ & = -(q-q^{-1})(\gamma,b)(\beta,c) - (q-q^{-1})(\gamma,b)(\beta,a) \frac{1}{1+(\alpha,a)}(\alpha,c) \\ & - (q-q^{-1})(\gamma,a) \frac{1}{1+(\alpha,a)}(\alpha,b)(\beta,c) \\ & + (\gamma,a) \frac{1}{1+(\alpha,a)}(\alpha,c)(\beta,a) \frac{1}{1+(\alpha,a)}(\alpha,b) - (\beta,a) \frac{1}{1+(\alpha,a)}(\alpha,b)(\gamma,a) \frac{1}{1+(\alpha,a)}(\alpha,c) \\ & = -(q-q^{-1}) \left[(\gamma,b) + (\gamma,a) \frac{1}{1+(\alpha,a)}(\alpha,b) \right] \left[(\beta,c) - (\beta,a) \frac{1}{1+(\alpha,a)}(\alpha,c) \right] = -(q-q^{-1}) \overline{(\gamma,b)} \overline{(\beta,c)}. \end{split}$$



$$\overline{[(\gamma,b),(\beta,c)]} = \left[\left((\gamma,b) + (\gamma,a) \frac{1}{1+(\alpha,a)} (\alpha,b) \right), \left((\beta,c) + (\beta,a) \frac{1}{1+(\alpha,a)} (\alpha,c) \right) \right] \\
= (q-q^{-1})(\beta,a) \frac{1}{1+(\alpha,a)} (\gamma,c)(\alpha,b) - (q-q^{-1})(\gamma,c)(\beta,a) \frac{1}{1+(\alpha,a)} (\alpha,b) \\
+ (\gamma,a) \frac{1}{1+(\alpha,a)} (\alpha,b)(\beta,a) \frac{1}{1+(\alpha,a)} (\alpha,c) - (\beta,a) \frac{1}{1+(\alpha,a)} (\alpha,c)(\gamma,a) \frac{1}{1+(\alpha,a)} (\alpha,b) = 0.$$

Variant (b): $\{\overline{(\gamma,c)},\overline{(\beta,b)}\}$.

$$\begin{split} & [\overline{(\gamma,c)},\overline{(\beta,b)}] = \left[\left((\gamma,c) + (\gamma,a) \frac{1}{1+(\alpha,a)}(\alpha,c) \right), \left((\beta,b) - (\beta,a) \frac{1}{1+(\alpha,a)}(\alpha,b) \right) \right] \\ & = - (q-q^{-1})(\gamma,a) \frac{1}{1+(\alpha,a)}(\alpha,b)(\beta,a) \frac{1}{1+(\alpha,a)}(\alpha,c) \\ & - (\gamma,a) \frac{1}{1+(\alpha,a)}(\alpha,c)(\beta,a) \frac{1}{1+(\alpha,a)}(\alpha,b) + (\beta,a) \frac{1}{1+(\alpha,a)}(\alpha,b)(\gamma,a) \frac{1}{1+(\alpha,a)}(\alpha,c) = 0. \end{split}$$

Case 6.
$$\gamma \rightarrow \beta$$
 Variant (a): $\{\overline{(\gamma,b)},\overline{(\beta,c)}\}$.

$$\overline{[(\gamma,b),(\beta,c)]} = \left[\left((\gamma,b) + (\gamma,a) \frac{1}{1+(\alpha,a)}(\alpha,b) \right), \left((\beta,c) - (\beta,a) \frac{1}{1+(\alpha,a)}(\alpha,c) \right) \right] \\
= (q-q^{-1})(\gamma,c)(\beta,b) - (q-q^{-1})(\beta,a) \frac{1}{1+(\alpha,a)}(\gamma,c)(\alpha,b) \\
- (q-q^{-1})(\gamma,a) \frac{1}{1+(\alpha,a)}(\alpha,c)(\beta,a) \frac{1}{1+(\alpha,a)}(\alpha,b) + (q-q^{-1})(\gamma,a) \frac{1}{1+(\alpha,a)}(\alpha,c)(\beta,b) \\
- (\gamma,a) \frac{1}{1+(\alpha,a)}(\alpha,b)(\beta,a) \frac{1}{1+(\alpha,a)}(\alpha,c) - (\beta,a) \frac{1}{1+(\alpha,a)}(\alpha,c)(\gamma,a) \frac{1}{1+(\alpha,a)}(\alpha,b)$$

(two last terms mutually cancelled

$$= (q-q^{-1}) \left[(\gamma,c) + (\gamma,a) \frac{1}{1+(\alpha,a)} (\alpha,c) \right] \left[(\beta,b) - (\beta,a) \frac{1}{1+(\alpha,a)} (\alpha,b) \right] = (q-q^{-1}) \overline{(\gamma,c)} \overline{(\beta,b)}.$$

Variant (b): $\{\overline{(\gamma,c)},\overline{(\beta,b)}\}.$

$$\begin{split} & [\overline{(\gamma,c)},\overline{(\beta,b)}] = \left[\left((\gamma,c) + (\gamma,a) \frac{1}{1+(\alpha,a)}(\alpha,c) \right), \left((\beta,b) - (\beta,a) \frac{1}{1+(\alpha,a)}(\alpha,b) \right) \right] \\ & = - \left(q - q^{-1} \right) (\gamma,a) \frac{1}{1+(\alpha,a)}(\alpha,b) (\beta,a) \frac{1}{1+(\alpha,a)}(\alpha,c) \\ & - (\gamma,a) \frac{1}{1+(\alpha,a)}(\alpha,c) (\beta,a) \frac{1}{1+(\alpha,a)}(\alpha,b) + (\beta,a) \frac{1}{1+(\alpha,a)}(\alpha,b) (\gamma,a) \frac{1}{1+(\alpha,a)}(\alpha,c) = 0. \end{split}$$

This concludes the proof of the theorem.

References

- A. Berenstein and A. Zelevinsky, Quantum cluster algebras Adv. Math. 195 (2005) 405-455; math/0404446.
- A. Berenstein and A. Zelevinsky, Quantum cluster algebras Adv. Math. 195 (2005) 405-455; math/0404446.
 P. P. Boalch, Stokes Matrices, Poisson Lie Groups and Frobenius Manifolds, Invent. Math. 146 (3) (2001) 479-506.
- A.I. Bondal, A symplectic groupoid of triangular bilinear forms and the braid groups, Izv. Math., 68:4 (2004), 659-708
- [4] V. Chari and A. Pressley, A Guide to Quantum Groups. Cambridge University Press, 1994.
- Chekhov L., Fock V., A quantum Techmüller space, Theoret. and Math. Phys. 120 (1999), 1245–1259.
- [6] Chekhov L., Fock V., Quantum mapping class group, pentagon relation, and geodesics, Proc. Steklov Inst. Math. no. 3, 226 (1999), 149–163.
- Chekhov L., Fock V., Observables in 3d gravity and geodesic algebras, Czech. J. Phys. 50 (2000) 1201–1208.
- Chekhov L.O., Mazzocco M., Isomonodromic deformations and twisted Yangians arising in Teichmüller theory, Adv. Math.
- L. Chekhov and M. Mazzocco, Block triangular bilinear forms and braid group action, Comm. Math. Phys. 322 (2013) 49-71.
- L. Chekhov and M. Mazzocco, On a Poisson space of bilinear forms with a Poisson Lie action, Russian Math. Surveys 72(6) (2017) 1109-1156.
- Chekhov L.O., Mazzocco M. and Rubtsov V., Algebras of quantum monodromy data and character varieties, Geometry and Physics: Volume I: A Festschrift in honour of Nigel Hitchin, edited by A.Dancer, J.E.Anderson, and O.Garcia-Prada, Oxford Scholarship Online, (2018), DOI: 10.1093/oso/9780198802013.001.0001.
- Chekhov, L. and Shapiro, M. Teichmüller spaces of Riemann surfaces with orbifold points of arbitrary order and cluster variables, Int. Math. Res. Not. (2014) 2746 - 2772; doi: 10.1093/imrn/rnt016.
- Chekhov, L., Shapiro, M., and Shibo, H., Characteristic equation for symplectic groupoid and cluster algebras, arXiv:2101.10323, 14pp
- [14] Coman, I., Gabella M, and Teschner J. 2015. Line Operators in Theories of Class S, Quantized Moduli Space of Flat Connections, and Toda Field Theory, J. High Energy Phys. 2015 (10). Springer Verlag, doi:10.1007/JHEP10(2015)143.
- [15] Dubrovin B., Geometry of 2D topological field theories, Integrable systems and quantum groups (Montecatini Terme, 1993), Lecture Notes in Math., 1620, Springer, Berlin, (1996) 120-348.
- Fock V.V., Dual Teichmüller spaces arXiv:dg-ga/9702018v3, (1997).
- [17] V. V. Fock and A. B. Goncharov, Moduli spaces of local systems and higher Teichmüller theory, Publ. Math. Inst. Hautes Études Sci. 103 (2006), 1-211.
- V. V. Fock and A. B. Goncharov, The quantum dilogarithm and representations of quantum cluster varieties, Invent. Math. **175**(2) (2008) 223–286.

- [19] V. Fock, A. Goncharov. Cluster X-varieties, amalgamation, and Poisson-Lie groups. Algebraic geometry and number theory. (2006): 27-68.
- [20] V. V. Fock and A. A. Rosly, Moduli space of flat connections as a Poisson manifold, Advances in quantum field theory and statistical mechanics: 2nd Italian-Russian collaboration (Como, 1996), Internat. J. Modern Phys. B 11 (1997), no. 26-27, 3195–3206.
- [21] S. Fomin and A. Zelevinsky, Cluster algebras I: Foundations. J. Amer. Math. Soc. 15 (2002), 497-529, DOI: https://doi.org/10.1090/S0894-0347-01-00385-X
- [22] Fomin S., Shapiro M., and Thurston D., Cluster algebras and triangulated surfaces. Part I: Cluster complexes, Acta Math. 201 (2008), no. 1, 83–146.
- [23] A. M. Gavrilik and A. U. Klimyk, q-Deformed orthogonal and pseudo-orthogonal algebras and their representations Lett. Math. Phys., 21 (1991) 215–220.
- [24] M. Gekhtman, M. Shapiro, and A. Vainshtein, Cluster algebra and Poisson geometry, Mosc. Math. J. 3(3) (2003) 899-934.
- [25] Goldman W.M., Invariant functions on Lie groups and Hamiltonian flows of surface group representations, Invent. Math. 85 (1986) 263–302.
- [26] A. Goncharov, L. Shen Quantum geometry of moduli spaces of local systems and representation theory, arXiv:1904.10491
- [27] Henneaux M. and Teitelboim Cl., Quantization of Gauge Systems, Princeton University Press, 1992.
- [28] M. V. Karasev, Analogues of objects of Lie group theory by nonlinear Poisson brackets, Math. USSR Izvestia 28 (1987) 497–527.
- [29] R. M. Kashaev, On the spectrum of Dehn twists in quantum Teichmüller theory, in: Physics and Combinatorics, (Nagoya 2000). River Edge, NJ, World Sci. Publ., 2001, 63–81.
- [30] R. M. Kaufmann and R. C. Penner, Closed/open string diagrammatics, Nucl. Phys. B748 (2006) 335–379.
- [31] Korotkin D. and Samtleben H., Quantization of coset space σ -models coupled to two-dimensional gravity, Comm. Math. Phys. 190(2) (1997) 411–457.
- [32] Machacek, J. and Ovenhouse, N. Log-canonical coordinates for Poisson brackets and rational changes of coordinates J. Geom. Phys. 121 (2017), pp. 288–296.
- [33] K. Mackenzie General Theory of Lie Groupoids and Lie Algebroids, LMS Lect. Note Series 213 (2005).
- [34] A. Molev, E. Ragoucy, P. Sorba, Coideal subalgebras in quantum affine algebras, Rev. Math. Phys., 15 (2003) 789–822.
- [35] Nelson J.E., Regge T., Homotopy groups and (2+1)-dimensional quantum gravity, Nucl. Phys. B 328 (1989), 190–199.
- [36] Nelson J.E., Regge T., Zertuche F., Homotopy groups and (2 + 1)-dimensional quantum de Sitter gravity, Nucl. Phys. B 339 (1990), 516–532.
- [37] Postnikov A., Total positivity, Grassmannians, and networks, arXiv:math/0609764
- [38] Postnikov, A., Speyer, D., Williams, L., Matching polytopes, toric geometry, and the non-negative part of the Grassmannian, J. Algebraic Combin. 30 (2009), no. 2, 173-191.
- [39] A. Reyman and M. Semenov-Tian-Shansky, Group-theoretical methods in the theory of finite-dimensional integrable systems. Encyclopaedia of Mathematical Sciences, vol.16, Springer, Berlin, 1994 pp.116–225.
- [40] G. Schrader and A. Shapiro, Continuous tensor categories from quantum groups I: algebraic aspects, arXiv:1708.08107.
- 41] G. Schrader and A. Shapiro, private communication.
- [42] Ugaglia M., On a Poisson structure on the space of Stokes matrices, Int. Math. Res. Not. 1999 (1999), no. 9, 473–493.
- [43] A. Weinstein, Coisotropic calculus and Poisson groupoids, J. Math. Soc. Japan 40(4) (1988) 705–727.
- [44] M. Yakimov, Symplectic leaves of complex reductive Poisson-Lie groups, Duke Math. J. 112 (2002) 453-509.